

AD-A075 400

NORTHEASTERN UNIV BOSTON MA DEPT OF CIVIL ENGINEERING

F/G 8/11

STATE-OF-THE-ART FOR ASSESSING EARTHQUAKE HAZARDS IN THE UNITED--ETC(U)

JUL 79 M K YEGIANJUL 79

DACW39-78-M-2652

UNCLASSIFIED

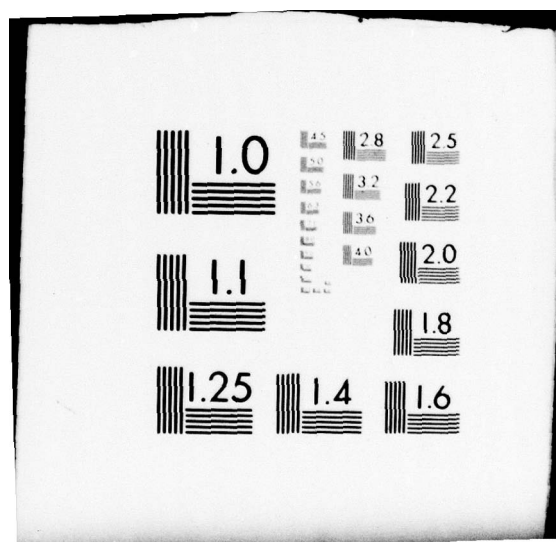
WES-MP-S-73-1

NL

1 OF 2

AD  
A075400





M. P. S-73-1

STATE-OF-THE-ART FOR ASSESSING EARTHQUAKE HAZAR



**LEVEL**



MISCELLANEOUS PAPER S-73-1

# STATE-OF-THE-ART FOR ASSESSING EARTHQUAKE HAZARDS IN THE UNITED STATES

Report 13

## PROBABILISTIC SEISMIC HAZARD ANALYSIS

by

M. K. Yegian

Department of Civil Engineering  
Northeastern University  
Boston, Mass. 02115

July 1979

Report 13 of a Series

Approved For Public Release; Distribution Unlimited

DDC  
RECEIVED  
OCT 22 1979  
E



DDC FILE COPY

Prepared for Office of Chief of Engineers, U. S. Army  
Washington, D. C. 20314

Under Contract No. DACW39-78-M-2652

Monitored by Geotechnical Laboratory  
U. S. Army Engineer Waterways Experiment Station  
P. O. Box 631, Vicksburg, Miss. 39180

70 22 10 000

When this report is no longer needed, return it to  
the originator.

The findings in this report are not to be construed as an official  
Department of the Army position unless so designated  
by other authorized documents.

The contents of this report are not to be used for  
advertising, publication, or promotional purposes.  
Citation of trade names does not constitute an  
official endorsement or approval of the use of  
such commercial products.

Unclassified

18 WES

SECURITY CLASSIFICATION OF THIS PAGE (When Data Entered)

REPORT DOCUMENTATION PAGE		READ INSTRUCTIONS BEFORE COMPLETING FORM
1. REPORT NUMBER Miscellaneous Paper S-73-1	2. GOVT ACCESSION NO.	3. RECIPIENT'S CATALOG NUMBER
4. TITLE (and Subtitle) STATE-OF-THE-ART FOR ASSESSING EARTHQUAKE HAZARDS IN THE UNITED STATES Report 13. PROBABILISTIC SEISMIC HAZARD ANALYSIS	5. TYPE OF REPORT & PERIOD COVERED Report 13 of a series	
7. AUTHOR(s) K. Yegian	6. PERFORMING ORG. REPORT NUMBER	
9. PERFORMING ORGANIZATION NAME AND ADDRESS Northeastern University Department of Civil Engineering Boston, Mass. 02115	8. CONTRACT OR GRANT NUMBER(s) Contract No. DACW39-78-M-2652	
11. CONTROLLING OFFICE NAME AND ADDRESS Office, Chief of Engineers, U. S. Army Washington, D. C. 20314	10. PROGRAM ELEMENT, PROJECT, TASK AREA & WORK UNIT NUMBERS	
14. MONITORING AGENCY NAME & ADDRESS (if different from Controlling Office) U. S. Army Engineer Waterways Experiment Station Geotechnical Laboratory P. O. Box 631, Vicksburg, Miss. 39180	12. REPORT DATE July 1979	
	13. NUMBER OF PAGES 132	
	15. SECURITY CLASS. (of this report) Unclassified	
	15a. DECLASSIFICATION/DOWNGRADING SCHEDULE	
16. DISTRIBUTION STATEMENT (of this Report) Approved for public release; distribution unlimited.		
17. DISTRIBUTION STATEMENT (of the abstract entered in Block 20, if different from Report)		
18. SUPPLEMENTARY NOTES		
19. KEY WORDS (Continue on reverse side if necessary and identify by block number) Earthquake engineering      Probability theory Earthquake hazards      Seismic investigations Earthquakes      Seismic risks Ground motion      State-of-the-art studies		
20. ABSTRACT (Continue on reverse side if necessary and identify by block number) This report presents a comprehensive review of the state of the art of probabilistic seismic hazard analysis. This type of analysis essentially provides information regarding the likelihood that various levels of a ground motion parameter will be exceeded in a given period of time.  The report begins with a discussion of the various seismic parameters required for the analysis and the calculation of these parameters based on seismic history data. Problems involved in the estimation of these (Continued)		

DD FORM 1 JAN 73 1473

EDITION OF 1 NOV 65 IS OBSOLETE

Unclassified

SECURITY CLASSIFICATION OF THIS PAGE (When Data Entered)

4p 292 411 416

Unclassified

SECURITY CLASSIFICATION OF THIS PAGE(When Data Entered)

20. ABSTRACT (Continued)

parameters exclusively on the basis of seismological data are outlined, and emphasis is placed on the need to utilize and incorporate geologic and geophysical information in the analysis.

A brief presentation of Baye's theorem and discussion of the procedure for seismic hazard estimation using the theorem are provided.

The report continues with a presentation of the various mathematical formulations used in the calculation of seismic hazard probabilities. This section also includes a discussion of the use of computer programs to facilitate the calculations involved in the analysis.

Concluding the report is a presentation and discussion of the various practical applications of seismic hazard analysis, emphasizing use in structural and geotechnical engineering. Some recent seismic hazard maps for the U. S. incorporating probability calculations are presented and reviewed in this section.

Unclassified

SECURITY CLASSIFICATION OF THIS PAGE(When Data Entered)

## PREFACE

This report was prepared by Dr. M. K. Megian of the Department of Civil Engineering, Northeastern University, Boston, Mass., under Contract No. DACW39-78-M-2652. It is part of ongoing work at the U. S. Army Engineer Waterways Experiment Station (WES) in Civil Works Investigation Study, "Seismic Effects of Reservoir Loading and Fluid Injection in Wells," sponsored by the Office, Chief of Engineers, U. S. Army. The report was reviewed by Ms. Mary Ellen Hynes Griffin and Dr. Frank K. Chang of WES.

Preparation of this report was under the direction of Dr. E. L. Krinitzsky, Engineering Geology and Rock Mechanics Division (EG&RMD), Geotechnical Laboratory (GL), WES. General direction was by Mr. J. P. Sale, Chief, GL, and Dr. D. C. Banks, Chief, EG&RMD.

COL J. L. Cannon, CE, and Mr. F. R. Brown were Director and Technical Director, respectively, of WES during the period of this study.

Accession For	
NTIS GRA&I	<input checked="checked" type="checkbox"/>
DDC TAB	<input type="checkbox"/>
Unannounced	<input type="checkbox"/>
Justification	
By _____	
Distribution/	
Availability Codes	
Dist	Avail and/or special
A	

## CONTENTS

	<u>Page</u>
PREFACE. . . . .	1
CONVERSION FACTORS, U. S. CUSTOMARY TO METRIC (SI) UNITS OF MEASUREMENT. . .	4
PART 1: INTRODUCTION. . . . .	5
Benefits of Seismic Hazard Analysis . . . . .	6
General Description of Methodology. . . . .	7
Scope of Report . . . . .	8
PART 2: SEISMIC HAZARD ANALYSIS--INPUT PARAMETERS . . . . .	9
Analysis of Seismic History Data. . . . .	10
Seismic Sources . . . . .	10
Rate of Earthquake Occurrence . . . . .	15
Magnitude-Frequency . . . . .	18
Upper Bound Magnitude . . . . .	37
Housner's Method. . . . .	40
Attenuation Laws. . . . .	44
Other Factors Influencing Attenuation Laws. . . . .	66
Geologic and Geophysical Information. . . . .	72
Bayesian Approach . . . . .	76
Bayesian Estimate of Seismic Hazard . . . . .	80
PART 3: SEISMIC HAZARD CALCULATIONS . . . . .	83
Basic Probability Concepts. . . . .	83
Mathematical Formulations . . . . .	89
Point Source. . . . .	89
Line Source . . . . .	91
Area Source . . . . .	96

## CONTENTS

	<u>Page</u>
PART 4: APPLICATIONS. . . . .	99
Input to Structural Analysis. . . . .	101
Intensity Data. . . . .	102
Magnitude Data. . . . .	103
Input to Geotechnical Analysis. . . . .	105
Seismic Hazard Maps . . . . .	108
Uniform Building Code . . . . .	108
California Division of Mines and Geology. . . . .	110
Milne and Davenport (1969). . . . .	110
Kiremidjian and Shah (1975) . . . . .	111
Algermissen and Perkins (1976). . . . .	111
Applied Technology Council (1978) . . . . .	111
Design Spectrum . . . . .	119
PART 5: CONCLUSIONS . . . . .	121
REFERENCES . . . . .	123
APPENDIX A: SEISMIC HAZARD ANALYSIS USING PROBABILISTIC ATTENUATION LAW . .	A1

CONVERSION FACTORS, U. S. CUSTOMARY TO METRIC (SI)  
UNITS OF MEASUREMENT

U. S. customary units of measurement used in this report can be converted to metric (SI) units as follows:

<u>Multiply</u>	<u>By</u>	<u>To Obtain</u>
feet	0.3048	metres
miles (U. S. statute)	1.609344	kilometres
square miles (U. S. statute)	2.589988	square kilometres

## PROBABILISTIC SEISMIC HAZARD ANALYSIS

### PART I: INTRODUCTION

There are two basic types of seismic hazard analysis which can be utilized in the determination of design earthquakes and ground motions: the deterministic analysis and the probabilistic analysis. The deterministic procedure bases the calculation for the seismic design of a facility on the largest expected earthquake or ground motion at the site of the facility. This method (which is the one generally adopted by the Army Corps of Engineers) is utilized in design situations where human safety is a crucial consideration, such as in the design of large dams. A probabilistic analysis is applied in situations where the failure of a facility does not pose a threat to human safety. A probabilistic analysis provides useful data regarding the likelihood of exceeding various levels of earthquake shaking within a given period of time, which can be used to perform cost-benefit analyses in order to select the criteria for the most economic design.

The following Report constitutes a review of the state of the art of probabilistic seismic analysis for estimating the expected occurrence of future seismic events. The use of the term "seismic risk analysis" in earthquake engineering literature to refer to such an analysis has caused some controversy in recent years, since seismic risk is also defined as the expected consequences of a future seismic event by planners and some earthquake engineers. In order to avoid any ambiguity in the definition, various investigators (24, 93) have adopted the term "hazard" to refer to the probability of occurrence of a seismic event and have reserved the term "risk" to refer to the consequences of a seismic event. This Report will adhere to the following definitions:

Seismic Hazard Analysis: The development of a probability versus ground motion intensity curve for a given site.

Seismic Risk Analysis: The development of a probability versus consequences curve for a given site. The consequences of a seismic event may include fatalities, injuries, economic losses and damages.

Thus, seismic risk analysis, as herein defined, constitutes a complete probabilistic analysis of the future occurrence of seismic events, as well as an analysis of the expected consequences to a constructed facility of such events. Thus, the results obtained from seismic hazard analysis are an input factor in the seismic risk analysis.

This Report specifically reviews the state of the art of probabilistic seismic hazard analysis for a single site.

#### Benefits of Seismic Hazard Analysis

Prior to the development of seismic hazard analysis procedures in the late 1960's, estimations of the likelihood of occurrence for seismic hazards of various intensities were based on experience and professional judgment. Use of seismic hazard analysis procedures now provides greater logic and consistency in such estimations as well as more reliable information regarding the occurrence of different seismic hazards over a given period of time. The benefits can be summarized as follows (23, 35):

- 1) Allows for maximum utilization in a logical and consistent manner of geologic, geophysical and historic data, combined with the professional judgment of trained seismologists and geologists.
- 2) Accounts for uncertainties in both the data used and the models developed for analysis.
- 3) Can provide comparative influences of various parameters and assumptions which contribute to the overall computed hazard, thus identifying the major parameters and/or sources of uncertainty which may require special consideration.

- 4) Provides crucial information toward well-balanced engineering designs, which require a trade-off between costly designs for greater resistance and more economical designs which run higher risks of economic loss (23, 50, 51, 88, 104).
- 5) Permits assessment of the seismic hazard in terms which allow comparison with other natural and man-made hazards.

#### General Description of Methodology

The basic procedure for conducting a seismic hazard analysis for a single site involves the steps outlined below.

1) Local Seismicity - A study is made of the geologic, tectonic and seismic history of the surrounding area, and potential earthquake source zones are identified. For each of the potential sources a prediction is made regarding the future activity within the source in terms of expected number of earthquake occurrences of different magnitudes within a given period of time. At this point in the study, the probability that an earthquake of a certain magnitude will occur within the region under study can be calculated by employing a probability model to describe the random nature of earthquake occurrences.

2) Regional Seismicity - An evaluation of the regional seismicity involves the computation of the probability distribution of earthquake intensities or other seismic parameters, such as peak acceleration, spectral velocity, or duration, at the site under investigation. An attenuation law is applied at this point to describe the earthquake at the site as a function of earthquake magnitude and distance from the site. For each source zone, the probability of a future earthquake exceeding a given value of the specific seismic parameter being used at the site is computed, accounting for the random nature of seismic activity and the uncertainties involved in the estimation of the parameter.

The total probability of exceedence within a given period of time is obtained by summing the various contributions to this probability of the sources identified in the first step.

3) Micro-regionalization - The attenuation law used in the preceding step very often provides an estimate of the earthquake parameter based on firm ground. The influence of the local soil properties and the details of the local geology upon the computed parameters for firm ground can be incorporated in this step to arrive at a seismic hazard curve which relates a suitably chosen seismic parameter describing earthquake shaking at the site to the probability of its exceedence in a given number of years.

#### Scope of the Report

This Report is limited to the review of the state of the art of seismic hazard analysis for a single site. Part 2 of the Report discusses the various sources of information with regard to local and regional seismicity. Detailed descriptions are presented of the different parameters employed in the analysis, as well as the uncertainties and problems involved in their estimation. A discussion regarding the application of Baye's theorem in order to combine data from various sources is also included. Part 3 is a presentation of the mathematical formulations required for the seismic hazard analysis, including a brief introduction to some of the probability concepts used in such an analysis. Part 4 deals with the various applications of a seismic hazard analysis and presents the recently published seismic hazard maps. Part 5 concludes the Report with a summary.

## PART 2: SEISMIC HAZARD ANALYSIS--INPUT PARAMETERS

The probabilistic assessment of maximum earthquake intensities which may occur at a given site requires input from a number of sources including geologic, geophysical and historic data regarding the seismicity of the area. None of these sources considered alone provides adequate information toward a reliable probabilistic assessment of seismic hazard.

It is clear, for example, that the use of historic seismicity data as the basis for prediction of future seismic activity in a certain region is a highly uncertain and unreliable method (3, 8, 43). The use of such historic data is problematic in that the available information is often quite scarce and the records are extremely recent in terms of geologic time. Furthermore, the information extracted from historic records often seems to contradict geologic evidence (43).

Allen (1976) has detailed the difficulties in estimating future seismicity on the basis of short historic records. Historic seismic records for Eastern Mediterranean regions and China, which date back between 2,000 to 3,000 years, show periods of up to several centuries of quiescence alternating with equally lengthy periods of intense earthquake activity. It is apparent that estimates of the frequency of seismic activity based on short-term historic data relative to the geological time scale are highly uncertain. Thus, in regions such as the Eastern United States where historic data is available for less than a 300-year period and does not, therefore, allow observation of a cyclical seismic energy release as observed in Asia, geologic and geophysical information is most valuable in making predictions of future seismicity. Baye's theorem, which

will be detailed later in this section of the Report, provides a rational procedure for combination of the various information sources to arrive at the most reliable estimate of probability of future earthquake occurrence.

The remainder of Part 2 will include a discussion of the parameters involved in seismic hazard analysis as well as the estimation of these parameters based on seismological data. Further discussion will deal with relevant geologic and geophysical information, followed by a brief review of Baye's theorem and an explanation of its application in seismic hazard analysis.

#### Analysis of Seismic History Data

A comprehensive study of the local seismicity of a region includes the identification of potential earthquake source zones; an estimation of the average rate of earthquake occurrence for each of the identified sources; and the establishment of an earthquake magnitude-frequency law.

#### Seismic Sources

The initial task of a seismic hazard study is to identify all potential seismic sources in the region of the given site. Cornell (1968) has outlined the following three basic seismic source types, shown in Fig. 2.1:

- 1) Point Source - Characterizes a potential source of earthquakes, closely concentrated in space relative to its distance from the site.
- 2) Line Source - Describes potential earthquakes originating from a known fault.
- 3) Area Source - Utilized when the occurrence of earthquakes in the given region does not correlate with the geologic structure of the area, or when the

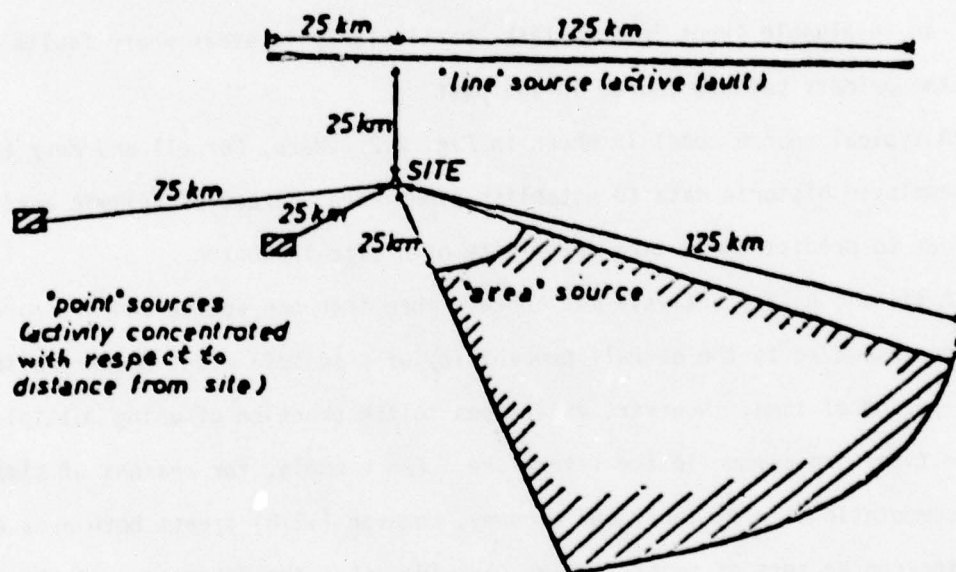


FIG. 2.1 Definition of Earthquake Sources  
(After Cornell 1968)

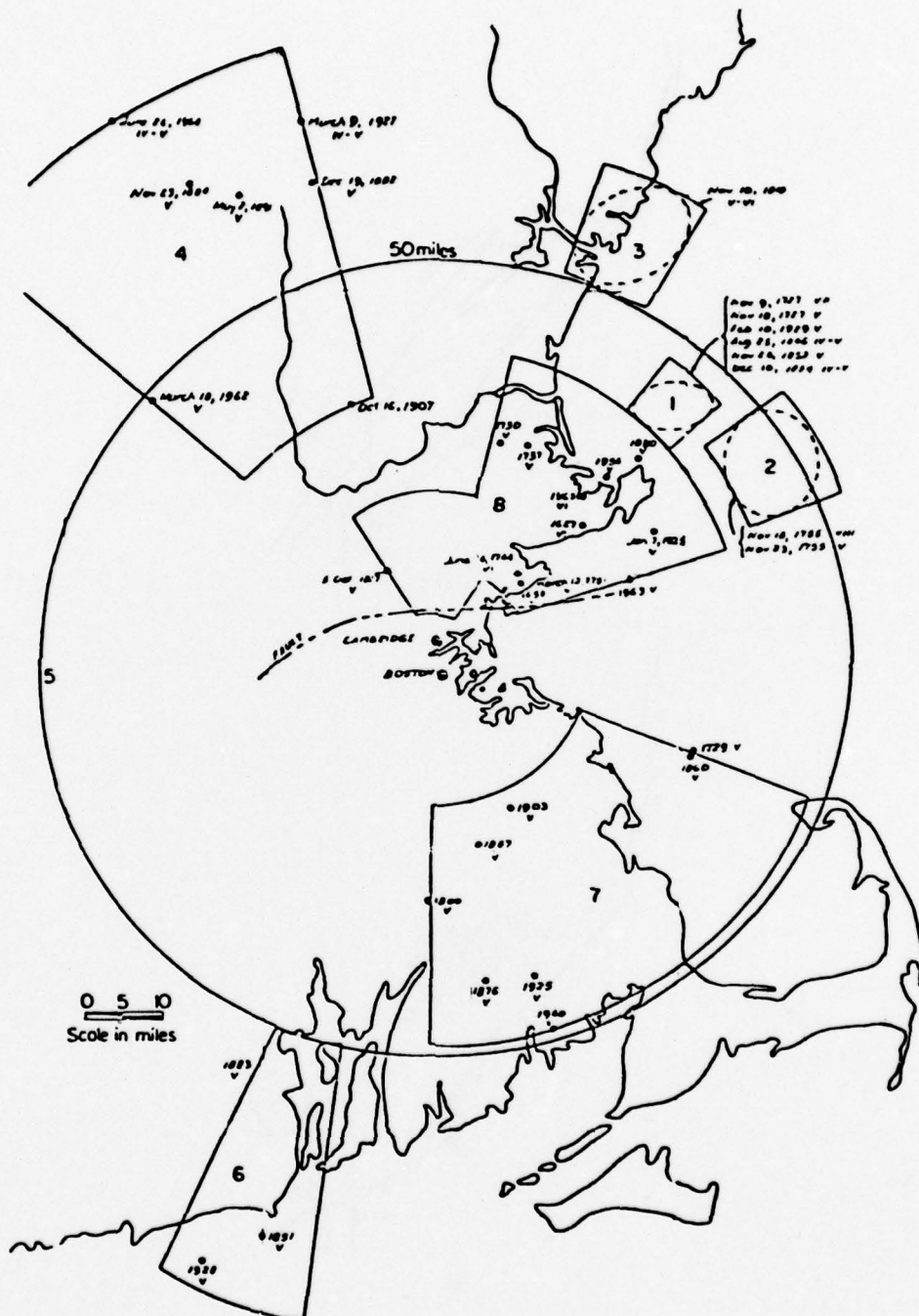
geologic structure is unobservable due to deep overburdens. In such an area, earthquakes are assumed to occur randomly and with an equal probability of occurrence throughout the source area.

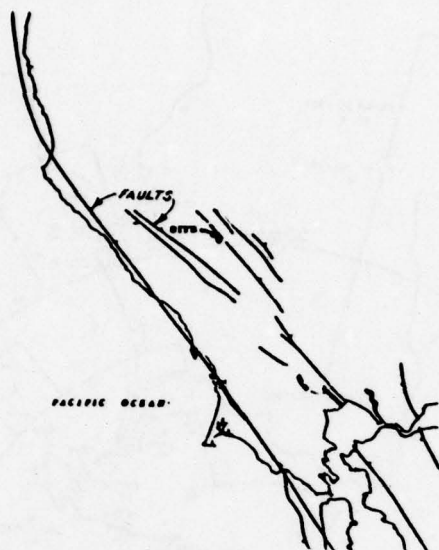
The initial establishment of all potential seismic sources, including their location in relation to the site, is essential to the seismic hazard analysis. The use of historic records can be useful in this determination, provided that the records cover a sufficiently large area. Geologic and geophysical data provide an invaluable input in this task, particularly in areas where faults have been the primary seismic source in the past.

A typical source model is shown in Fig. 2.2. Here, Cornell and Merz (1975) have employed historic data to establish eight area sources of seismic activity in order to predict the future seismicity of a site in Boston.

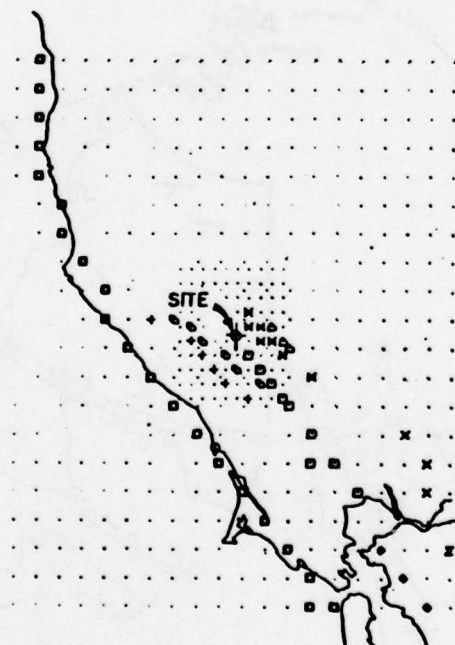
A seismic hazard analysis may contain more than one source and/or source type contributing to the overall probability of a seismic event occurring in a given period of time. However, exceptions to the practice of using multiple source types are common in the literature. For example, for reasons of simplicity, computational efficiency and economy, Donovan (1978) treats both area and line sources as sets of point sources, provided that the dimensions of the area or length which the point represents is considerably smaller than the distance from the equivalent point source to the site. A typical source model used by Donovan is shown in Fig. 2.3, in which the active faults located in the region under study are represented by point sources.

For similar reasons, McGuire (1976) treats faults as narrow area sources of 1 to 2 kilometres in width. Probabilities calculated using this model of fault representation, when evaluated with regard to calculations based on more accurate models which treat faults as line sources, have indicated approximately





(a)



(b)

FIG. 2.3 Fault Map of Northern California (a) and Computer Model of Regional and Fault Activity (b) Used in Risk Analysis (After Donovan 1978)

a 9% error in the estimated hazard at all levels of intensity for a site located a distance of 16 km from a fault which is 100 km in length. Studies show that this inaccuracy or error decreases as the distance from the source to the site increases.

Ayyaswamy et al. (1974) describe their preference of using faults as the only seismic source to be considered, particularly in a region such as California where active faults are scattered throughout the entire state. Lomnitz (1964), in his study of seismic risk in Chile, has employed a rather simple source model establishing each location of an historic seismic event as a future point source. It is necessary to point out that the validity of such a simple model is highly questionable, particularly if the historic records cover only a limited time span. The heavy emphasis in this approach on historic and instrumental data disregards possible valuable input from geologic and geophysical information.

Proper identification of all potential earthquake sources within a region, and most importantly those sources which are located near to a given site of interest, is an absolutely essential prerequisite to the calculation of seismic hazard for the given site. Cornell and Vanmarcke (1969) have shown that small and/or frequent events originating from sources close to the site provide the most significant information contributing to the total computed hazard for the site when the hazard is described in terms of peak ground acceleration. Thus, the oversight of a potential source close to the site could result in a significant understatement of the calculated hazard.

#### Rate of Earthquake Occurrence

Following identification of potential seismic sources, an average annual rate of occurrence of earthquakes,  $\lambda(m_0)$ , is assigned for each source. Rate of

occurrence can be estimated by counting the number of earthquakes of engineering interest with a magnitude exceeding an arbitrary lower bound,  $m_0$ , and dividing this by the observational period in years of the historic data. Very often in seismic hazard studies, a lower bound magnitude,  $m_0$ , is chosen representing a magnitude cutoff point below which earthquakes are considered to have negligible damaging effects and may be disregarded for the purpose of the study.

Thus, the parameter  $\lambda(m_0)$  describes the average number of earthquakes with magnitudes larger than  $m_0$  occurring annually within a specific source. The actual number to occur in a specific source over a given period of time is random. In order to model this randomness, seismic hazard analysis most commonly acts on the assumption that earthquake occurrence follows a poisson process, a model which assumes that earthquakes are both spatially and temporally independent. The general form of the poisson distribution is given by Eq. 2.1:

$$P(n, \lambda(m_0)) = \frac{\lambda(m_0)^n e^{-\lambda(m_0)}}{n!} \quad n = 0, 1, 2, \dots \quad (2.1)$$

where  $P(n, \lambda(m_0))$  represents the probability of  $n$  events with magnitudes equal to or exceeding  $m_0$  occurring in a time interval of  $t$ ; and  $\lambda(m_0)$  is the mean annual rate of occurrence of events with  $m \geq m_0$ .

Use of the poisson process to determine the rate of earthquake occurrence has been shown to be inaccurate by a number of investigators. Ferraes (1967b, 1973) tested the poisson model for earthquakes in Mexico City and concluded that the resulting data indicated non-randomness and thus the historic earthquakes in that region were actually not statistically independent events. Ferraes (1973) attributed this deviation from randomness to "the fact that the energy dissipated

by most of the large earthquakes is so large that the disturbance by these earthquakes affects the chances of the occurrence of subsequent discrete earthquakes." Based on data from southern California, Knopoff (1964) concluded that seismic events in that region registering a magnitude of 3.0 or greater did not correspond to a poisson distribution, thus suggesting a causal connection between successive seismic events. Lomnitz (1966) has suggested that observed deviation from the poisson process using statistics of past earthquakes may be due to a lack of spatial rather than temporal randomness. Isacks and Page (1968), in their comments regarding the data presented by Lomnitz (1966), suggest that the average rate of occurrence of seismic events,  $\lambda$ , is a random variable, and that discrepancies regarding the poisson process may be attributed to this variation of  $\lambda$  with time. As previously stated, variations of  $\lambda$  with time are observed in historic data of Eastern Mediterranean countries and in China, where seismological records span 2,000 to 3,000 years.

Esteva (1975) describes the distribution of waiting times between earthquakes, using geophysical information, by a gamma function, of which the poisson process is a specific case. A comparison of the expected costs of failure for the two processes has shown significant differences. Using the poisson model, the expected cost of failure is greater than that for the gamma function for a short time following the occurrence of an earthquake. As the period of time increases with no further occurrence, the computed risk based on the gamma distribution increases, eventually to twice the risk computed for the poisson process.

Although it is presently very difficult to substantiate any assumption that the occurrence of seismic activity follows a poisson process, it is equally difficult to dismiss the assumption on the basis of what little statistical data exists. Thus, the poisson distribution is frequently employed in seismic hazard

and seismic risk studies. Rosenblueth (1969) suggests that the poisson assumption may be an acceptable model in the design of structures with life-spans of several decades. However, the non-poisson nature of seismic activity should be carefully considered in decision-making immediately following a destructive earthquake.

#### Magnitude-Frequency

Two separate steps are involved in the probabilistic estimation of future earthquake occurrence of a specified magnitude,  $m$ . The initial step is a calculation of the probability of occurrence of seismic activity within a given period of time, and the second step is the estimation of the probability that should an earthquake occur it will reach or exceed a specified magnitude,  $m$ . The first probability calculation can be made utilizing the poisson model and the earthquake occurrence rate,  $\lambda$ , as previously discussed. The second probability estimation, commonly referred to as the conditional probability, requires an earthquake magnitude vs frequency law, which establishes a relationship between the number of earthquake occurrences and their respective magnitudes. The law most commonly applied in seismic hazard studies for this purpose is that suggested by Gutenberg and Richter (1954), which assumes the existence of an exponential relationship between the number of earthquakes and their respective magnitudes, as shown in Eq. 2.2:

$$\lambda(m) = 10^a e^{-\beta m} \quad (2.2)$$

This recurrence relationship, illustrated on a semi-log plot, yields a straight

line given by Eq. 2.3:

$$\log_{10} \lambda(m) = a - bm \quad ; \quad b = \beta / \ln 10 \quad (2.3)$$

where  $\lambda(m)$  refers to the mean number of earthquakes with magnitudes equal to or exceeding the specified magnitude,  $m$ , occurring within a unit time;  $a$  is a constant that is dependent on the location and time of the earthquake sample used; and  $b$  represents a constant thought to be characteristic of a particular region (54).

Assuming that there is an equal likelihood of occurrence for future earthquakes along a fault of length  $l$ , or over a source with an area  $A$ , then Eq. 2.3 can also be written as follows:

$$\log_{10} \bar{\lambda}(m) = \bar{a} - \bar{b} m \quad (2.4)$$

where  $\bar{\lambda}(m)$  gives the number of earthquakes with magnitudes equal to or greater than  $m$  per unit area or length, and per unit time;  $\bar{a}$  is equal to  $a - \log(A \text{ or } l \times \text{period of record})$ ; and  $\bar{b} = b = \beta / \ln 10$ .

The recurrence relationship of Eq. 2.3 or Eq. 2.4 can be used in order to determine the conditional probability of occurrence of an earthquake having or exceeding a magnitude of  $m$ .

If  $\lambda(m_0)$  designates the total number of earthquakes occurring within a unit time and exceeding magnitude  $m_0$ , then the ratio  $\lambda(m)/\lambda(m_0)$  gives the probability of a future earthquake having or exceeding a magnitude of  $m$ .

For the purpose of illustration, consider the example of a region with historic records documenting the occurrence of twenty earthquakes with magnitudes

equaling or exceeding  $m_0 = 4.0$ , and further documenting that five of the twenty earthquakes either reached or exceeded a magnitude of 6.0 on the Richter scale. Based on historic seismicity, the probability that a future earthquake in the region will have a magnitude equaling or exceeding 6.0 can be expressed by the ratio 5/20.

Therefore, the complementary cumulative distribution function for earthquake magnitude  $G_M(m)$  can be expressed by Eq. 2.5:

$$\begin{aligned} G_M(m) &= P[M \geq m|E] = 1 - F_M(m) = \frac{\lambda(m)}{\lambda(m_0)} = \frac{\bar{\lambda}(m)}{\bar{\lambda}(m_0)} \\ &= e^{-\beta(m - m_0)} \end{aligned} \quad (2.5)$$

where  $P[M \geq m|E]$  is the conditional probability of exceeding  $m$  given that an earthquake will occur. The probability density function for  $M$  is given by Eq. 2.6:

$$f_M(m) = \frac{dF_M(m)}{dm} = \beta e^{-\beta(m - m_0)} \quad (2.6)$$

Frequently, the seismic history data available for a region is given in terms of earthquake intensity. In such cases, the establishment of a magnitude-frequency law can be accomplished by writing the recurrence relationship of Eq. 2.2 in terms of earthquake intensity as follows:

$$\lambda(I) = 10^c e^{-\beta I I_0} \quad (2.7)$$

where  $I_0$  represents the epicentral intensity; and  $c$  and  $\beta_I$  are parameters which are comparable to  $a$  and  $\beta$  in Eq. 2.2. The parameter  $\beta_I$  can be related to  $\beta$ , provided that there is an assumed relationship between  $m$  and  $I_0$ . The most commonly used equation regarding this relationship is that given by Gutenberg and Richter (1954):

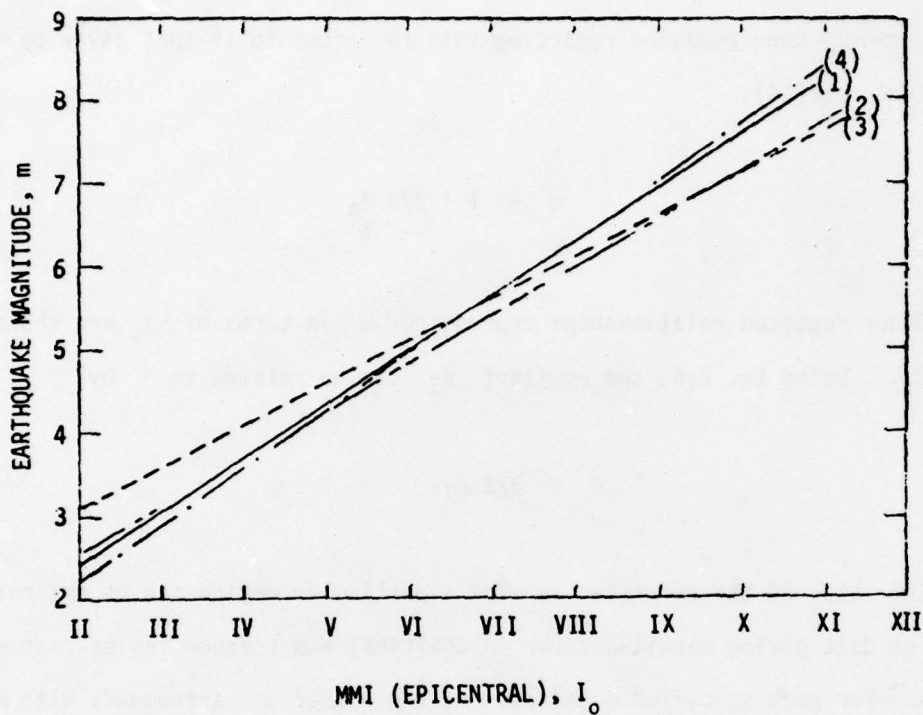
$$m = 1 + 2/3 I_0 \quad (2.8)$$

Other reported relationships expressing  $m$  in terms of  $I_0$  are shown in Fig. 2.4. Using Eq. 2.8, the constant  $\beta_I$  can be related to  $\beta$  by:

$$\beta = 3/2 \beta_I \quad (2.9)$$

The value of the parameter  $\beta$  for a particular region can be estimated based on data giving magnitudes (or intensities) and frequencies of past earthquakes. For each specified magnitude  $m$ , the number of earthquakes with magnitudes equal to or exceeding  $m$  is counted and plotted as a function of  $m$ . When this number is then divided by the time length of the record and the area it covers, the recurrence equation will be given as in Eq. 2.4. The value of  $\beta$  is always equal to the slope,  $b$ , of the best fit line in the semi-log plot multiplied by  $\ln 10$ . Fig. 2.5 shows typical earthquake magnitude distributions for the United States.

Alternatively, the seismic history data can be presented by plotting the ratio  $\lambda(m)/\lambda(m_0)$  vs  $m$ . The resulting relationship gives the probability of exceedence of  $m$  vs  $m$ . The slope of the best fit line on a semi-log plot will be equal to  $\beta$ , as shown in Eq. 2.5.



<u>CURVE</u>	<u>EQUATION</u>	<u>REFERENCE</u>
(1)	$m = 1 + \frac{2}{3} I_o$	Gutenberg & Richter (1954)
(2)	$m = 1.2 + 0.6 I_o$	Northeastern U.S. Chinnery & Rogers (1973)
(3)	$m = 2.1 + 0.5 I_o$	Western U.S. Krinitzsky & Chang (1977)
(4)	$m = 0.82 + 0.69 I_o$	Washington & Oregon Algermissen (1969)

FIG. 2.4 Earthquake Magnitude and MMI Relationships

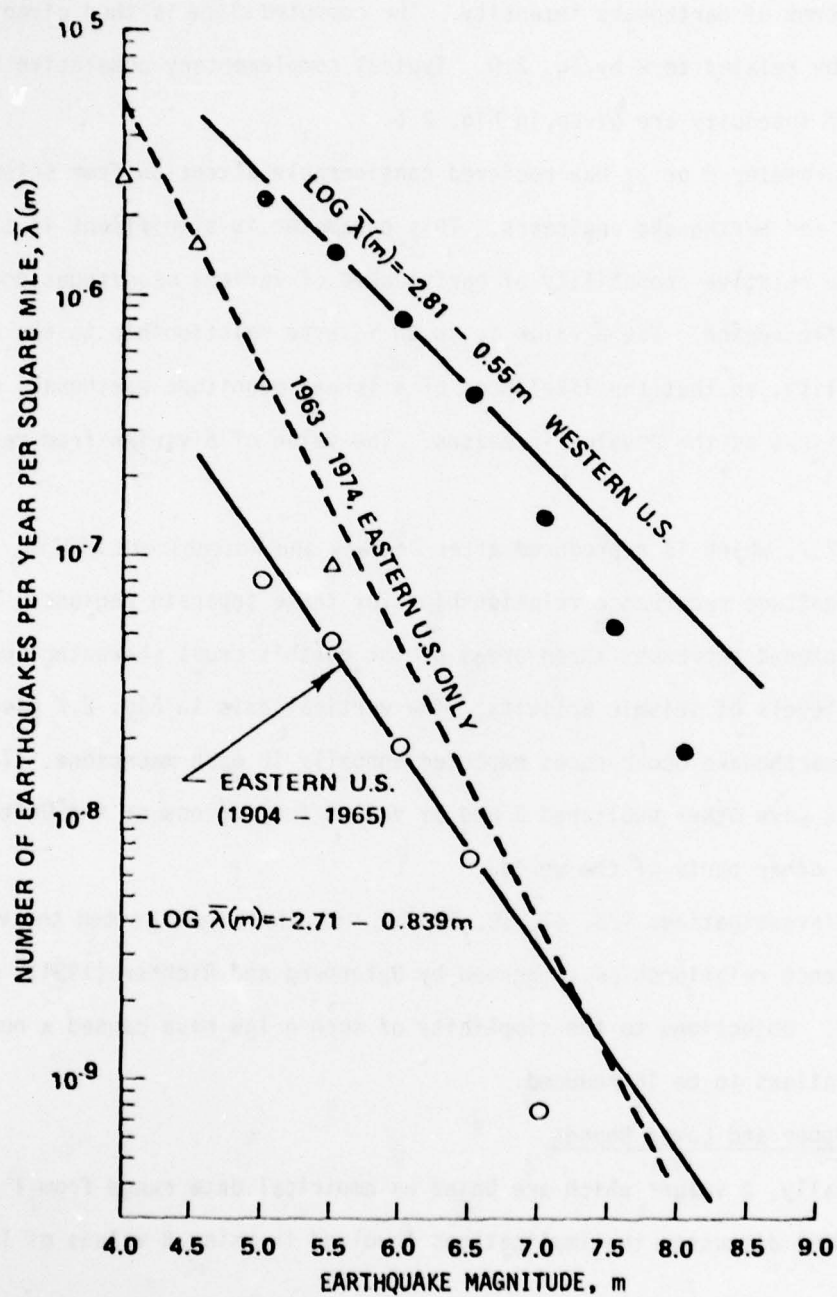


FIG. 2.5 Earthquake Distribution in the United States  
(After Hsieh et al. 1975)

This procedure can be applied to earthquake intensities as opposed to magnitudes where necessary, as in cases where the available historic records are given in terms of earthquake intensity. The computed slope is then given by  $\beta_I$ , which can be related to  $\beta$  by Eq. 2.9. Typical complementary cumulative functions in terms of intensity are given in Fig. 2.6.

The parameter  $\beta$  or  $\beta_I$  has received considerable attention from seismologists, geologists and earthquake engineers. This parameter is significant in that it defines the relative probability of earthquakes of various magnitudes occurring in a specific region. The  $\beta$  value is in an inverse relationship to the degree of probability, so that the likelihood of a larger magnitude earthquake occurring diminishes as the  $\beta$  value increases. The value of  $\beta$  varies from region to region.

Fig. 2.7, which is reproduced after Newmark and Rosenblueth (1971), gives typical magnitude recurrence relationships for three separate regions. The three macrozones represent three areas of the earth's crust characterized by different levels of seismic activity. The vertical axis in Fig. 2.7 gives the number of earthquake occurrences expected annually in each macrozone. Tables 2.1 and 2.2 give other published  $\beta$  and  $\beta_I$  values for regions of the United States and other parts of the world.

Some investigations (28, 47, 58, 79, 81, 102, 103) have tested the validity of the recurrence relationships suggested by Gutenberg and Richter (1954), given in Eq. 2.2. Objections to the simplicity of such a law have caused a number of modifications to be introduced.

#### A. Upper and Lower Bounds

Typically,  $\beta$  values which are based on empirical data range from 1 to 3. Esteva (1969) discusses the implications involved in using  $\beta$  values of less

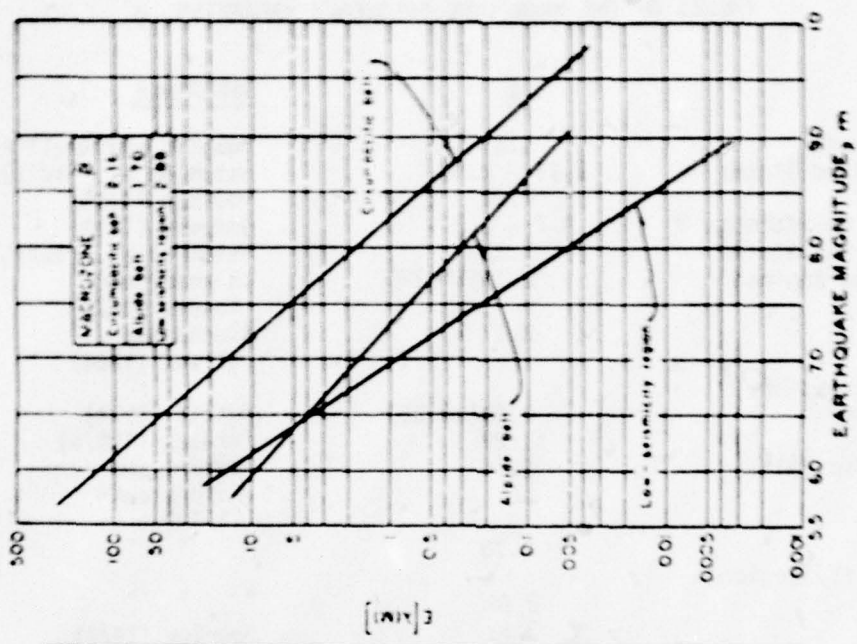


FIG. 2.6 Epicentral Intensity vs Frequency Curves  
(After Cornell and Merz 1975)

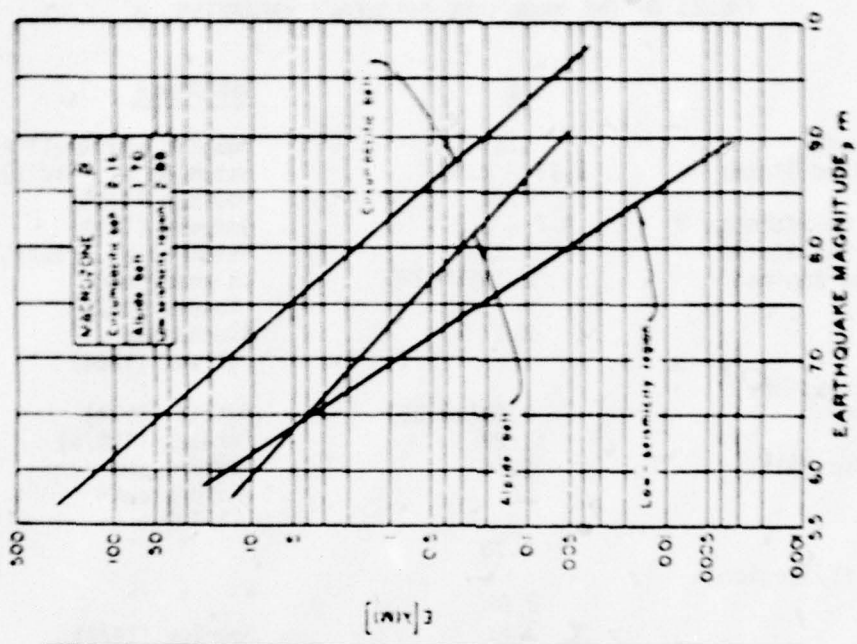


FIG. 2.7 Expected  $\lambda$ 's in Each Macrozone  
(After Newmark and Rosenblueth 1971)

TABLE 2.1  
VALUES OF THE MAGNITUDE-FREQUENCY PARAMETER,  $\beta$

<u>REGION</u>	<u><math>\beta</math></u>	<u>REFERENCE</u>
Western Nevada	2.1	Douglas and Ryall (1975)
Western United States	1.17 - 2.00	Hsieh et al. (1975)
California	2.07	Housner (1969)
San Jose', California	1.2 - 1.3	Donovan (1978)
Eastern United States	1.93	Hsieh et al. (1975)
Southern New England	2.19( $\pm 0.12$ )	Chinnery and Rogers (1973)
New Jersey	2.17	Isacks and Oliver (1964)
Central Mississippi River Valley	2.00( $\pm 0.25$ )	Nuttli (1974)
Mexico City	1.27	Ferraes (1967a)
Circumpacific Belt	2.16	Newmark and Rosenblueth (1971)
Alpide Belt	1.70	" " "
Low-Seismicity Region of World	2.88	" " "
Japan	2.81	Dowrick (1977)
New Guinea	3.1	" "
New Zealand	2.4	" "
Western Canada	2.5	" "
Central America	3.34	" "
Columbia-Peru	2.55	" "
Northern Chile	2.0	" "
Southern Chile	2.12	" "
Mediterranean	2.5	" "
Iran-Turkmenia	2.7	" "
Java	2.16	" "
East Africa	2.00	" "

TABLE 2.2  
VALUES OF THE INTENSITY-FREQUENCY PARAMETER,  $\beta_1$

<u>REGION</u>	<u><math>\beta_1</math></u>	<u>REFERENCES</u>
New York State and Surrounding Area	1.0	Decapua and Liu (1974)
Northern United States	1.05	Cornell and Merz (1975)
Boston Area	1.10	" "
Southern New England	1.31 ( $\pm 0.07$ )	Chinnery and Rogers (1973)
Southeastern United States	1.36	Bollinger (1973)
New Madrid Zone	1.43	Mann and Howe (1973)
Mississippi Valley - St. Lawrence	1.17	Algermissen (1969)
Mississippi Valley	0.93	McClain and Myers (1970)
Montana, Idaho	1.29	Algermissen (1969)
Puget Sound, Washington	1.43	" "
Wyoming, Colorado, New Mexico	1.57	" "
Nebraska, Kansas, Oklahoma	1.13	" "
Oklahoma, North Texas	1.27	" "
California	1.24	" "
Central United States	1.15	Liu and Fagel (1972)
World	1.35	Cornell and Merz (1975)
All Turkey	1.14	Gulkan and Yuceman (1975)

than 3 in the recurrence relationship shown in Eq. 2.2. This equation, when used in conjunction with the relationship between magnitude and energy released suggested by Gutenberg and Richter, predicts the liberation of infinite amounts of energy in earthquake activity per unit time, if the value of  $\beta$  is less than 3. For this reason, Cornell and Vanmarcke (1969) have proposed a modified magnitude-frequency relationship which considers an upper and a lower bound. Such a truncated linear relationship between the log of  $\lambda(m)$  and magnitude  $m$  is obtained by: 1) assigning a probability of one to the chance that a future earthquake, should it occur, will exceed the minimum magnitude of engineering interest,  $m_0$ ; and 2) assigning a probability of zero to the chance that a future earthquake will exceed a maximum "credible" magnitude,  $m_1$ . The proposed complementary cumulative probability distribution function of magnitude is given by Eq. 2.10:

$$P[M > m|E] = 1 - F_M(m) = 1 - K_{m_1} (1 - e^{-\beta(m - m_1)}); m_0 < m < m_1 \quad (2.10)$$

where

$$K_{m_1} = [1 - e^{-\beta(m_1 - m_0)}]^{-1}$$

Fig. 2.8 shows the influence of the truncated form of the recurrence relationship upon the complementary cumulative function for magnitude. The comparison made in Fig. 2.8 shows that truncation has significance only if the values of  $\beta$  and  $m_1$  are both small.

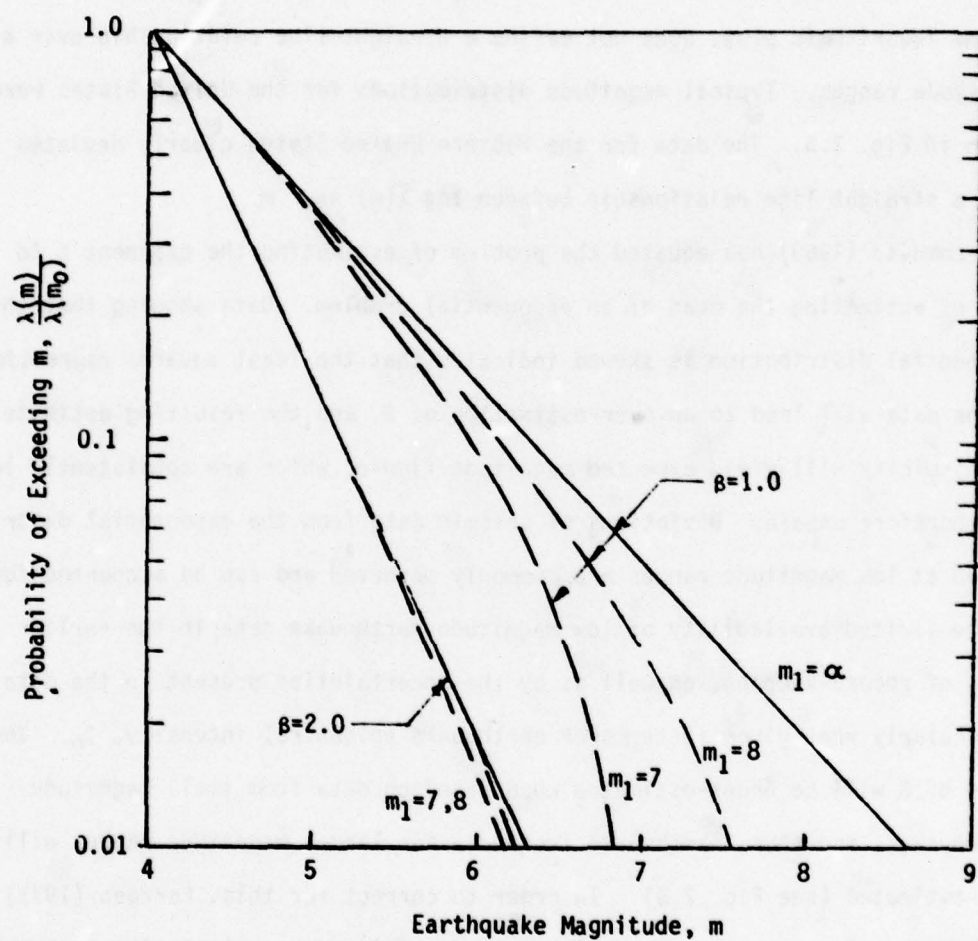


FIG. 2.8 Influence of  $\beta$  and  $m_1$  on Magnitude-Frequency Relationship

### B. "Nonlinear" Law

The estimation of the value of  $\beta$  using Eq. 2.2 and seismological data is not only difficult, but contains great uncertainties. Numerous examples are present in the literature in which magnitude-frequency data, when plotted on a semi-logarithmic plot, does not define a straight-line relationship over all magnitude ranges. Typical magnitude distributions for the United States were shown in Fig. 2.5. The data for the Western United States clearly deviates from a straight line relationship between  $\log \bar{\lambda}(m)$  and  $m$ .

Lomnitz (1969) has equated the problem of estimating the exponent  $\beta$  to that of estimating the mean of an exponential problem. Data showing that this exponential distribution is skewed indicates that the least squares regression on the data will lead to an over-estimation of  $\beta$ , and the resulting estimate of seismicity will yield expected magnitude figures which are consistently low, and therefore unsafe. Deviations of seismic data from the exponential distribution at low magnitude ranges are commonly observed and can be accounted for by the limited availability of low magnitude earthquake data in the earlier years of record-keeping, as well as by the uncertainties present in the data, particularly when given in terms of earthquake epicentral intensity,  $I_0$ . The value of  $\beta$  will be under-estimated when based on data from small magnitude earthquakes, and thus, earthquake frequency for larger magnitude ranges will be over-estimated (see Fig. 2.5). In order to correct for this, Ferraes (1973) recommends using a shorter time span and restricting the calculation to magnitude ranges where the data is reasonably complete and the recurrence relationship is approximately a straight line on the semi-log plot.

Rosenblueth (1969) states that the usefulness of the magnitude-frequency calculation is dependent on the nature of the structure being considered for

design. He explains that the frequency calculation of large magnitude earthquakes is most important in regard to structures with long economic life spans, while the frequency calculation of smaller magnitude earthquakes will affect the design of structures with very uncertain strengths. He maintains that a recurrence relationship which is obtained by a good curve fitting over a wide range of magnitudes may be adequate for some types of structures, but that its use may not be appropriate in the design of all types of structures.

In an attempt to resolve some of the difficulties encountered in estimating the value of  $\beta$ , bilinear frequency laws have been employed by some investigators. Fig. 2.9 shows a recurrence relationship used by Mortgart et al. (1977) in their seismic risk study of Costa Rica. Two regression lines were fitted to the data, and a cutoff point for magnitude was introduced based on geologic considerations.

Ferrares (1967b) introduced a polynomial to describe the logarithm of the magnitude-frequency relationship,  $\lambda(m)$ :

$$\log_{10} \lambda(m) = b_0 + b_1 m + b_2 m^2 + b_3 m^3 + \dots \quad (2.11)$$

In 1973, Merz and Cornell, using only the second order polynomial, introduced both lower and upper bound magnitudes into the magnitude-frequency law. The resulting quadratic law is as follows:

$$\log_{10} \lambda(m) = \begin{cases} b_0 & ; m < m_0 \\ b_0 + b_1 (m - m_0) + b_2 (m^2 - m_0^2) & ; m_0 < m < m_1 \\ 0 & ; m > m_1 \end{cases} \quad (2.12)$$

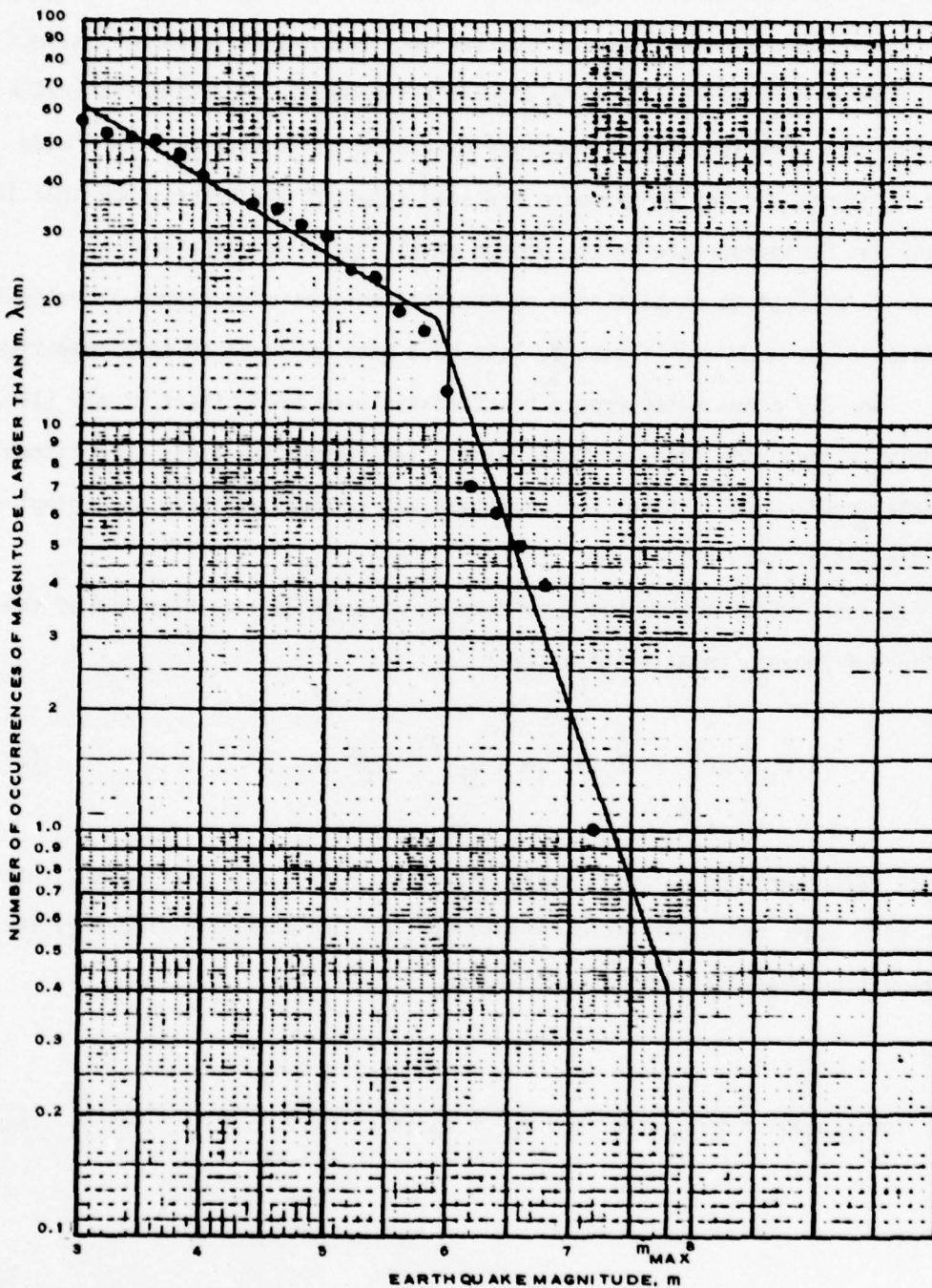


FIG. 2.9 Bilinear Magnitude-Frequency Relationship Used by Mortgart et al. (1977)

The cumulative function for  $m$  will then be:

$$F_M(m) = P[M \leq m|E] = K_{m_1}^* [1 - \exp \left\{ \beta_1(m - m_0) + \beta_2(m^2 - m_0^2) \right\}] \quad (2.13)$$

where

$$K_{m_1}^* = 1 - \exp \left\{ \beta(m_1 - m_0) + \beta_2(m_1^2 - m_0^2) \right\}$$

$$\beta_1 = b_1 \ln 10$$

$$\beta_2 = b_2 \ln 10$$

Studies have shown that this proposed quadratic magnitude-frequency function corresponds well to both regional and global earthquake data. Fig. 2.10 gives a typical magnitude-frequency function used by Merz and Cornell (1973). A comparison of the hazard results based on the quadratic relationship given in Figure 2.10 vs those based on the "linear" relationship is shown in Fig. 2.11. From this comparison it can be concluded that a seismic hazard analysis which is based on a "linear" recurrence relationship obtained by emphasizing the data at small intensities may result in an over-estimation of the hazard.

It must be emphasized that "bilinear" or quadratic formulations of magnitude-frequency laws should not be indiscriminately applied whenever the data indicates a deviation from linearity. Careful examination of the historic data and an evaluation of its validity and adequacy are essential prior to the application of more sophisticated relationships to account for such deviations.

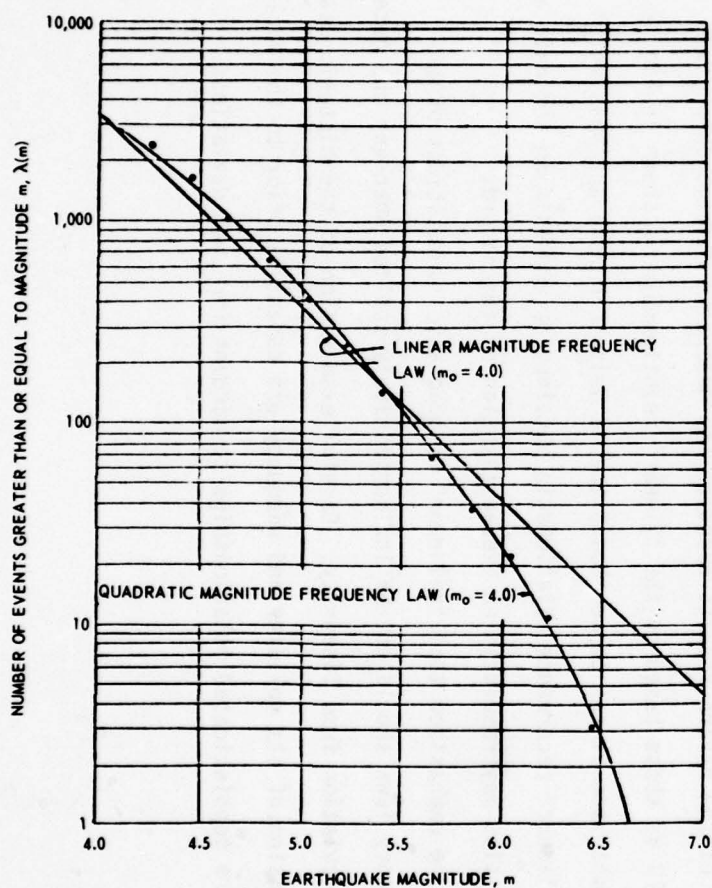


FIG. 2.10 Linear and Quadratic Magnitude-Frequency Relationships (After Merz and Cornell 1973)

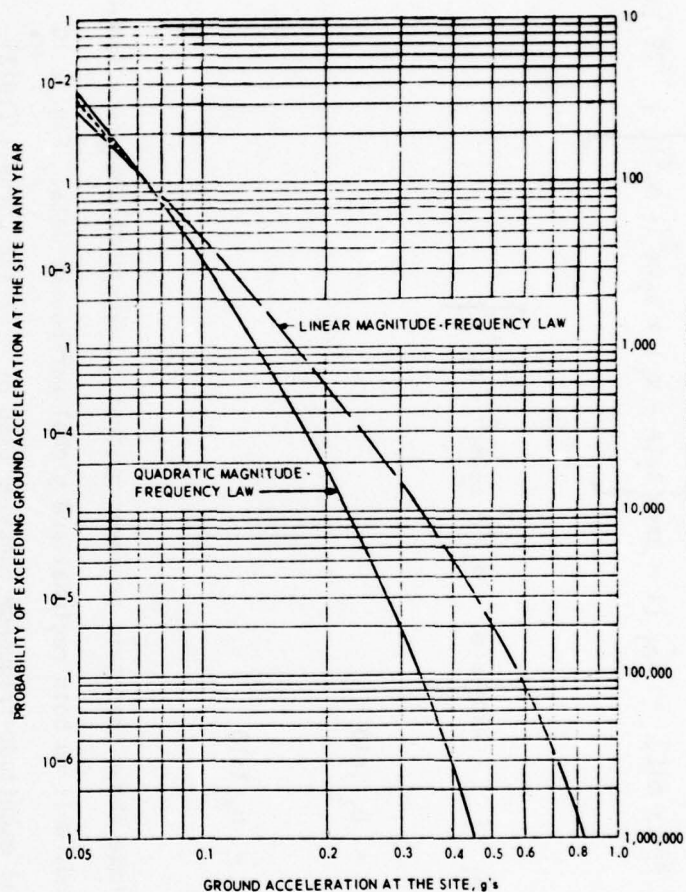


FIG. 2.11 Comparison of Hazard Results Using Linear and Quadratic Frequency Laws (After Merz and Cornell 1973)

All of the preceding methods of estimating the probability that an earthquake of a specified magnitude will occur in a given region and within a given period of time have involved two basic assumptions:

- 1) That the number of earthquakes occurring per unit time follows the poisson distribution; and
- 2) That the magnitude-frequency distribution is basically linear on semi-log paper.

An alternate procedure for estimating the magnitude-frequency distribution is based on Gumbel's theory of extreme values (55). Based on this theory, the cumulative distribution function of the largest earthquakes occurring annually in a specific region and having magnitudes less than or equal to  $m$  is given by:

$$F_M(m) = e^{-\alpha e^{-\beta m}}$$

or

(2.14)

$$\ln(-\ln F_M(m)) = \ln \alpha - \beta m$$

The parameters  $\alpha$  and  $\beta$  are estimated through the following process:

- 1) Select the largest annual earthquake magnitudes over a period of  $t$  years and arrange them in ascending order.
- 2) Assign probability values  $F_i(m)$  for each event using Eq. 2.15 and beginning with the smallest magnitude:

$$F_i(m) = \frac{i}{t+1} \quad i = 1, 2, \dots, t \quad (2.15)$$

- 3) Plot these probabilities vs  $m$  on Gumbel probability paper, and estimate  $\alpha$  and  $\beta$  based on the best fit straight line.

Using the theory of extreme values, studies of global data and data from southern California to determine the probability of occurrence of maximum earthquake magnitudes have shown that the calculated probabilities plotted fairly well as a straight line on Gumbel's probability paper (31, 34, 43, 108). Such an observation is not surprising and proves to be mathematically correct, assuming that earthquakes occur as independent events (poisson arrivals) and that the Gutenberg and Richter magnitude-frequency law is valid. It is, in fact, possible to relate the constants  $a$  and  $b$  in Eq. 2.3 to  $\alpha$  and  $\beta$  in Eq. 2.14, as follows: Given that the number of years covered by the record is  $t$ , then the average annual rate of occurrence for earthquakes with magnitudes equal to or exceeding  $m$  can be obtained from the Gutenberg and Richter relationship of Eq. 2.3.

By assuming poisson arrivals of events, the probability of at least one earthquake exceeding magnitude  $m$  occurring annually is given by:

$$P[M > m] = 1 - e^{-\lambda(m)}$$

thus,

$$P[M < m] = e^{-\lambda(m)} = e^{-10^a e^{-b \ln 10 m}} \quad (2.16)$$

A comparison of Eq. 2.16 with Eq. 2.14 yields the following relationship:

$$\begin{aligned} a &= \log(\alpha) \\ b &= \beta / \ln 10 \end{aligned} \quad (2.17)$$

Dick (1965) has made similar observations and has concluded that

"the statistical theory of extreme values gives formulae that might very well be expected from seismological evidence, principally the frequency-magnitude law and the fact that the time of occurrence of the largest earthquake in a six-monthly period tends to be randomly distributed in time."

Thus, the theory of extreme values provides an alternate method of computing the same parameters as computed in the Gutenberg and Richter relationship. Further, it allows for examination of the effects of after-shocks or for their elimination from the study, if necessary (35). Donovan (1978) states that, if the list of earthquake records is complete, the actual differences between the two approaches may be small. For example, Fig. 2.12 presents the results of the seismic recurrence studies by Donovan for a region in San Jose, California. This figure shows a straight line relationship on Gumbel paper established between the maximum annual magnitude,  $m$ , and the probability that that magnitude will not be exceeded,  $F(m)$ . The results shown in Fig. 2.12 were converted by Eq. 2.17 and replotted in Fig. 2.13 in order to compare the recurrence relationship obtained using the theory of extreme values to the Gutenberg and Richter relationship. The third line of the figure is obtained by using the maximum number of events occurring during a five-year period. The results are quite similar.

#### Upper Bound Magnitude

The truncated form of the recurrence relationship discussed earlier applies an upper bound for earthquake magnitude. Often referred to as the "maximum credible earthquake", this upper bound magnitude is defined as the largest earthquake likely to occur along a seismically active fault in a given region. The return period associated with such an event is generally very large as compared to the

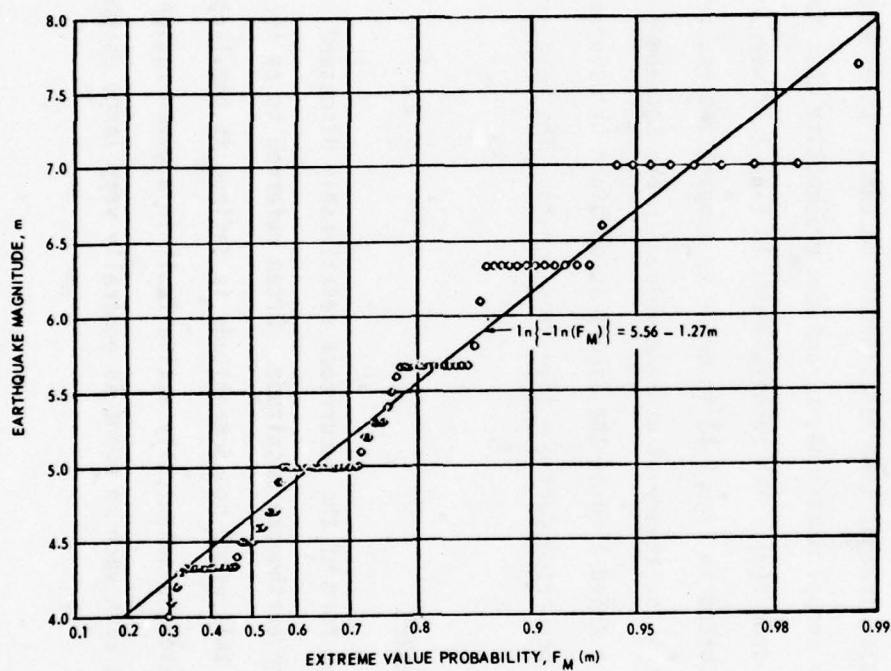


FIG. 2.12 Extreme Value Derivation of Seismic Recurrence Information (After Donovan 1978)

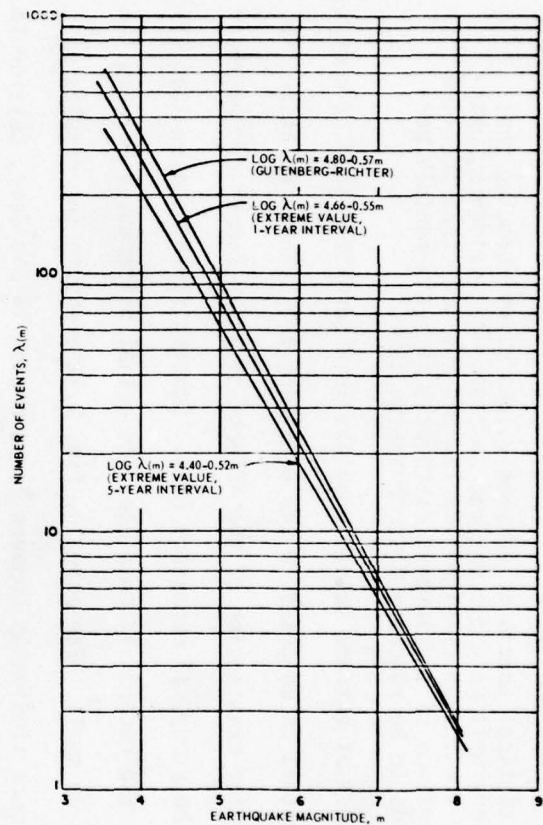


FIG. 2.13 Comparison of Derived Recurrence Relationships for San Jose, California, Using Gutenberg and Richter and Extreme Value Techniques (After Donovan 1978)

life span of a typical structure.

The existence of a finite upper bound has been widely accepted, and in many countries the design level earthquake shaking for such structures as nuclear reactors and large dams is based on the maximum credible earthquake intensity (21, 44, 94).

The estimation of  $m_1$  for a given region or for a potential earthquake source should be based on available geologic and seismological data. Housner (1969) states that low seismicity of a particular region does not discount the possibility of that region experiencing a large magnitude earthquake, and cites examples in the United States where large earthquakes occurred in regions of relatively low seismicity - specifically New Madrid, Missouri, in 1811-12; and Charleston, South Carolina, in 1886. Further Chinnery and Rogers (1973), in their statistical study of earthquakes in southern New England, argue that existing records for the region are too recent to assume that large magnitude events have not occurred in the past, and they consider the possibility that large earthquakes may occur in the region at infrequent intervals.

It is clear that the determination of  $m_1$  cannot be based on historic data exclusively, and that geologic data and professional judgment are invaluable in such an estimation. However, the estimated value of  $m_1$  will always contain a certain degree of uncertainty. Esteva and Villaverde (1973) studied the influence of  $m_1$  upon the computed annual probability of exceeding the peak acceleration and have found that errors in the estimated value of  $m_1$  had little influence relative to high probabilities but showed significant influence at low probabilities. Yegian and Whitman (1978) have concluded that the influence of  $m_1$  upon the computed probability of liquefaction is greater for smaller values of  $\beta$ . Fig. 2.8 shows recurrence relationships for various estimations of  $\beta$  and  $m_1$ . It is clear

that the influence of  $m_1$  is most significant in cases of a small  $\beta$  value and when the design level probability is low. The procedure for estimating  $m_1$  suggested by Housner (based on seismological data) will be outlined and discussed herein. Other procedures based on geologic data will be presented subsequently.

#### Housner's Method

Housner (1969) suggests two different approaches to the estimation of the upper bound magnitude  $m_1$ . The first method is based on a seismic zoning map and involves the assumption that the frequency distribution curves for regions of varying seismicity have different slopes. Table 2.3 presents the maximum earthquake magnitudes corresponding to each zone. Housner states that "these values are more or less arbitrary and are used as a matter of expediency."

The second method involves the assumption that the probability distribution for  $m$ , ranging from zero to infinity, is the same for all regions. This assumption allows the maximum credible earthquake magnitudes for different regions to be related through the use of Eq. 2.18:

$$m_2 = \frac{\beta_2}{\beta_1} m_1 - \beta_2 \ln\left(\frac{\lambda_1(m_0)}{\lambda_2(m_0)}\right) \quad (2.18)$$

where  $m_1$  represents the upper bound magnitude;  $\beta$  represents the magnitude-frequency parameter defined in Eq. 2.2;  $\lambda$  is the average seismicity expressed in terms of the number of earthquakes occurring per unit time; and the numbers 1 and 2 refer to the two regions under consideration. Thus, given that the seismicity for one region is reliably determined, then the upper bound magnitude for another can be predicted by assigning the proper  $\beta$  and  $\lambda$  values for the two re-

TABLE 2.3

ESTIMATED MAXIMUM ZONAL ACCELERATION AND MAGNITUDE  
(After Housner 1969)

	<u>MAXIMUM ACCELERATION</u>	<u>MAGNITUDE</u>
Zone 3 (near a great fault)	50% g	8.5
Zone 3 (not near a great fault)	33% g	7.0
Zone 2	16% g	5.75
Zone 1	8% g	4.75
Zone 0	4% g	4.25

gions. Table 2.4 presents computed upper bound magnitudes using California as the known region, where  $m_1 = 8.5$  and  $\beta_1 = 0.48$ . Based on results shown in Table 2.4, one can conclude that the upper bound magnitude for a region with  $\beta = 0.48$  and with an average number of earthquakes 10 times smaller per unit area and unit time will be approximately 7.4.

In general, if only statistical data is used, the maximum credible earthquake magnitude for a region can be estimated based on curves of intensity and return period and the choice of acceptable failure probability for a given time interval. Using a different approach,  $m_1$  can be estimated based on the judgmental assessment of a geologist. Ideally, both sources of information should be rationally combined (41), a procedure to be discussed in a later section of this Report.

Previous discussion has been limited to the study of local seismicity and to the estimation of the likelihood of occurrence of earthquakes having different magnitudes or intensities. A complete seismic hazard analysis for a site should further provide an estimation of the probability that the chosen earthquake intensity parameter will exceed a specified value at the site. In order to accomplish this, an attenuation law is applied, essentially relating earthquake magnitude or intensity (MMI) and the distance between the site and the epicenter or hypocenter to an appropriate parameter which describes the intensity of the earthquake ground shaking at the site. The use of an attenuation law for estimating earthquake shaking on firm ground constitutes a study of the regional seismicity. A discussion will follow regarding the use of attenuation laws for firm ground, and a later discussion will deal with site effects.

TABLE 2.4

UPPER BOUND MAGNITUDE AS DETERMINED BY SEISMICITY RATIO  
(From Housner 1969)

$\lambda_1(m_0)/\lambda_2(m_0)$	$m_1$
1	8.5 (California)
2	8.15
4	7.8
5	7.7
10	7.4
20	7.1
30	6.9
100	6.3

### Attenuation Laws

Earthquake engineering utilizes various parameters in order to describe the seismic hazard for a particular site. In seismic hazard analysis, the two most widely used parameters have been peak ground acceleration and site intensity, generally expressed in terms of Modified Mercalli Intensity (MMI). Neither of these provides an adequate description of the severity of earthquake activity at a given site for most structural and geotechnical design purposes. Recent studies have attempted to consider other parameters in seismic hazard analysis, including peak ground velocity, displacement and spectral velocity.

Choice of the proper attenuation law is a crucial step in the seismic hazard analysis. Numerous investigations have been conducted regarding the attenuation of earthquake motions with distance, using seismological data. Table 2.5, reproduced from McGuire (1976), summarizes most of the published attenuation laws. While a detailed explanation of these laws and their limitations is beyond the scope of this Report, the following brief discussion will point out some of the factors influencing the attenuation laws used in seismic hazard studies.

#### A. Acceleration attenuation law

The most commonly used attenuation law is one which relates peak acceleration,  $a$ , to earthquake magnitude,  $m$ , and epicentral or hypocentral distance,  $R$ . The form of this function is given by Eq. 2.19:

$$a = b_1 e^{b_2 m} R^{-b_3} \quad (2.19)$$

where  $b_1$ ,  $b_2$  and  $b_3$  represent empirical constants. Studies have shown that appli-

TABLE 2.5  
PUBLISHED ATTENUATION FUNCTIONS  
(From McGuire 1976)

Reference*	Data Source	Distance Parameter	Dependent Variable	Equation	Standard Deviation
Blume (1966)	Southern California	Epical distance $\Delta$ (mi)	Peak ground acceleration $a_g$ (g)	$a_g = \frac{a_0}{1+(\Delta/h)^2}$ where $a_0$ is epicentral acceleration, $h$ is focal depth	Not reported
Brazee (1972)	United States east of long. 106° W	Epical distance $\Delta$ (mi)	Distance over which a Modified Mercalli Intensity is felt	$\log \Delta = a_I + b_I I_e$ where $I_e$ is epicentral intensity, $a_I$ and $b_I$ are tabulated	Not reported
Cloud and Perez (1971)	North and South America	Epical distance or distance to fault $\Delta$ (mi)	Maximum single component ground acceleration $a_g$ (g)	$a_g = 3.0 - 2 \log (\Delta + 43)$ $a_g = 3.5 - 2 \log (\Delta + 80)$	Not reported
Cornell and Merz (1971)	Northeastern United States, rock sites	Epical distance $\Delta$ (mi)	Modified Mercalli Intensity	$I = 2.6 + I_e - 1.3 \ln \Delta$ $\Delta \geq 10$ mi	$\sigma_I = 0.2$
	Northwestern United States, all sites	-----do-----	-----do-----	$I = 3.1 + I_e - 1.3 \ln \Delta$ $\Delta \geq 10$ mi where $I_e$ is epicentral intensity	$\sigma_I = 0.5$

(Continued)

\* These references are McGuire's (1976).

TABLE 2.5 (Continued)

Reference	Data Source	Distance Parameter	Dependent Variable	Equation	Standard Deviation
Donovan (1974)	San Fernando, rock sites	Distance to energy center R (km)	Peak ground acceleration $a_g$ (gals)	$a_g = 12.783 \times 10^6 (R+25)^{-2.77}$	Not reported
	San Fernando, soil sites	-----do-----	-----do-----	$a_g = 2.054 \times 10^5 (R+25)^{-1.83}$	Not reported
	San Fernando, all sites	-----do-----	-----do-----	$a_g = 5.165 \times 10^5 (R+25)^{-2.04}$	$\sigma_{\ln a_g} = 0.481$
	-----do-----	-----do-----	-----do-----	$a_g = 1.84 \times 10^4 R^{-1.42}$	Not reported
	Western North America, Japan Papua-New Guinea	-----do-----	-----do-----	$a_g = 1080 e^{0.5M} (R+25)^{-1.32}$	$\sigma_{\ln a_g} = 0.707$
Donovan (1973)	Worldwide	Hypocentral distance, epicentral distance, or distance to fault R (km)	Peak ground acceleration $a_g$ (gals)	$a_g = 1320 e^{0.58M} (R+25)^{-1.52}$	$\sigma_{\ln a_g} = 0.84$
Duke and others (1972)	San Fernando, all sites	Distance to energy center R (km)	Peak ground acceleration $a_g$ (gals)	$a_g = \frac{6.69}{R} e^{-0.0097R}$	$\sigma_{a_g} = 0.052 \text{ g}$
	-----do-----	-----do-----	Spectral acceleration $s_g$ (g)	$s_g = \frac{5.34}{R} e^{-0.0068R}$	$\sigma_{s_g} = 0.053 \text{ g}$
Esteve (1970)	See reference	Hypocentral distance R (km)	Peak ground acceleration $a_g$ (gals)	$a_g = 1230 e^{0.8M} (R+25)^{-2}$	$\sigma_{\ln a_g} = 1.2$
	-----do-----	-----do-----	Peak ground velocity $v_g$ (cm/sec)	$v_g = 15 e^M (R+0.17 e^{0.59M})^{-1.7}$	$\sigma_{\ln v_g} = 0.84$

(Continued)

(Sheet 2 of 6)

TABLE 2.5 (Continued)

Reference	Data Source	Distance Parameter	Dependent Variable	Equation	Standard Deviation
Esteve and Rosenblueth (1964)	West Coast of United States	Hypocentral distance R (km)	Peak ground acceleration $a_g$ (gals)	$a_g = 2000 e^{0.8M} R^{-2}$	See reference
	-----do-----	-----do-----	Peak ground velocity $v_g$ (cm/sec)	$v_g = 20 e^M R^{-1.7}$	See reference
Esteve and Villaverde (1974)	Western United States	Hypocentral distance R (km)	Peak ground acceleration $a_g$ (gals)	$a_g = 5600 e^{0.8M} (R+40)^{-2}$	$\sigma_{1n} a_g = 0.64$
	-----do-----	-----do-----	Peak ground velocity $v_g$ (cm/sec)	$v_g = 32 e^M (R+25)^{-1.7}$	$\sigma_{1n} v_g = 0.74$
	-----do-----	-----do-----	Maximum average spectral acceleration $\bar{\lambda}$ (gals)	$\bar{\lambda} = 69600 e^{0.8M} (R+70)^{-2}$	$\sigma_{1n} \bar{\lambda} = 0.75$
	-----do-----	-----do-----	Maximum average spectral velocity $\bar{V}$ (cm/sec)	$\bar{V} = 250 e^M (R+60)^{-1.7}$	$\sigma_{1n} \bar{V} = 0.64$
Gupta and Nuttli (1975)	Central United States	Epicentral distance to isoseismal $\Delta$ (km)	Modified Mercalli Intensity	$I = I_e + 3.7 - 0.0011 \Delta - 2.7 \log \Delta$ where $I_e$ is epicentral intensity	Not reported
Gutenberg and Richter (1956)	California	Epicentral distance	Peak ground acceleration	Graphical	Not reported
Housner (1965)	Western United States, Central and South America	Distance to fault	Peak ground acceleration	Graphical	Not reported

(Continued)

(Sheet 3 of 6)

TABLE 2.5 (Continued)

Reference	Data Source	Distance Parameter	Dependent Variable	Equation	Standard Deviation
Howell and Schultz (1975)	California coast	Epicentral distance to isoseismal $\Delta$ (km)	Modified Mercalli Intensity	$I = I_e + 0.874 - 0.422 \ln \Delta - 0.0186 \Delta$	$\sigma_I = 0.64$
	-----do-----	-----do-----	Logarithm of Modified Mercalli Intensity	$\ln I = \ln I_e + 0.16 - 0.0763 \ln \Delta - 0.0023 \Delta$	$\sigma_I = 0.44$
	Rocky Mountains, Washington, Oregon	Epicentral distance to isoseismal $\Delta$ (km)	Modified Mercalli Intensity	$I = I_e + 1.802 - 0.628 \ln \Delta - 0.009 \Delta$	$\sigma_I = 0.61$
	-----do-----	-----do-----	Logarithm of Modified Mercalli Intensity	$\ln I = \ln I_e + 0.322 - 0.1098 \ln \Delta - 0.0012 \Delta$	$\sigma_I = 0.47$
	Central and Eastern United States, Canada	Epicentral distance to isoseismal $\Delta$ (km)	Modified Mercalli Intensity	$I = I_e + 3.278 - 0.989 \ln \Delta - 0.0029 \Delta$	$\sigma_I = 0.64$
	-----do-----	-----do-----	Logarithm of Modified Mercalli Intensity (Other forms of equations examined and reported also)	$\ln I = \ln I_e + 0.480 - 0.139 \ln \Delta - 0.00075 \Delta$ where $I_e$ is epicentral intensity	$\sigma_I = 0.43$
McGuire (1974)	West Coast of United States	Hypocentral distance R (km)	Peak ground acceleration $a_g$ (gals)	$a_g = 472 \times 10^{0.28M} (R+25)^{-1.3}$	$\sigma_{\log a_g} = 0.222$
	-----do-----	-----do-----	Peak ground velocity $v_g$ (cm/sec)	$v_g = 5.64 \times 10^{0.40M} (R+25)^{-1.2}$	$\sigma_{\log v_g} = 0.273$
	-----do-----	-----do-----	Peak ground displacement $d_g$ (cm)	$d_g = 0.393 \times 10^{0.43M} (R+25)^{-0.88}$	$\sigma_{\log d_g} = 0.330$
	-----do-----	-----do-----	Spectral velocity ( $T=1$ sec; $\beta=0.02$ ) $s$ (in/sec)	$s = 0.428 \times 10^{0.38M} (R+25)^{-0.59}$	$\sigma_{\log s} = 0.274$
			(Spectral attenuation equations given for other periods and dampings also)		

(Continued)

(Sheet 4 of 6)

TABLE 2.5 (Continued)

Reference	Data Source	Distance Parameter	Dependent Variable	Equation	Standard Deviation
Mickey (1971)	See reference	Hypocentral distance R (km)	Peak particle acceleration a (g)	$a = 3.04 \times 10^{0.74m-4} R^{-1.4}$	See reference
	-----do-----	-----do-----	Peak particle velocity v (cm/sec)	$v = 4.06 \times 10^{0.88m-3} R^{-1.5}$	-----do-----
	-----do-----	-----do-----	Peak particle displacement d (cm)	$d = 5.66 \times 10^{1.1m-5} R^{-1.2}$ where m is body-wave magnitude	-----do-----
Milne and Davenport (1969)	Western United States, Central America, Chile	Epicentral distance $\Delta$ (km)	Peak ground acceleration $a_g$ (g)	$a_g = \frac{0.69 e^{1.64M}}{1.1 e^{1.1M} + \Delta^2}$	Not reported
	Eastern Canada	-----do-----	Modified Mercalli Intensity	$I = I_7 - 9.66 - 0.0037 \Delta + 1.38 M + 0.00528 \Delta M$ where $I_7$ is site intensity of M=7 event at distance $\Delta$	$\sigma_I = 0.53$
Neumann (1954)	West Coast of United States	Epicentral distance $\Delta$ (mi)	Modified Mercalli Intensity	$I = I_e + 0.15 - 3.17 \log R$ $R \geq 1.12$ miles	Not reported
Nuttli (1973a)	Central United States	Epicentral distance	Vertical particle acceleration, velocity, and displacement at 3 frequencies for Rayleigh waves	Graphical and tabular for various earthquakes	Not reported
Nuttli (1973b)	Central United States	Epicentral distance	Sustained ground acceleration, velocity, and displacement at 3 frequencies for surface waves	Graphical and tabular	Not reported

(Continued)

(Sheet 5 of 6)

TABLE 2.5 (Concluded)

<u>Reference</u>	<u>Data Source</u>	<u>Distance Parameter</u>	<u>Dependent Variable</u>	<u>Equation</u>	<u>Standard Deviation</u>
Orphal and Laboud (1974)	California	Hypocentral distance R (km)	Peak ground acceleration $a_g$ (g)	$a_g = 0.066 \times 10^{0.4M_R - 1.39}$	See reference
	California and nuclear explosions	-----do-----	Peak ground velocity $v_g$ (cm/sec)	$v_g = 0.726 \times 10^{0.52M_R - 1.34}$	-----do-----
	-----do-----	-----do-----	Peak ground displacement $d_g$ (cm)	$d_g = 0.0471 \times 10^{0.57M_R - 1.18}$	-----do-----
Rasmussen and others (1974)	Puget Sound, Washington	Epicentral distance	Modified Mercalli Intensity	Graphical: data and limits given for each earthquake	Not calculated; data shown
Schnabel and Seed (1973)	Western United States	Distance to fault	Peak ground acceleration	Graphical	Not reported
Stapp (1971)	Puget Sound, Washington	Hypocentral distance to isoseismal R (km)	Modified Mercalli Intensity	$I = I_e - 2.017 \log(R/h) - 0.008(R/h)$ where $I_e$ is epicentral intensity, h is focal depth	Not reported

cation of this equation in cases of small distances results in ground acceleration values which are significantly larger than the observed values. For this reason, the term "R" in Eq. 2.19 has been replaced with "R + 25".

Fig. 2.14 shows typical acceleration attenuation relationships for eastern and western regions of the United States. These curves, which represent maximum horizontal acceleration in rock, were applied in the development of a new earthquake hazard map for the United States by Algermissen and Perkins (1976). The dashed curves, together with the solid lines at close distances, correspond to curves recommended by Schnabel and Seed (1973). The solid curves given for eastern regions were generated through the introduction of various modifications to the curves suggested by Schnabel and Seed.

Problems of uncertainties in acceleration attenuation laws have been studied by various investigators. Merz and Cornell (1973) have suggested that an error term be included in the attenuation law, as follows:

$$a = b_1 e^{b_2 m} R^{-b_3} \cdot \epsilon \quad (2.20)$$

where  $\epsilon$  represents a random error term lognormally distributed with median 1 and standard deviation of  $\sigma_{1\epsilon}$ . Donovan (1973) has confirmed the lognormal distribution of the data points around the mean. Values of  $\sigma_{1\epsilon}$  for different attenuation laws are listed in Table 2.5.

The parameters  $b_1$ ,  $b_2$  and  $b_3$  have been treated as constants in most attenuation laws. Donovan and Bornstein (1978) have argued that earthquake magnitude and distance are not independently related to acceleration, and have conducted a study in which they have treated  $b$  as a parameter dependent on distance. Results based on data for rock and hard soil indicated that this parameter is indeed de-

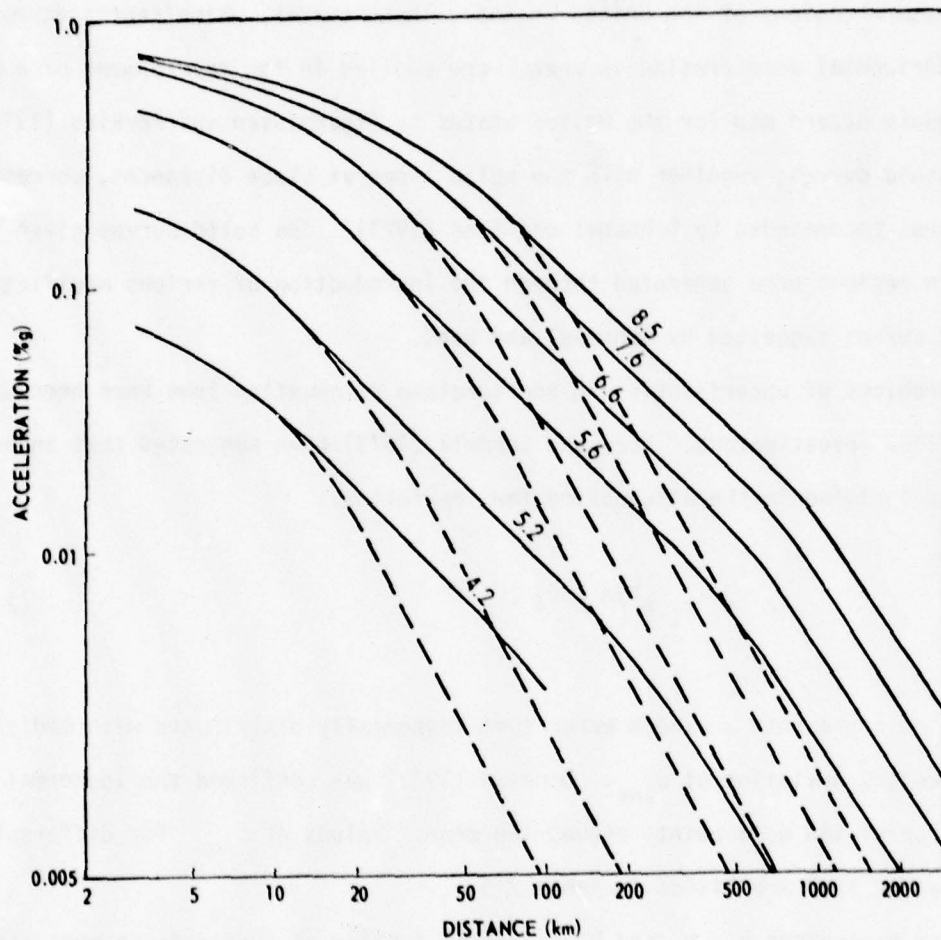


FIG. 2.14 Acceleration Attenuation Curves. The solid lines are curves used for the eastern region. The dashed lines together with solid lines at close distances are the attenuation curves used for the western region (From Algermissen and Perkins 1976)

pendent on distance. The following are the values obtained for  $b$  from this study:

$$b_1 = 2,154,000 (R)^{-2.10}$$

$$b_2 = 0.046 + 0.445 \log (R) \quad (2.21)$$

$$b_3 = 2.515 - 0.486 \log (R)$$

where  $R$  represents the distance to the energy center or the causative fault in kilometres.

Fig. 2.15 gives the attenuation relationship developed from these values. The standard deviation was found to decrease as acceleration increased. This variation is shown in Fig. 2.16.

#### B. Intensity Attenuation Law

As stated earlier, the Modified Mercalli Intensity (MMI) is the most commonly used term for the expression of site intensity. A description of this scale is given in Fig. 2.17. A seismic hazard analysis is performed in terms of intensity when the seismological data for the region is given in terms of intensity, in which case an intensity attenuation law is required (26). Such a situation applies, for example, to New England, where most available seismological data is based on subjective interpretation of historic records of earthquake occurrence and damage. A second situation in which results of the hazard analysis should be stated in terms of intensity exists when the risk analysis (which is based on the results of the hazard analysis) employs earthquake intensities in relation to damages. The seismic design decision analysis developed by Whitman et al. (1975) employs a damage probability matrix which summarizes the observed behavior of

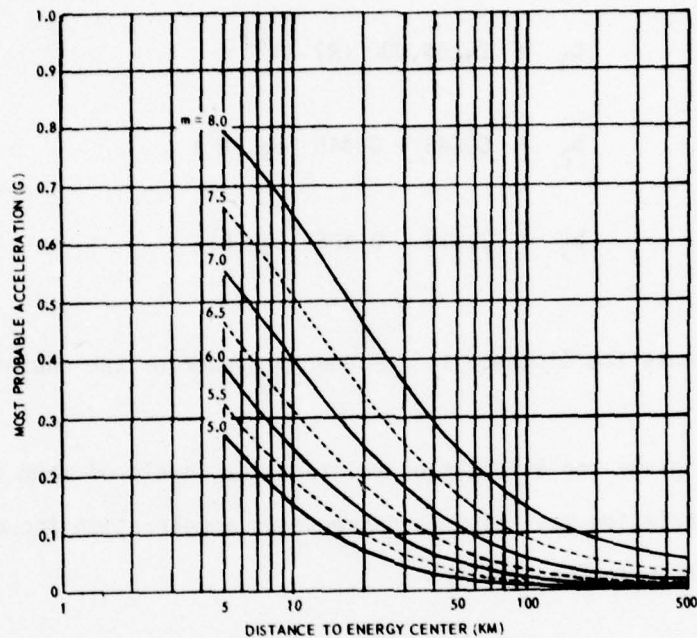


FIG. 2.15 Attenuation Relationship for Mean Risk Acceleration at Rock and Hard Soil Site (After Donovan and Bornstein 1978)

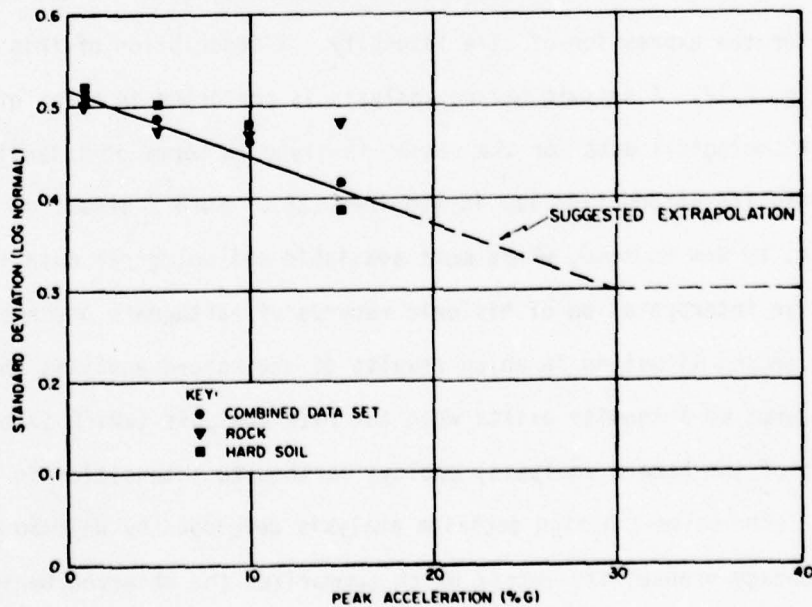


FIG. 2.16 Variation of Attenuation Uncertainty with Increased Acceleration Values (From Donovan and Bornstein 1978)

ABRIDGED  
MODIFIED MERCALLI INTENSITY SCALE

I	Not felt except by a very few under especially favourable circumstances.	
II	Felt only by a few persons at rest, especially on upper floors of buildings. Delicately suspended objects may swing.	
III	Felt quite noticeably indoors, especially on upper floors of buildings, but many people do not recognize it as an earthquake. Standing motor cars	may rock slightly. Vibration like passing of truck. Duration estimated.
IV	During the day felt indoors by many, outdoors by few. At night some awakened. Dishes, windows, doors disturbed; walls make creaking sound. Sen-	sation like heavy truck striking building. Stand- ing motor cars rocked noticeably.
V	Felt by nearly everyone; many awakened. Some dishes, windows, etc., broken; a few instances of cracked plaster; unstable objects overturned.	Disturbance of trees, poles and other tall objects sometimes noticed. Pendulum clocks may stop.
VI	Felt by all; many frightened and run outdoors. Some heavy furniture moved; a few instances of fallen plaster or damaged chimneys. Damage slight.	
VII	Everybody runs outdoors. Damage negligible in buildings of good design and construction; slight to moderate in well-built ordinary structures;	considerable in poorly built or badly designed structures; some chimneys broken. Noticed by persons driving motor cars.
VIII	Damage slight in specially designed structures; considerable in ordinary substantial buildings with partial collapse; great in poorly built structures. Panel walls thrown out of frame structures.	Fall of chimneys, factory stacks, columns, monu- ments, walls. Heavy furniture overturned. Sand and mud ejected in small amounts. Changes in well water. Persons driving motor cars disturbed.
IX	Damage considerable in specially designed structures; well designed frame structures thrown out of plumb; great in substantial buildings, with	partial collapse. Buildings shifted off foundations. Ground cracked conspicuously. Underground pipes broken.
X	Some well-built wooden structures destroyed; most masonry and frame structures destroyed with foundations; ground badly cracked. Rails	bent. Landslides considerable from river banks and steep slopes. Shifted sand and mud. Water splashed (sprayed) over banks.

FIG. 2.17 Modified Mercalli Intensity Scale

structures during earthquakes as a function of earthquake intensity. Thus, the risk studies described by Whitman et al. use seismic hazard results given in terms of MMI.

The general form of the attenuation relation can be expressed by:

$$I_{\text{site}} = C_1 + C_2 (I_{\text{epicenter or m}}) - C_3 \ln \Delta \quad (2.22)$$

where  $\Delta$  represents the hypocentral, epicentral or isoseismal distance; and  $C_1$ ,  $C_2$  and  $C_3$  are constants dependent on the geological features of the area. Intensity-magnitude-distance relationships for the Eastern and Western United States were presented by Chang and Krinitzsky (1977). It has been shown that intensity attenuates at a much slower rate in the eastern portion of the country than in the western regions. McGuire (1977c) has proposed relationships relating site intensity to peak ground acceleration, velocity and displacement. Tables 2.6 and 2.7 give these relationships for soft and medium sites.

The form of the attenuation law shown in Eq. 2.22 implies that the predicted isoseismals or lines of equal site intensities are circular. Hence, the orientation of a potential earthquake source relative to the site under study is immaterial, and only its distance from the site is of relevance. However, in many cases, true isoseismals on firm ground are roughly elliptical in shape, and the orientation of the corresponding axes are often correlated to the local or regional geologic trends (44). Esteva (1975) explains that, in some regions such as the eastern United States and Mexico, "The isoseismals seem to elongate systematically in a direction that is a function of the epicentral coordinates." In such cases, the assessment of the seismic hazard at a site should consider

TABLE 2.6

REGRESSION COEFFICIENTS FOR SOFT SITES  
(From McGuire 1977c)

$$\ln p = C_1 + C_2 m + C_3 \ln \Delta + C_4 I_s$$

$\ln p$	$C_1$	$C_2$	$C_3$	$C_4$	$\sigma_{\ln p}$
$\ln a_g$	.271	x	x	.601	.781
(peak ground acceleration)	2.01	x	-.313	.506	.723
cm/sec <sup>2</sup>	1.81	.904	-.901	x	.696
$\ln v_g$	-1.51	x	x	.543	.770
(peak ground velocity)	-1.11	x	-.072	.521	.771
cm/sec	-1.58	.997	-.710	x	.715
$\ln d_g$	-1.47	x	x	.415	.791
(peak ground displacement)	-2.35	x	.157	.463	.780
cm	-2.67	.863	-.398	x	.746

TABLE 2.7

REGRESSION COEFFICIENTS FOR MEDIUM SITES  
(From McGuire 1977c)

$$\ln p = C_1 + C_2 m + C_3 \ln \Delta + C_4 I_s$$

$\ln p$	$C_1$	$C_2$	$C_3$	$C_4$	$\sigma_{\ln p}$
$\ln a_g$	-.831	x	x	.851	.753
(peak ground acceleration)	1.45	x	-.359	.680	.703
cm/sec <sup>2</sup>	1.47	1.01	-.884	x	.619
$\ln v_g$	-4.02	x	x	.952	.751
(peak ground velocity)	-3.61	x	-.064	.923	.758
cm/sec	-3.61	1.37	-.776	x	.605
$\ln d_g$	-4.68	x	x	.899	.664
(peak ground displacement)	-5.75	x	.168	.979	.658
cm	-4.81	1.25	-.509	x	.581

the coordinates of the site in relation to the sources.

Uncertainties in intensity attenuation laws are caused by errors in data (which is subjectively recorded), as well as by possible errors in the evaluation of the mean curve. Donovan (1978) discusses the bias involved in the mean intensity attenuation curve based on isoseismal maps of a region. A comparison between the mean attenuation line based on recorded intensities for individual sites during an event in Washington State and the mean attenuation line obtained from the isoseismals for the same earthquake showed a difference between the curves of 0.73 units of MMI scale, representing only the probable error in the mean and not considering the scatter of data about the mean. Cornell and Merz (1975) have used a standard deviation of  $\sigma_I = 0.5$  MMI for the scatter in the mean, considering all site conditions. Table 2.5 gives a list of standard deviation values for various attenuation laws.

#### C. Other Attenuation Laws Used

The use of peak acceleration to describe the seismic hazard at a site without due consideration to the frequency characteristic of the design motions is sometimes inadequate for design purposes. Seismic design criteria usually employ a level of design ground acceleration in order to scale a set of standardized response spectra. This practice may be adequate for the design of short period structures, but may require modification in order to accommodate the design requirements of intermediate and long period structures. Cornell and Vanmarcke (1975) have concluded that the response of long period structures such as offshore drilling platforms is poorly correlated to peak acceleration and suggest that peak ground displacement may be a more appropriate parameter for use in such designs. Therefore, a peak displacement attenuation law may be more useful in seismic hazard studies concerned with long period structures. Cornell and Vanmarcke warn that the use of a peak displacement attenuation law results in

seismic hazard estimates which are more sensitive to the choice of the upper bound magnitude than estimates which are based on peak acceleration. This difference in sensitivity is attributed to the fact that peak ground displacement is dependent on magnitude to a greater extent than peak acceleration, as is indicated by the value of  $b_2$  in the attenuation law. Further, while seismic hazard probabilities based on an acceleration attenuation law are sensitive to close potential earthquake sources, probabilities based on a displacement attenuation law are more sensitive to distant sources (28).

Similar studies by McGuire (1977b) have shown that the scaling of standardized response spectra for design purposes using peak acceleration together with velocity leads to inconsistencies regarding the calculated risk for medium to long period structures. McGuire recommends the use of an attenuation law which relates spectral velocity,  $S_v$ , to earthquake magnitude,  $m$ , and hypocentral distance,  $R$ , as follows:

$$S_v(T) = a10^{bm}(R + 25)^{-c} \quad (2.23)$$

The coefficients  $a$ ,  $b$  and  $c$  are obtained for each period of a one-degree-of-freedom system and for a specific damping value by applying regression analysis on computed response spectra from recorded motions. Table 2.8 gives the values of the coefficients for various frequencies and for 2% damping. McGuire (1977a) has also provided an attenuation function relating Fourier amplitude spectra of horizontal ground acceleration to earthquake magnitude,  $m$ , and source to site distance,  $R$ , as follows:

TABLE 2.8

SUMMARY OF REGRESSION COEFFICIENTS FOR MAXIMUM PSEUDO-VELOCITY (IN INCHES/SEC)  
OF OSCILLATORS WITH 2% DAMPING  
(From McGuire 1977b)

$$S_v = a 10^{bM} (R + 25)^{-c}$$

$$\log S_v = a + bM - c \log (R + 25)$$

Frequency, cps	a	a'	b	-c
10	12.27	1.051	.225	-1.324
6.67	56.89	1.719	.185	-1.368
5	32.16	1.476	.232	-1.292
3.33	29.88	1.447	.295	-1.386
2.5	11.42	1.025	.321	-1.205
2	5.44	.708	.360	-1.146
1.67	2.48	.364	.440	-1.203
1.25	1.158	.0318	.406	- .913
1	.428	- .416	.382	- .587
0.67	.1085	-1.020	.428	- .434
0.5	.0918	-1.100	.456	- .519
0.33	.0900	-1.114	.473	- .615
0.25	.0552	-1.344	.539	- .742
0.2	.0735	-1.223	.565	- .931
0.167	.0995	-1.087	.465	- .694
0.125	.1825	- .802	.413	- .705

$$FS(T) = \exp (b_1 + b_2 m + b_4 Y_s) R^{b_3} \quad (2.24)$$

where  $FS(T)$  is the Fourier spectrum ordinate for period  $T$ ;  $Y_s$  is a soil amplification term and is equal to one for soil sites and zero for rock sites. The coefficients  $b_1$ ,  $b_2$ ,  $b_3$  and  $b_4$  and the standard deviation of  $\ln FS$  are given in Table 2.9 for different values of the period  $T$ .

Eqs. 2.23 and 2.24 can be applied in seismic hazard analysis to compute the annual probability of exceeding of  $S_v$  or  $FS$  vs the parameter itself.

Another parameter of significance in the determination of earthquake intensity or in the specification of design criteria is duration of earthquake motion. In geotechnical problems, peak ground acceleration and duration of motion are very often adopted to describe the intensity measure at a site. For example, it is known that the susceptibility of a site to liquefaction depends on the level of acceleration and the duration of the sustained motion.

Reported examples of seismic hazard analyses which have explicitly taken into consideration the effects of duration are very few. Douglas and Ryall (1975) have described a seismic hazard analysis procedure which allows for the determination of return period of acceleration as a function of magnitude. Since duration of earthquake motion can be correlated to magnitude, the design criteria corresponding to an acceptable risk level can be expressed in terms of peak ground acceleration and duration, as in Fig. 2.18. A procedure which is able to explicitly consider duration in seismic hazard analysis will require the use of an attenuation law for duration. The literature offers various definitions of and attenuation laws for duration (14, 19, 101). A state-of-the-art review of duration, spectral content and predominant period of strong motion earthquake records has been compiled by Chang and Krinitzsky (1977). The most

TABLE 2.9  
SUMMARY OF REGRESSION COEFFICIENTS FOR FOURIER AMPLITUDE SPECTRUM FOR 2% DAMPING  
(From McGuire 1977a)

T	b <sub>1</sub>	b <sub>2</sub>	b <sub>3</sub>	b <sub>4</sub>	$\sigma_{1nFS}$
0.04	-3.38	0.90	-1.20	-0.43	1.26
.05	-1.59	.75	-1.21	- .31	1.17
.06	-0.47	.73	-1.23	- .48	.95
.08	-0.47	.92	-1.33	- .43	1.07
.1	-0.02	1.04	-1.37	- .70	.98
.13	-0.62	.81	-1.07	- .49	.96
.17	1.06	.92	-1.23	- .42	.89
.2	- .35	1.01	-1.11	- .45	.92
.24	- .80	.99	-1.19	- .12	.86
.3	- .82	1.02	-1.22	.02	.86
.34	- .64	1.05	-1.16	- .02	.93
.4	1.04	.88	- .97	- .13	.90
.5	- .05	1.09	-1.11	.25	.91
.6	-1.03	1.16	- .96	.39	.82
.8	-1.03	1.04	- .75	.36	.92
1	-1.24	1.12	- .89	.68	.91
1.3	-1.84	1.08	- .69	.60	.91
1.7	-2.55	1.32	- .85	.31	.98
2	-3.40	1.44	- .89	.53	1.00
2.4	-3.08	1.23	- .65	.38	1.05
3	-2.54	1.00	- .46	.35	1.03
3.4	-2.57	1.08	- .59	.31	1.11
4	-3.93	1.28	- .59	.30	1.00
5	-3.36	1.20	- .61	.32	1.11

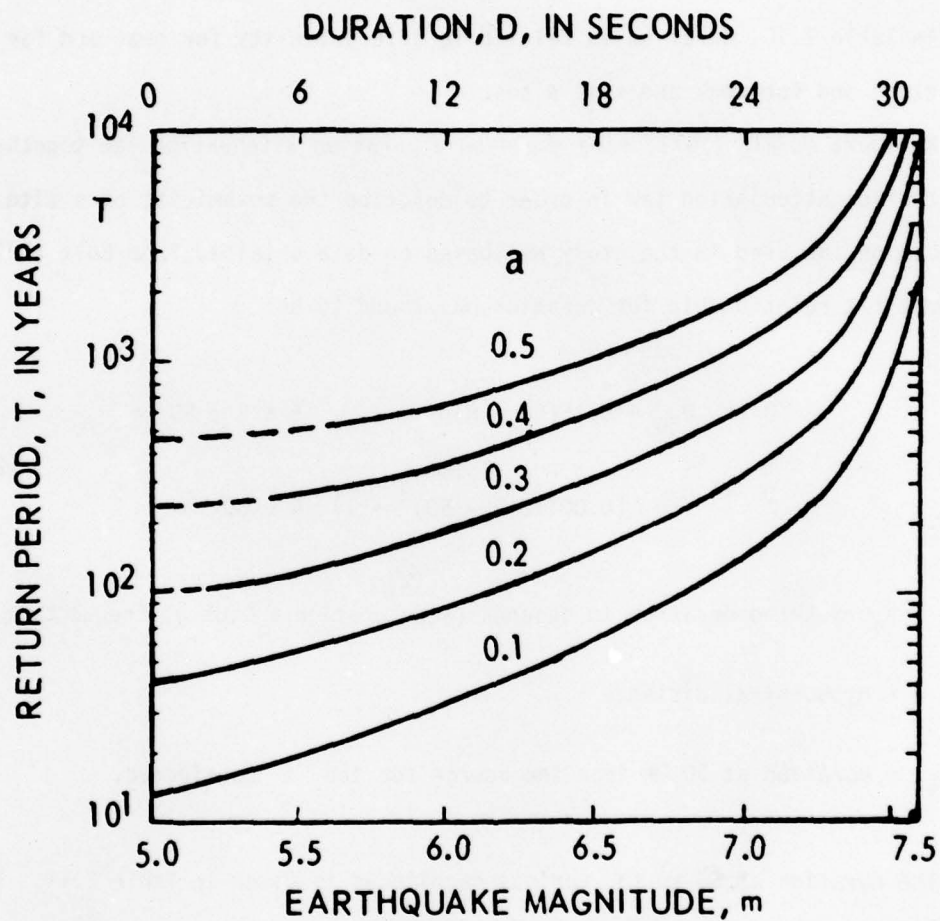


FIG. 2.18 Return Period  $T$ , in years for Selected Values of Rock Acceleration  $a$  (in g's), as a Function of Magnitude  $m$  and Duration  $D$  (in seconds) of Strong Shaking (After Douglas and Ryall 1975)

common definition of duration is the "bracketed" duration defined as the time interval between the first and last peaks of acceleration equal to or greater than 0.05 g for the strong earthquake record. Typical duration attenuation laws for soil and rock sites were presented by Chang and Krinitzsky (1977).

In Table 2.10, duration is related to site intensity for near and far field conditions and for rock and soil sites.

Mortgart et al. (1977) have employed a duration attenuation law together with an acceleration attenuation law in order to describe the seismicity of a site. The attenuation law used in the study was based on data obtained from Bolt (1973). The best fit relationship for duration was found to be:

$$D = D_{50} + 0.15(50 - R) \quad 5 \leq R \leq 50 \text{ km}$$

and

$$D = D_{50} / (0.00112(R - 50)^2 + 1) \quad R \geq 50 \text{ km} \quad (2.25)$$

where D = bracketed duration in seconds (acceleration  $\geq$  0.05 g; frequency  $\geq$  2 Hz)

R = hypocentral distance

$D_{50}$  = duration at 50 km from the source for the m considered.

The duration at 50 km for various magnitudes is given in Table 2.11. These values were used in Eq. 2.25 to define a complete duration attenuation law in terms of m and R. Variance studies indicate that the coefficient of variation was approximately 0.15.

TABLE 2.10  
DURATION AS A FUNCTION OF SITE INTENSITY IN THE NEAR AND FAR FIELDS  
(From Chang and Krinitzsky 1977)

LOCAL MM INTENSITY	NEAR FIELD DURATION seconds		FAR FIELD DURATION seconds	
	ROCK SITE	SOIL SITE	ROCK SITE	SOIL SITE
V	6.4	17.5	9 to 10	17 to 19
VI	7.3	20.0	" "	" "
VII	8.3	23.0	" "	" "
VIII	9.6	26.5	" "	" "
IX	11.0	30.0	" "	" "
X	12.5	35.0	" "	" "
XI	14.5	40.0	" "	" "
XII	16.5	46.0	" "	" "

TABLE 2.11  
BRACKETED DURATION (SEC) AT 50. KM FROM SOURCE  
(Accel.  $\geq$  0.05 g's; Freq.  $\geq$  2 Hz)  
(From Mortgart et al. 1977)

<u>Duration seconds</u>	<u>Magnitude m</u>	<u>Duration seconds</u>	<u>Magnitude m</u>
1.5	4.0	17.0	6.75
1.5	4.25	22.0	7.0
1.5	4.50	24.25	7.25
1.5	4.75	26.0	7.50
2.0	5.0	27.25	7.75
2.0	5.25	28.0	8.0
2.0	5.50	28.5	8.25
2.5	5.75	29.0	8.50
3.0	6.0	29.5	8.75
5.5	6.25	29.5	9.0
10.0	6.50		

## Other Factors Influencing Attenuation Laws

### A. Site Condition

Incorporation of the influence of the soil at a site is a part of micro-regionalization. Empirical and theoretical procedures have been devised to account for this influence (4, 5, 12, 26, 39, 46, 77, 90, 91, 92). In his statistical analysis of the data on the 1971 San Fernando earthquake, Donovan (1973) evaluated the differences between the attenuation characteristics of soil and rock. His results indicated that the peak ground accelerations at short distances on rock were higher than those on soil. Results further showed a reversal of this trend at distances of more than 60 km, or at acceleration levels of less than 8% gravity. The resulting attenuation law suggested for soil and rock is given in Table 2.5.

Another method of incorporating the influence of soil conditions utilizes the curves by Seed et al. (1976), which are reproduced in Fig. 2.19. Additional procedures, which relate peak ground surface acceleration on soil to bedrock for generalized site conditions, are present in the literature (8, 17).

For a site where there is adequate information regarding the site and soil conditions, a theoretical analysis based on the wave propagation theory can be made to assess the modification of the ground motions propagating from bedrock to the surface of the ground. Faccioli (1977) has described a stochastic method of one-dimensional soil amplification analysis which employs nonlinear soil properties. Using this procedure, probabilistic assessments of earthquake parameters on local soil sediments can be made from the distributions of the parameters for rock or firm ground.

Modifications in the common form of the attenuation law have been made

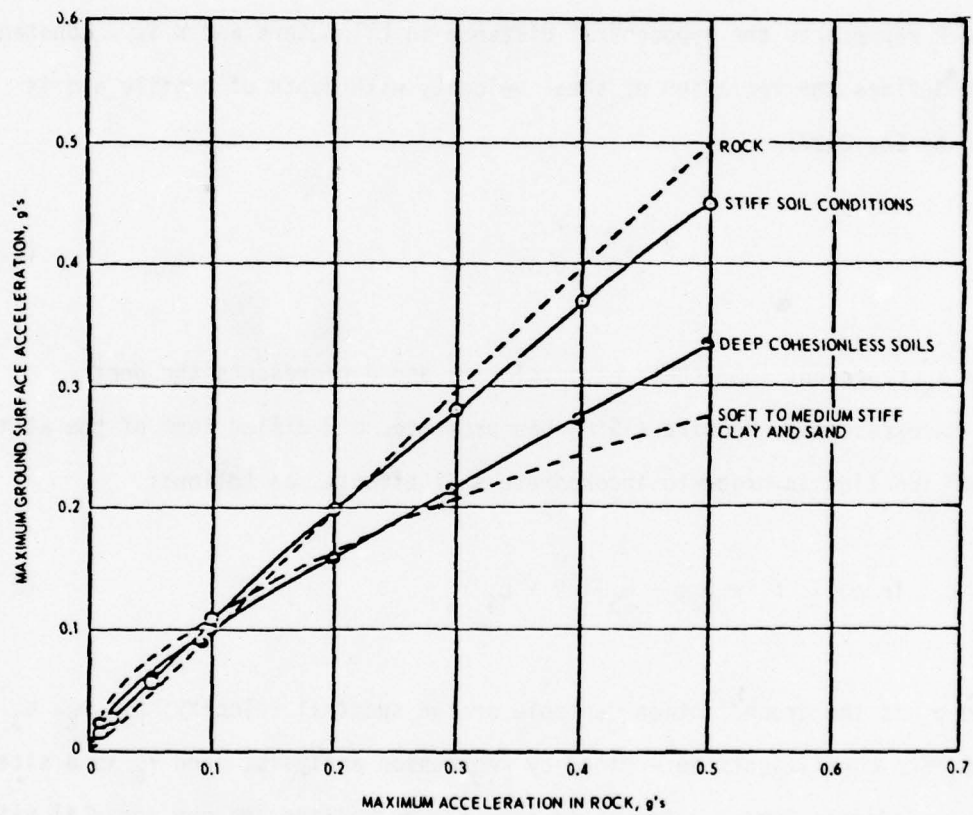


FIG. 2.19 Approximate Relationships between Maximum Accelerations on Rock and Other Local Site Conditions (From Seed et al. 1976)

introducing a suitable parameter to the equation in order to represent the influence of site properties. Performing multiple regression on the 1971 San Fernando data, Eguchi (1977) has proposed Eq. 2.26 for peak particle velocity, V:

$$V(\text{cm/sec}) = e^{4.69} k^{0.33} e^{1.2(m - 6.4)} R^{-1.05} \quad (2.26)$$

where R represents the hypocentral distance in kilometers and K is a constant which defines the variation of shear velocity with depth of profile and is given by Eq. 2.27:

$$K = \frac{V_s}{d^{0.37}} \quad (2.27)$$

where  $V_s$  represents the shear wave velocity and d represents the depth.

More recently, McGuire (1978) has presented a modified form of the attenuation function in order to incorporate soil effects, as follows:

$$\ln p = b_1 + b_2 m + b_3 \ln R + b_4 Y_s \quad (2.28)$$

where p is the ground motion variable or the spectral velocity;  $b_1$ ,  $b_2$ ,  $b_3$  and  $b_4$  are coefficients determined by regression analysis; and  $Y_s$  is a site geology indicator which is equal to zero for rock sites and one for soil sites. Table 2.12 provides the regression coefficients for peak ground acceleration, velocity, displacement and spectral velocity at a period of 1 second with 2% damping.

A similar study by Blume (1977) has resulted in site-acceleration-mag-

TABLE 2.12  
COEFFICIENTS AND STANDARD DEVIATIONS OBTAINED FROM REGRESSION ANALYSIS  
(After McGuire 1978)

$$\ln p = b_1 + b_2 M + b_3 \ln R + b_4 Y_s$$

p	b <sub>1</sub>	b <sub>2</sub>	b <sub>3</sub>	b <sub>4</sub>	c <sub>ln p</sub>
a <sub>g</sub> , peak ground acceleration	3.40	.89	-1.17	- .20	.62
v <sub>g</sub> , peak ground velocity	-1.00	1.07	- .96	+ .07	.64
d <sub>g</sub> , peak ground displacement	-2.72	1.00	- .63	.12	.69
PSRV, response spectrum velocity (1-sec period, 2 percent damping)	-1.61	1.16	- .83	.31	.72

a<sub>g</sub> is cm/sec<sup>2</sup>

v<sub>g</sub> is cm/sec

d<sub>g</sub> is cm

PSRV is cm/sec

nitude (SAM) relationships which incorporate the site effects. The proposed expressions for the acceleration at any probability level,  $y$ , in lognormal form are, for  $m < 6.5$ :

$$A_y = 0.318e^{1.03m}(29)^{1.14\bar{b}}(R + 25)^{-1.14\bar{b}}(2.54)^y$$

and for  $m > 6.5$ :

(2.29)

$$A_y = 26.0e^{0.432m}(29)^{1.22\bar{b}}(R + 25)^{-1.22\bar{b}}(1.81)^y$$

where

$$\bar{b} = \frac{1}{2} \log_{10}(\rho V_s)$$

in which  $A_y$  is the estimated peak acceleration that would be recorded by an instrument during an earthquake of  $m$  and  $R$ ; and  $\rho V_s$  gives the site impedance in feet per second. The parameter  $y$  is the standardized variable of the lognormal distribution: when  $y = 0$ , the estimated acceleration corresponds to the mean value.

The influence of soil conditions upon the intensity attenuation laws is more difficult to assess. The available data on intensities corresponds to a number of different earthquake locations and site conditions. This, coupled with the fact that the intensity scales are based on subjective judgments, renders site influence determination nearly impossible. Because intensity scales are based on damage and cause effects, it follows that for a given earthquake

the poorer the site conditions are, the larger the intensity will be at a given distance from the source. For this reason, Cornell and Merz (1975) have assigned to the parameter  $C_1$  (in Eq. 2.22) values of 2.6 for rock and 3.1 for all sites, a difference of 0.5 between the two corresponding intensities.

Duration of earthquake motion, generally speaking, is significantly longer on soil sites than rock sites, as observed from Table 2.10.

#### B. Near Source Effects

Because attenuation laws are generated from data observed at long distances from earthquake sources, the validity of such laws regarding short distances from earthquake sources, the validity of such laws regarding short distances from a source is questionable. Algermissen and Perkins (1976) suggest that acceleration obtained from the Schnabel and Seed (1973) curves.

One method for accounting for near source effects on the law is the use of  $R + 25$  to replace  $R$ , as mentioned earlier. Donovan and Bornstein's (1978) recommendations for distance dependent parameters  $b_1$ ,  $b_2$ , and  $b_3$  (Eq. 2.21) are another attempt to account for near source effects. The attenuation law suggested by Milne and Davenport (1969) and given in Table 2.5 implies that the acceleration has a variation of  $e^{1.64mR^{-2}}$  at long distances, and of  $e^{0.5m}$  at short distances from the source.

Espinosa (1977) studied the intensity attenuation relationships for near and intermediate distances using the data from the 1971 San Fernando earthquake. The recommended relationship is given by:

$$\log \Delta = 3.05 - 0.21 I \quad (2.30)$$

where  $\Delta$  represents the epicentral distance in kilometres, and  $I$  is the Modified Mercalli Intensity. Krinitzsky and Chang (1977) have presented relationships between acceleration velocity or displacement vs MM Intensity for near and far field conditions.

Cornell and Merz (1975), in their study of seismic risk in Boston, have assumed that there is no attenuation of intensity within a 10-km radius around the site. Near source effects on acceleration attenuation are not yet very well understood. Recent papers have discussed the characteristics of near field ground motions which are determined based on physical models describing the faulting process and near field wave propagation (11, 15, 32, 52, 86, 99). Due to the scarcity of near field data for large magnitude earthquakes, reliable predictions of acceleration close to the source cannot yet be made.

A seismic hazard study will always face questions regarding the proper selection of an attenuation law. Following careful selection, the uncertainties in the law can be incorporated in the hazard analysis following the procedure suggested by Cornell and Merz (1975). If more than one attenuation law is thought to be applicable, the analysis may be repeated for each law and a Bayesian estimate of seismic hazard, using subjective weights, can be made. The Bayesian approach will be described in the following section.

#### Geologic and Geophysical Information

To this point, discussion has been limited to the evaluation of local and regional seismicity, based on parameters obtained from statistical data. Problems and limitations involved in the estimation of seismicity based on seismological data have been outlined. In summary, existing historic records are, in most cases, too recent and too incomplete, and do not, therefore, represent the

true nature of the tectonic process. For example, the absence of large earthquake occurrence indicated in the historic data for a particular region may erroneously be interpreted as an indication of low seismicity, whereas a detailed geologic investigation may establish the existence of active faults in the region which might have been the source of large earthquakes predating the historic record. Thus, studies of the seismicity of a region based solely on statistical information are limited in the conclusions they can realistically or safely draw. Bell and Hoffman (1978) have made a comparative study between the computed seismic hazard based on geologic evidence and the computed hazard based on instrumental data for a site near Los Angeles (Fig. 2.20). They concluded that, for "normal levels of acceptable seismic risk", the accelerations which were computed based on geologic evidence exceeded those based on instrumental data by as much as 50%.

It is now accepted that geologic and geophysical information can contribute significantly to the determination of local seismicity, particularly where there exists a strong correlation between past earthquake occurrence and the surface faults present, such as in California. So extensive is the information regarding faults and fault activity that Allen (1976) suggests that a seismic zoning map for California based on geologic data alone would be more reliable than a map based on purely statistical data. However, the most rational procedure in seismic hazard analysis is to utilize the various types of data stemming from different sources, incorporating the subjective judgments of the geologist and the seismologist. Baye's theorem provides a rational procedure toward this end.

Seismic hazard analysis following the Bayesian approach was first introduced by Esteva (1969). Various other researchers have since discussed the application of Baye's theorem to the evaluation of local seismicity. However,

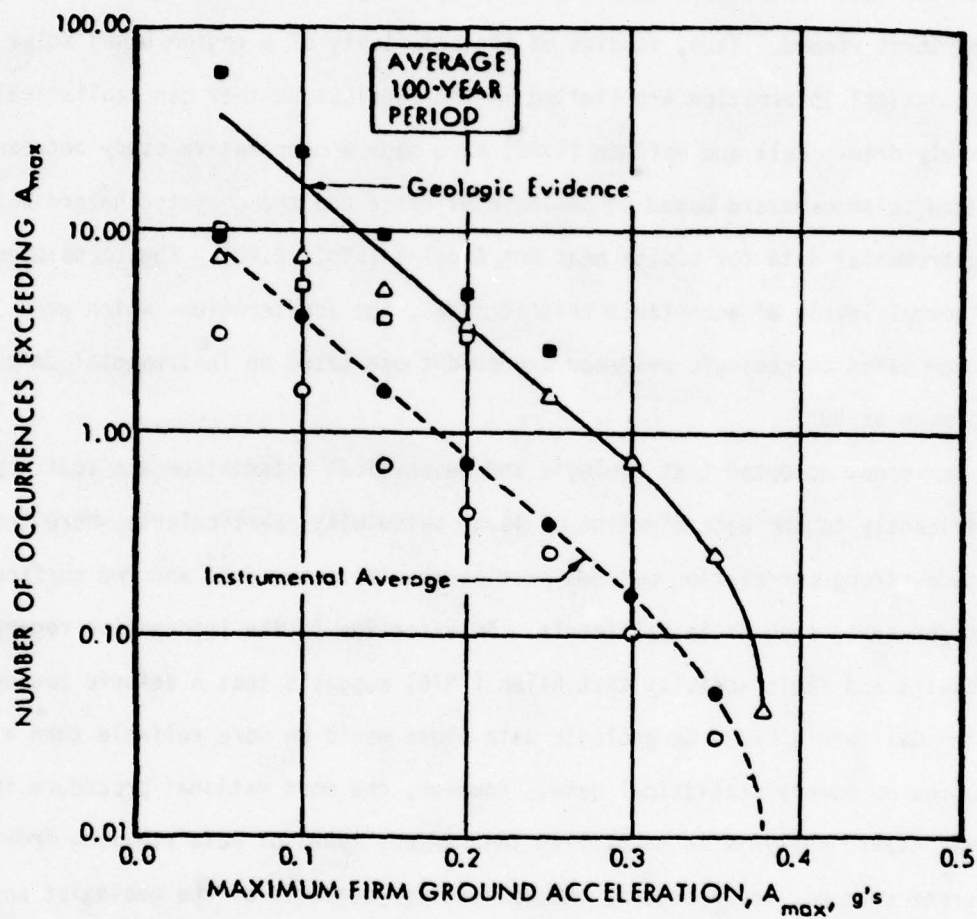


FIG. 2.20 Comparison Between Computed Seismic Hazards Based on Geologic Data versus Instrumental Data. (From Bell and Hoffman 1978)

only recently have complete formulations of the Bayesian approach and its practical applications in seismic hazard analysis been properly and extensively presented.

In brief, the Bayesian approach requires the cooperative effort and input from geologists, geophysicists and earthquake engineers. The pertinent geologic information includes the identification of all active faults in the given region and the assignment of activity levels for each fault. Such an evaluation of fault activity involves various investigative approaches, including geologic mapping, interpretation of aerial photographs and remote sensing imagery, direct subsurface investigation, geophysical surveys, age-dating of geologic material, geodetic measurements, and seismological studies (22, 59).

Various definitions of fault activity are present in the literature (22, 59). Table 2.13 presents the fault classification used by Bell and Hoffman (1978). In

TABLE 2.13  
FAULT ACTIVITY CLASSIFICATION (After Bell and Hoffman 1978)

<u>Fault Activity Classification</u>	<u>Geologic Time</u>	<u>Displacement Age (Years before Present)</u>
Historically active	Historic	0 to 200
Active	Holocene	200 to 11,000
Potentially Active	Pleistocene	11,000 to 3,000,000
Inactive	Pre-Pleistocene	Older than 3,000,000

addition to the classification of a fault, the degree of activity for each fault must be determined, most often in terms of slip rate, cumulative slip during a given interval, and amount of slip during one event (22).

The recurrence intervals of given magnitude events can be determined by the estimation of creep and energy liberated by shocks, based on measured fault displacements per unit time in the recent geologic time scale (43, 44). Slemmons (1977) has presented recurrence intervals as a function of earthquake magnitude and strain rates across fault zones.

Geologic data for a region can also provide a basis for estimating the maximum credible earthquake,  $m_1$ , that can occur along a known fault. Such an estimate is usually based on the length of the fault rupture and the type of fault movement. Various relationships between fault rupture length and earthquake magnitude have been summarized by Slemmons (1977). Cluff (1978) warns that estimates of  $m_1$  made solely on the basis of the length of fault rupture may be unrealistic, and recommends consideration of the following five factors in order to obtain more reliable estimates:

- 1) Geologic evaluation of the regional tectonic framework.
- 2) History of seismic activity along the fault and the surrounding region.
- 3) Geologic history of displacement along the fault.
- 4) Relationship between earthquake magnitude and fault rupture length.
- 5) The relationship between earthquake magnitude and the amount of fault displacement.

#### Bayesian Approach

Due to variations and uncertainties in the seismic parameters  $\lambda(m)$ ,  $\beta$ , and  $m_1$ , estimated on the basis of statistical data, these parameters are often treated as random variables (16, 41, 43, 81, 82, 102). Reliable probability distributions for these parameters can be determined by incorporating geologic, geophysical and statistical data, along with professional judgment, into a cohesive information source. Application of Bayes's theorem allows for such a rational combination of the widely varying data sources (10, 89).

For illustrative purposes, the parameter  $\lambda(m)$ , defining the annual rate of occurrence of earthquakes with magnitudes equal to or greater than  $m$  will be used to present the basic Bayesian probability theory applied in seismic hazard

analysis. In Eq. 2.2, an exponential function was used to relate  $\lambda(m)$  to  $m$ . The application of Baye's theorem requires that  $\lambda(m)$  be treated as a random variable and not a function of  $m$ . This can be accomplished by assuming that the  $\lambda$ 's for various magnitudes are independent of one another. Thus, Baye's theorem can be systematically applied for each  $\lambda(m_i)$ , independently for various values of  $m_i$ . The updated values of  $\lambda(m_i)$  obtained by the application of Baye's theorem will indicate discontinuity when plotted against  $m_i$ . This can be corrected by fitting a continuous curve through the computed  $\lambda(m_i)$  values (82).

For purposes of convenience, let  $\lambda(m_i)$  be denoted by  $\lambda_i$ . Baye's theorem can be expressed in mathematical terms as in Eq. 2.31:

$$f(\lambda_i | \text{data}) = \frac{f(\text{data} | \lambda_i) f(\lambda_i)}{\int f(\text{data} | \lambda_i) f(\lambda_i) d\lambda_i} \quad (2.31)$$

where  $f(\lambda_i)$  represents the initial or prior estimate of the probability density function of the random variable  $\lambda_i$ ;  $f(\text{data} | \lambda_i)$  represents the sample likelihood function defining the probability of observing the data, given  $\lambda_i$ ; and  $f(\lambda_i | \text{data})$  is the posterior or improved probability density function of  $\lambda_i$ , given the data. The numerator on the right side of the equation is a normalizing factor, so that when  $f(\lambda_i | \text{data})$  is integrated over all  $\lambda_i$ , the summation will equal 1.0.

Eq. 2.31 is applied in the following manner. A prior distribution for  $\lambda_i$  is chosen. The choice of this distribution is difficult and at times even arbitrary, yet Rosenblueth (1969) has stated in a discussion of the Bayesian approach that this difficulty "is a poor reason to drop this approach in favor of irrational, even if traditional, statistical methods." The prior distribution most

commonly chosen for  $\lambda_i$  is gamma with parameters  $\lambda_1$  and  $K_1$ , obtained from either geologic or subjective input. Newmark and Rosenblueth (1971) discuss procedures for evaluating such prior information based on geologic and seismological data corresponding to the three macrozones shown in Fig. 2.7.

The sample likelihood function can be obtained by using statistical data on earthquake occurrence, and assuming that earthquake occurrence generally follows a poisson process. If the available data for any given source indicates that during a period of time  $t$  years in length,  $n$  number of earthquakes of magnitude equal to or greater than  $m$  have occurred, then:

$$f(\text{data}|\lambda_i) = \frac{(\lambda_i t)^n e^{-\lambda_i t}}{n!} \quad (2.32)$$

Substituting Eq. 2.32 and the prior probability with the parameters  $\lambda_1$  and  $K_1$  in Eq. 2.31, and evaluating the normalizing factor, the posterior probability density function,  $f(\lambda_i|\text{data})$ , may be evaluated. Mortgart et al. (1977) present results of the calculations which indicate that the posterior density function of  $\lambda_i$  is also gamma with parameters

$$\begin{aligned} \lambda_2 &= \lambda_1 + t \\ K_2 &= K_1 + n \\ \text{and} \quad \mu &= \frac{K_1 + n}{\lambda_1 + t} \\ \sigma^2 &= \frac{K_1 + n}{(\lambda_1 + t)^2} \end{aligned} \quad (2.33)$$

where  $\lambda_2$  and  $K_2$  are the posterior, "updated" values of the parameters  $\lambda_1$  and  $K_1$ ; and  $\mu$  and  $\sigma^2$  are the mean and variance, respectively, of  $\lambda_i$ .

Newmark and Rosenblueth (1971) explain the application of Baye's theorem where the prior information on  $\lambda_i$  is given as  $n_1$  expected occurrences of magnitudes of  $m > m_i$  in a period of  $t_1$  years. Assuming a gamma distribution for  $\lambda_i$  and a prior coefficient of variation of  $\lambda_i$  equal to  $n_1^{-1/2}$ , the expected value and the variance of the posterior density function for  $\lambda_i$  are given by:

$$\begin{aligned}\mu &= \frac{n_1 + n}{t_1 + t} \\ \sigma^2 &= \frac{n_1 + n}{(t_1 + t)^2}\end{aligned}\tag{2.34}$$

Making the assumption that the prior coefficient of variation of  $\lambda_i$  is equal to  $n_1^{-1/2}$  is, in effect, equivalent to assigning to  $K_1$  a value of  $n_1$ . Thus, Eqs. 2.33 and 2.34 yield the same result. Eq. 2.33 expresses the posterior results in general terms as a function of the prior parameter for the gamma distribution, whereas Eq. 2.34 is valid only if the prior coefficient of the variation of  $\lambda_i$  is assumed to be equal to  $n_1^{-1/2}$ , or essentially, if  $K_1$  is equal to  $n_1$ .

Thus, application of Baye's theorem, which utilizes statistical data, improves the initial or prior estimation of  $\lambda_i$ , which is based on conceptual models and non-statistical information. As resources of statistical data increase, Baye's theorem can be applied to continuously update the seismicity evaluation of a given region.

In general, the value of the contribution of statistical information to the Bayesian estimation is dependent on the extent of the available historic data, as well as on the degree of uncertainty in the prior estimate. If the available seismological records are both relatively long and reliable, the posterior estimates should not differ too greatly from those based on the statistical data. However, if the prior estimates are based on thorough assessments of geologic evidence, then the statistical data should not significantly change the prior estimates (42).

In Eq. 2.1 the estimated probability of  $n$  events with magnitude  $m > m_i$  occurring in  $t$  years was conditional on  $\lambda_i$ , and because  $\lambda_i$  is a random variable with a distribution of  $f(\lambda_i|\text{data})$ , the unconditional Bayesian estimate of this probability will be given by Eq. 2.35:

$$P(n) = \int_0^{\infty} P(n, \lambda_i) f(\lambda_i|\text{data}) d\lambda_i \quad (2.35)$$

#### Bayesian Estimate of Seismic Hazard

The presence of uncertainties in several of the parameters used and in the steps followed in a seismic hazard analysis have been emphasized in this Report. Cornell and Merz (1975) have employed a rather simple method to account for these uncertainties and to allow for incorporation of subjective evaluation in the hazard studies. The procedure involves repeating the analysis for a number of alternative values of the questionable parameters and assumptions. The resultant hazard estimate is made by assigning a subjective weight to each alternative and summing the weighted results for all the alternatives. This estimate is referred to as a Bayesian estimate, which Cornell and Merz state "reflects the

uncertainty induced both by the behavior of nature and by man's incomplete state of knowledge about that behavior." Fig. 2.21 shows the subjective weights assigned by Cornell and Merz (1975) to the various assumptions made in their study of seismic risk in Boston. In this example, three assumptions were made on the attenuation law, three on source configuration, and four on the upper bound magnitude. The relative weights for each of the 36 studies are calculated by multiplying the subjective weights corresponding to each outcome. For example, for the most likely hazard curve, the relative weight is equal to  $0.5 \times 0.5 \times 0.3 = 0.075$ . The resulting Bayesian weighted estimate curve is then obtained by summing the products of each of the 36 hazard curves by the relative weight associated with that curve.

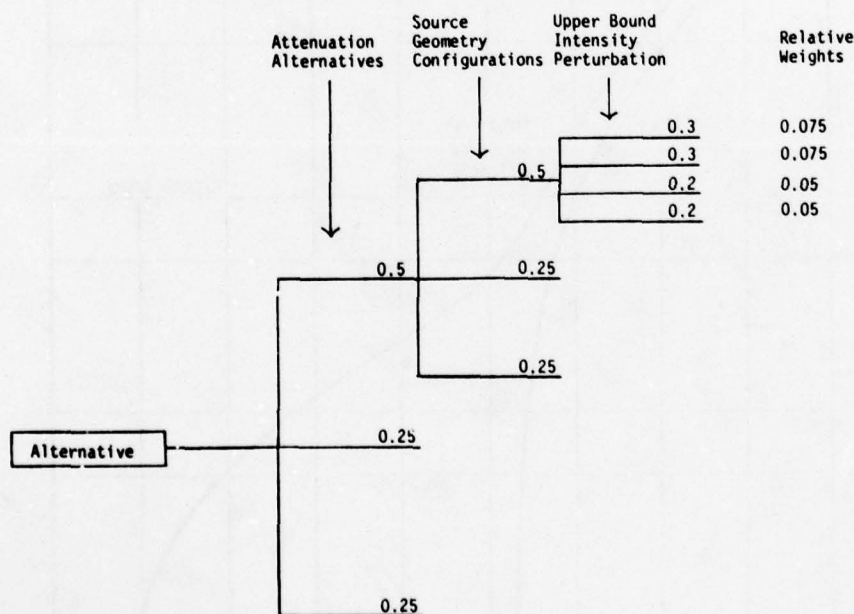


FIG. 2.21 Subjective Relative Weights Corresponding to Different Alternatives Used by Cornell and Merz (1975)

Fig. 2.22 shows a comparison between the most likely estimate of risk and the Bayesian estimate. The two results differ significantly at site intensities greater than VII, a discrepancy which is attributed to the perturbation in which the upper bound intensities in the near source areas were raised from (7.7, 8.7) to XII.

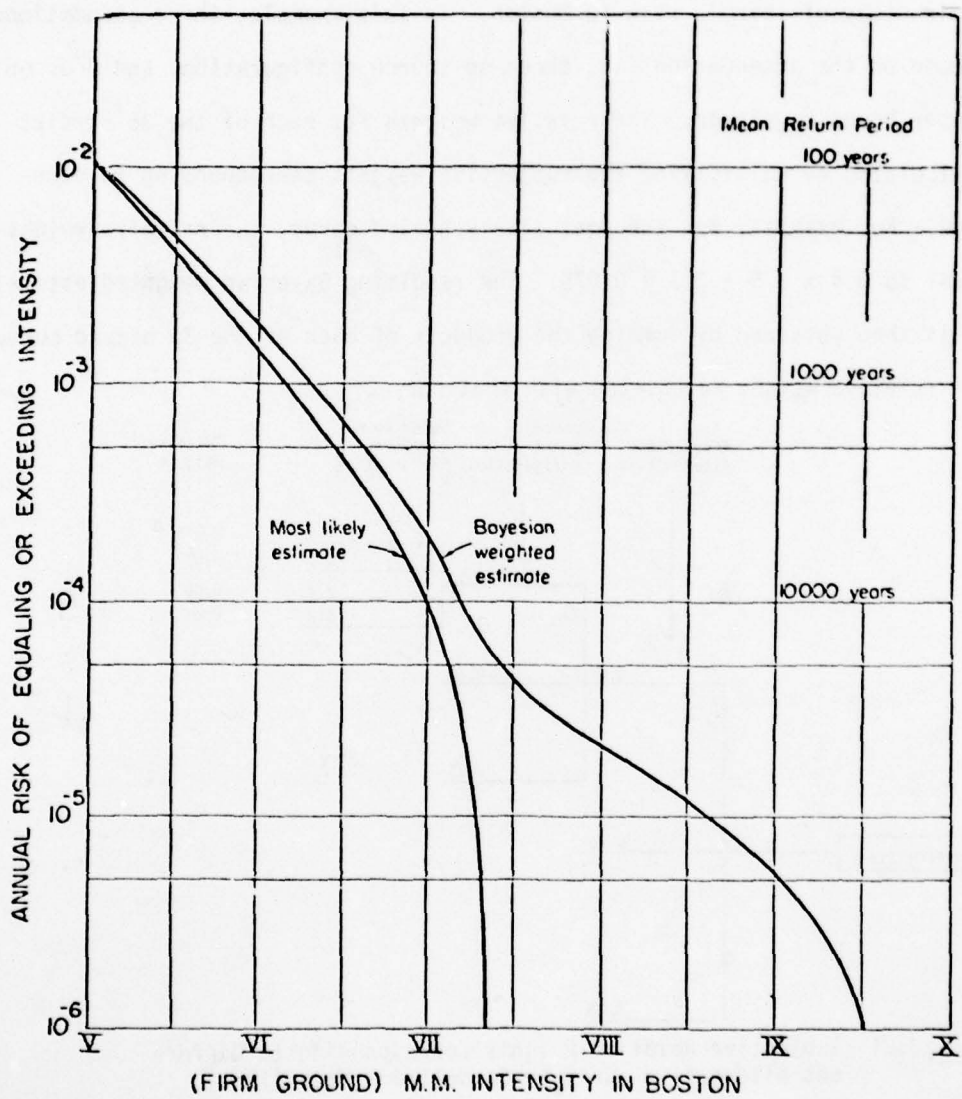


FIG. 2.22 Comparison Between Most Likely Estimate of Risk and Bayesian Estimate  
(From Cornell and Merz 1975)

### PART 3: SEISMIC HAZARD CALCULATIONS

The calculated seismic hazard at a site can be expressed in terms of a curve which represents the probability of exceeding a given seismic parameter at the site, vs the parameter itself. Previous discussion has provided a procedural basis for the performance of the hazard analysis. Fig. 3.1, which is reproduced after Shah (1978), gives a schematic outline of the major steps involved in hazard calculations. In Step 1, potential earthquake sources are identified, and the length or area, position and location of each source are established. Step 2 involves the determination of the recurrence relationship for each source, based on geologic, geophysical and historic data. In Step 3, an attenuation law is selected in order to describe the seismic parameter thought to best represent the ground motion intensity at the site. Finally, Step 4 involves the actual calculations of the seismic hazard and the estimation of the probability of exceedence (or non-exceedence) within a given time period of various values of the selected parameter.

The next section of the Report will present a brief discussion regarding a number of the basic probability concepts used in seismic hazard studies, followed by a presentation of the methodology and the mathematical formulations used in Step 4 of the analysis.

#### Basic Probability Concepts

The recurrence relationship given in Step 2 of Fig. 3.1 is established by a study of the local seismicity. This relationship was expressed in Part 2 in terms of two parameters: 1)  $\lambda(m_0)$ , the annual number of earthquake occurrences with magnitudes equal to or exceeding  $m_0$ , representing the minimum mag-

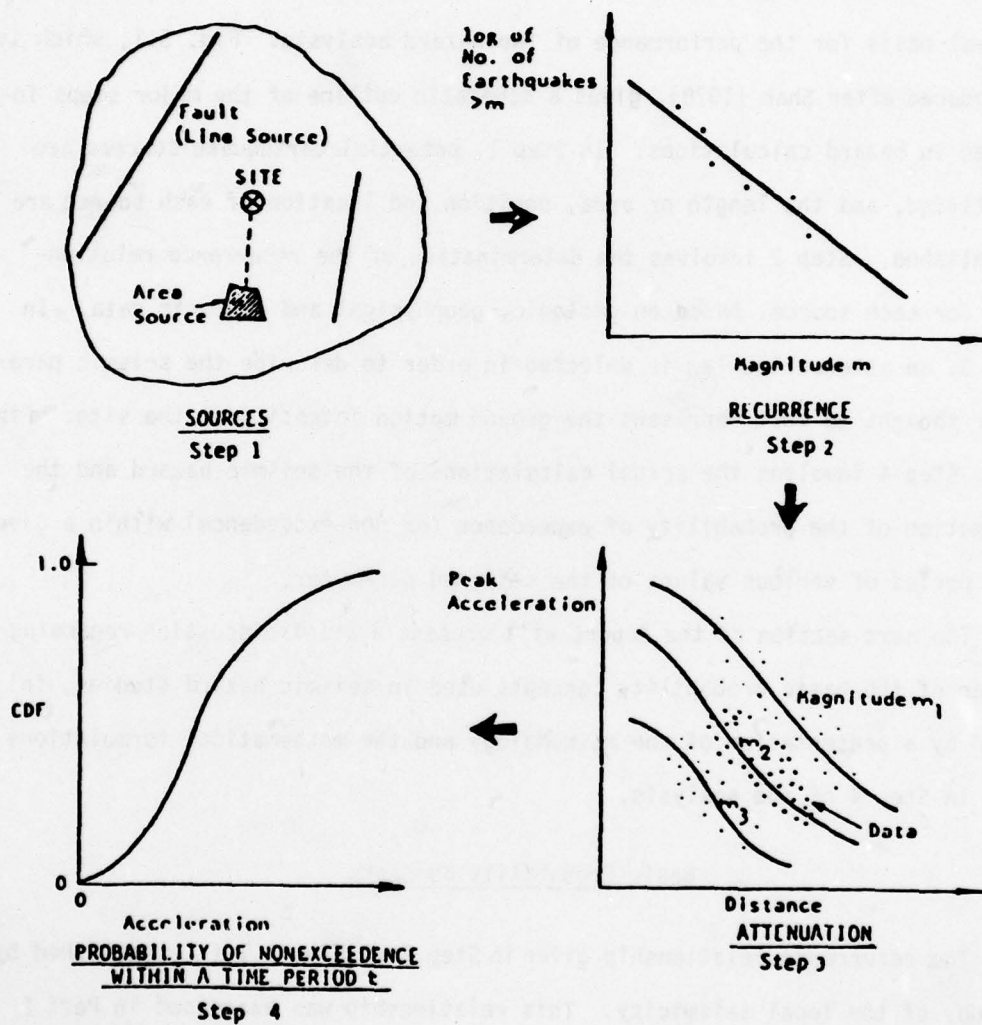


FIG. 3.1 Steps Involved in Seismic Hazard Calculations  
(After Shah 1978)

nitude of engineering interest, and 2)  $\beta$ , the magnitude-frequency parameter which defines the conditional probability of exceedence,  $P[M > m|E]$ , as given by Eq. 2.5. Seismic hazard calculations are performed in order to obtain an estimate of the probability that at least one event will occur in  $t$  years, causing the value of a parameter  $A$  to exceed  $a$ . This estimated probability figure is arrived at by calculating the conditional probability of  $A$  exceeding  $a$ , given that an earthquake  $E$  will occur:

$$P[A > a|E] = P[M > m|E] \quad (3.1)$$

where  $m$  is determined from the attenuation law (which relates  $A$  to  $M$  and  $R$ ), using  $A = a$ . The conditional probability shown in the right-hand side of Eq. 3.1 can be evaluated using Eq. 2.5, and thus the value of  $P[A > a|E]$  is estimated.

If  $\lambda(m_0)$  earthquakes are expected to occur annually, the expected number of special events causing  $A$  to exceed  $a$  is given by:

$$\lambda(a) = \lambda(m_0) P[A > a|E] \quad (3.2)$$

Provided that earthquake occurrence is assumed to follow a poisson process of arrival, these special events with an annual rate of occurrence of  $\lambda(a)$  will also follow a poisson process, assuming that they are independent events. Therefore, the unconditional probability of at least one event causing  $A > a$  occurring within a period of  $t$  years is given by:

$$P[A > a, t] \text{ at least one} = 1 - e^{-\lambda(a)t} \quad (3.3)$$

The annual probability of exceedence will then be given by:

$$P[A > a, t = 1] = 1 - e^{-\lambda(a)} \quad (3.4)$$

$$\approx \lambda(a); \quad \text{for small } \lambda(a)$$

If the annual probability of exceedence is known, then the corresponding probability for  $t$  years can be obtained following one of two alternate procedures. One method is to calculate  $\lambda(a)$  from Eq. 3.4 and simply substitute it in Eq. 3.3 to obtain the probability for  $t$  years. Alternatively,  $P[A > a, t]$  can be calculated directly from the annual probability, using Eq. 3.5:

$$P[A > a, t] = 1 - (1 - P[A > a, t = 1])^t \quad (3.5)$$

$$\approx P[A > a, t = 1] \times t; \text{ for probabilities less than 0.1}$$

These two procedures are essentially the same and should yield identical results.

In the literature, the estimated probability of a seismic event occurring is often expressed in terms of its return period. The return period,  $T_r(a)$ , of an event causing  $A$  to exceed  $a$ , is defined as the inverse of the annual probability of at least one event occurring (10):

$$T_r(a) = \frac{1}{1 - e^{-\lambda(a)}} \quad (3.6)$$

$$\approx \frac{1}{\lambda(a)} \quad \text{for small } \lambda(a)$$

A second parameter used in seismic hazard studies involves the average inter-arrival times, referred to as the recurrence interval,  $T_a(a)$ , which is defined by the inverse of the mean number of annual events causing  $A$  to exceed  $a$ :

$$T_a(a) = \frac{1}{\lambda(a)} \quad (3.7)$$

These two parameters are commonly used interchangeably, and therefore have been confused. A comparison between Eq. 3.6 and Eq. 3.7 leads to the conclusion that the return period and the recurrence interval are identical only if the computed probability is low. Fig. 3.2 gives the ratio of return period to recurrence interval as a function of the mean annual number of events,  $\lambda$ . It is clear that the return period and the recurrence interval are comparable only if  $\lambda$  is less than 0.1, or  $T_a(a)$  is greater than 10 years. In addition, the concept of recurrence interval is often misinterpreted (2). For example, the probability of at least one event with a recurrence interval of  $T_a(a)$  occurring in  $T_a(a)$  years is not equal to 1.0, as might be expected, but rather is equal to 0.63, as shown in Eq. 3.8:

$$P[A > a, t = T_a(a)] = 1 - e^{-\lambda(a) \cdot 1/\lambda(a)} = 0.63 \quad (3.8)$$

In order to avoid confusion, it is advised that the computed hazard results be stated in terms of the probability of exceedence within a given period of time. This manner of presenting the results provides for a direct association of the hazard to the design life span of a structure.

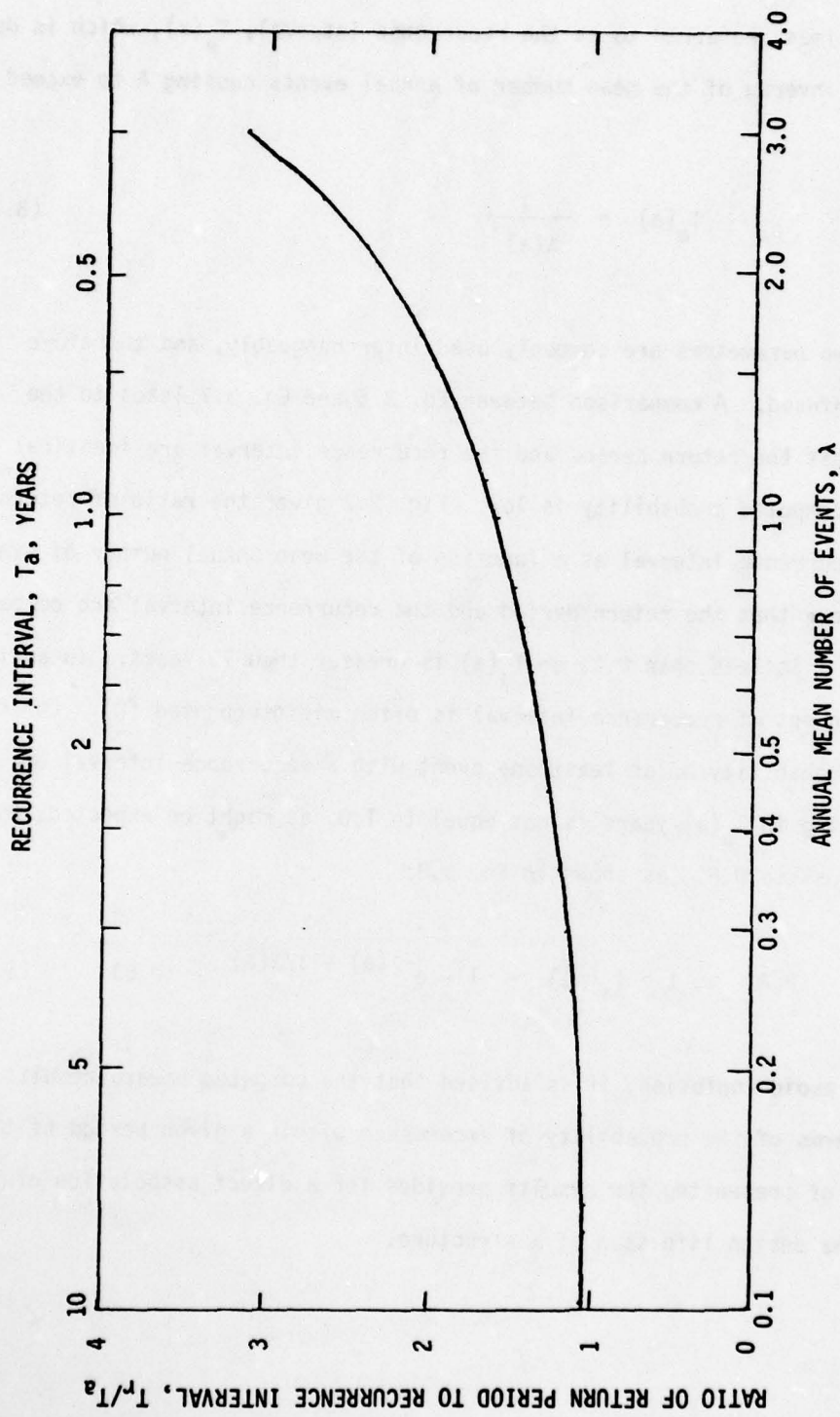


FIG. 3.2 Comparison Between Return Period,  $T_r$ , and Recurrence Interval,  $T_a$

### Mathematical Formulations

A seismic hazard analysis can employ three general earthquake source types in order to describe the potential future seismic activity for a region. This section of the Report presents the basic methodology involved in the analysis considering the three source types, which are referred to as point, line and area sources. For reasons of simplicity, the attenuation law will be assumed to be deterministic, having the form  $A = b_1 e^{b_2 m} (R + 25)^{-b_3}$ , and it will be further assumed that  $m_1 = \infty$ . A general procedure for a hazard analysis which employs a probabilistic rather than deterministic attenuation function is presented by McGuire (1976) and summarized in Appendix A.

#### Point Source

Fig. 3.3 shows a site located  $R$  km from a point source. The conditional probability,  $P[A > a|E]$  of acceleration  $A$  exceeding an assumed value,  $a$ , given that an earthquake  $E$  will occur, is obtained by Eq. 3.9:

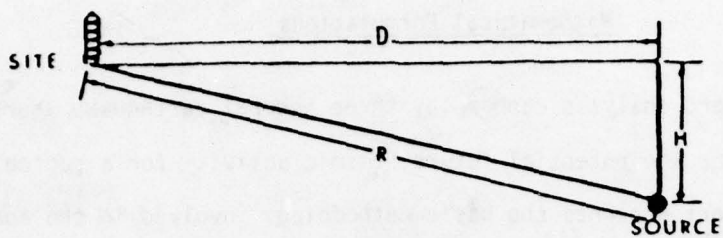
$$P[A > a|E] = P[M > m|E] \quad (3.9)$$

where  $a > b_1 e^{b_2 m_0} (R + 25)^{-b_3}$

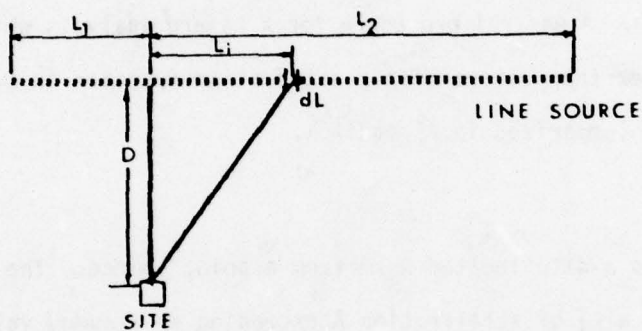
and  $m = \ln \left[ \frac{a}{b_1} (R + 25)^{-b_3} \right]^{-1/b_2}$

Employing the complementary cumulative distribution function for  $m$ , given by Eq. 2.5, the conditional probability of  $A$  exceeding  $a$  can be expressed by:

$$P[A > a|E] = \exp \left\{ -\beta \left[ \ln \left[ \frac{a}{b_1} (R + 25)^{-b_3} \right]^{-1/b_2} - m_0 \right] \right\} \quad (3.10)$$



POINT SOURCE



TOP VIEW

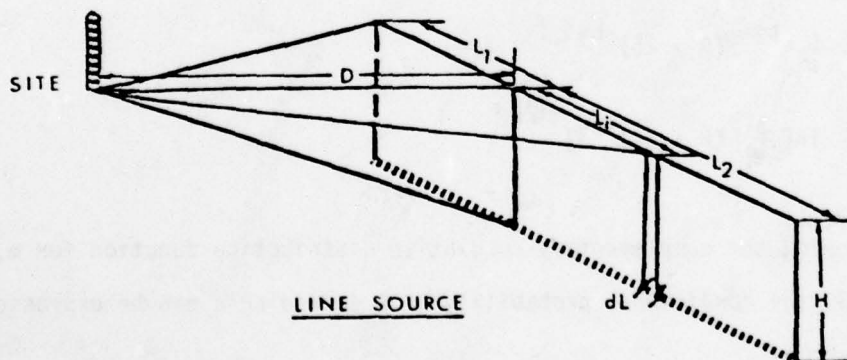


FIG. 3.3 Definitions of Source Geometry Parameters  
(After Shah et al. 1975)

$$= e^{\beta m_0} \left( \frac{a}{b_1} \right)^{-\beta/b_2} (R + 25)^{-b_3\beta/b_2}$$

Therefore, the mean annual number of seismic events causing acceleration  $A$  to exceed  $a$  is given by Eq. 3.11:

$$\lambda(a) = \lambda(m_0) \left[ e^{\beta m_0} \left( \frac{a}{b_1} \right)^{-\beta/b_2} (R + 25)^{-b_3\beta/b_2} \right] \quad (3.11)$$

where  $\lambda(m_0)$  represents the mean annual number of earthquakes with  $M > m_0$ . Assuming a poisson process of arrival for these events, the annual probability of occurrence at the site of at least one event having  $A > a$  is given by:

$$P[A > a, t = 1] = 1 - \exp[-\lambda(m_0) e^{\beta m_0} \left( \frac{a}{b_1} \right)^{-\beta/b_2} (R + 25)^{-b_3\beta/b_2}] \quad (3.12)$$

#### Line Source

The line source was originally proposed as a model for a potential earthquake source by Cornell (1968) and is employed in cases where the epicenters of historic earthquakes fall along a line, or when geologic and geophysical investigations indicate the presence of an active fault. Shah (1975) describes one method for modeling known faults, which divides the line representing the fault into  $k$  small segments of length  $dL$ , as shown in Fig. 3.3. Each segment is then treated as a point source, with a hypocentral distance equal to the distance of the segment from the site. An attenuation law is then applied, relating acceleration to earthquake magnitude and hypocentral distance, and the calculations for the hazard analysis are as follows. Based on the assumption

that a future earthquake, should it occur, has an equal likelihood of occurrence anywhere along the entire length of the fault, the mean annual rate of earthquake occurrence for each segment,  $i$ , will be equal to  $\bar{\lambda}(m_0)dl$ , where  $\bar{\lambda}(m_0)$  represents the mean annual rate of occurrence of earthquakes having  $M > m_0$  per unit length.

The contribution of each segment  $i$  to the mean number of events with  $A$  exceeding  $a$  can be expressed by:

$$\lambda_i(a) = \bar{\lambda}(m_0) dl \left[ e^{\beta m_0} \left( \frac{a}{b_1} \right)^{-\beta/b_2} (R + 25)^{-b_3\beta/b_2} \right] \quad (3.13)$$

From Fig. 3.3,  $R$  can be expressed in terms of the perpendicular distance to the fault, the focal depth and  $L_i$ , the distance of the segment  $i$  from the perpendicular on the line source:

$$R = (D^2 + L_i^2 + H^2)^{1/2} \quad (3.14)$$

Substituting the value of  $R$  into Eq. 3.13 and adding the contributions of all the segments to the mean rate of occurrence,  $\lambda(a)$ ,

$$\lambda(a) = \bar{\lambda}(m_0) e^{\beta m_0} \left( \frac{a}{b_1} \right)^{-\beta/b_2} \sum_{i=1}^k [(D^2 + L_i^2 + H^2)^{1/2} + 25]^{-b_3\beta/b_2} dL_i \quad (3.15)$$

Thus, the annual probability of  $A$  exceeding  $a$  is given by:

$$P[A > a, t = 1] = 1 - e^{-\lambda(a)} \quad (3.16)$$

AD-A075 400

NORTHEASTERN UNIV BOSTON MA DEPT OF CIVIL ENGINEERING F/G 8/11  
STATE-OF-THE-ART FOR ASSESSING EARTHQUAKE HAZARDS IN THE UNITED--ETC(U)  
JUL 79 M K YEGIANJUL 79 DACW39-78-M-2652

UNCLASSIFIED

WES-MP-S-73-1

NL

2 OF 2

AD  
A075400



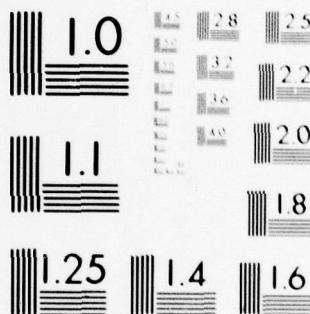
END

DATE

FILMED

11-79

DDC



MICROCOPY RESOLUTION TEST CHART  
NATIONAL BUREAU OF STANDARDS-1963-A

Arguments have been presented that such a treatment of a fault, i.e., dividing it into small segments or into areas as described in Part 2, does not consider the fault as a line source. Rather, dividing a fault into small segments and using an attenuation law which is based on hypocentral distance (in this case, distance of the site from the segment) is actually equivalent to treating the fault as a series of point sources. For this reason, as well as for computational efficiency, Donovan (1978) has preferred to use only point sources in seismic hazard analysis.

DerKiureghian and Ang (1977) have described the problems associated with modeling a fault as a point source. Such so-called "point source" models for faults assume that during an earthquake, energy is radiated from the focus of the earthquake. While such an assumption is valid for small earthquakes, during a large magnitude earthquake the energy released would be distributed along the rupture zone which may be propagated close to the site under study. Indicating that ignoring the effect of the rupture length would tend to underestimate the real hazard, Der Kiureghian and Ang (1977) have proposed a research model for faults which is based on the assumption "That an earthquake originates at the focus and propagates as an intermittent series of fault ruptures or slips, and that the maximum intensity of ground shaking at a site is determined by the slip that is closest to the site."

DerKiureghian and Ang (1977) have outlined three types of sources in describing the fault-rupture model, which are: 1) a well-defined fault line; 2) an area of known fault direction; and 3) an area of unknown faults. A brief presentation of the type 1 fault-rupture model follows.

Fig. 3.4 shows the location, position and length of a known fault. The distance  $x$  of the focus from the perpendicular line to the fault line is

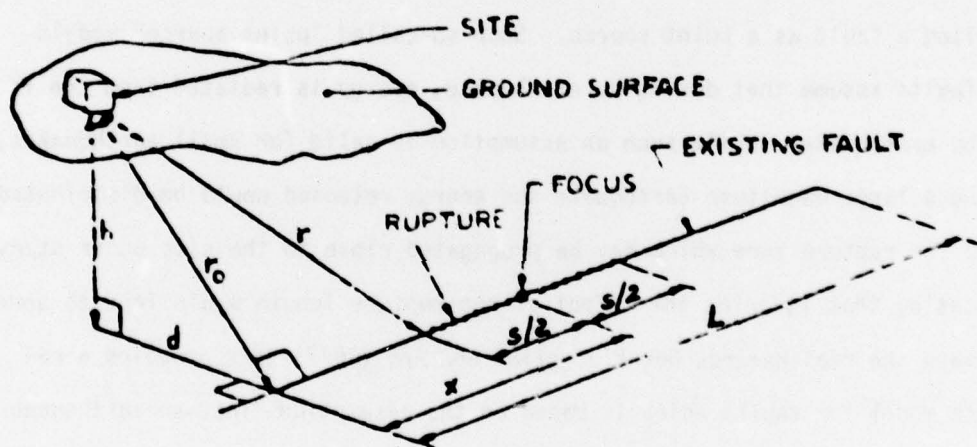


FIG. 3.4 Definitions of Parameters for the Fault-Rupture Model  
(From DerKiureghian and Ang 1977)

given by Eq. 3.17:

$$x = (r^2 - r_0^2)^{1/2} + s/2 \quad (3.17)$$

where  $s$  represents the length of the slip, which is related to earthquake magnitude:

$$s = \exp(am - b) \quad (3.18)$$

where  $a$  and  $b$  are constants (97). If it is assumed that the focus of a future earthquake would have an equal likelihood of occurrence anywhere along the length of the fault, the probability distribution  $f_R(r)$  for  $r$ , the minimum distance from the site to the slip, can be derived from Eq. 3.17 and the probability distribution for  $x$

$$f_x(x) = \begin{cases} \frac{1}{L} & 0 \leq x \leq L \\ 0 & \text{otherwise} \end{cases} \quad (3.19)$$

After the distribution  $f_R(r)$  has been determined, the conditional probability distribution for  $A$ , site intensity, given that an earthquake of magnitude  $m$  occurs in source  $i$ , can be obtained from the attenuation function which relates  $A$  to  $m$  and  $r$ . The probability that  $A$  exceeds  $a$ , conditional on the occurrence of an earthquake at source  $i$ , is obtained by integration over the appropriate values of  $a$  and  $m$ :

$$P[A > a | E] = \int_{m_0}^{m_1} \int_a^{a_{\max}} f_{A|E,m}(a) f_M(m) da dm \quad (3.20)$$

The annual probability of exceedence can then be obtained using Eqs. 3.2 and 3.4.

### Area Source

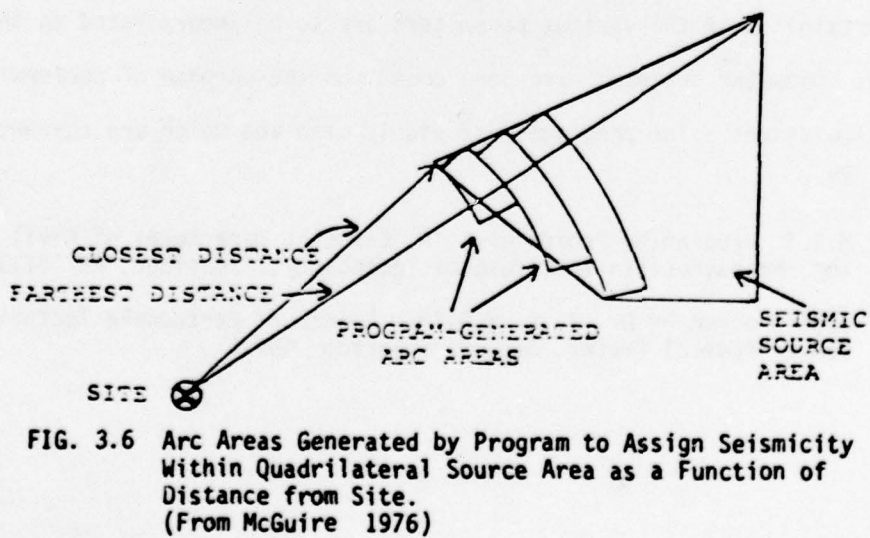
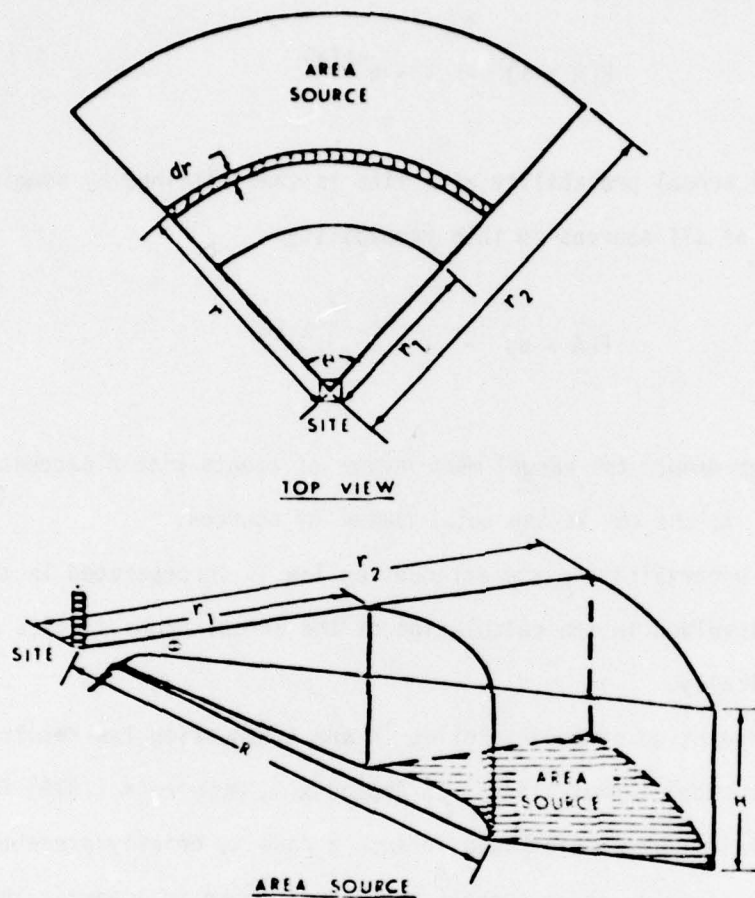
If in a particular region the epicenters of historic earthquakes are scattered randomly due to the presence of numerous faults and/or errors in the estimations of epicentral locations of past earthquakes, an area source model may be most appropriate to describe the future seismicity of the region. If the rate of occurrence per unit area, the focal depth and the attenuation are the same for all earthquakes originating within an area source, that source is commonly referred to as a "uniform" source. For computational efficiency, an area source is often represented by a segment of an annular ring, as shown in Fig. 3.5. If the area source considered in an analysis does not have an annular shape, the source is divided into subsources having annular shapes, as shown in Fig. 3.6.

The annual probability calculations for an area source are as follows. An example area source has an elemental area of  $rdr\theta$ , with a hypocentral distance of  $(r^2 + H^2)^{1/2}$  (see Fig. 3.5). The mean annual number of earthquakes occurring in this area is given by  $\bar{\lambda}(m_0) \cdot rdr\theta$ , and the conditional probability of an earthquake occurring with  $A$  exceeding  $a$  is given by Eq. 3.10. Therefore, the annual mean number of events with  $A$  exceeding  $a$  occurring in the elemental area is given by:

$$\lambda(a) = \bar{\lambda}(m_0) \left[ e^{\beta m_0} \left( \frac{a}{b_1} \right)^{-\beta/b_2} (R + 25)^{-b_3\beta/b_2} \right] rdr\theta \quad (3.21)$$

The total mean number of events with  $A$  exceeding  $a$  occurring in the annular ring defined by the two radii  $r_1$  and  $r_2$  and the angle  $\theta$  is given by:

$$\lambda(a) = \bar{\lambda}(m_0)\theta e^{\beta m_0} \left( \frac{a}{b_1} \right)^{-\beta/b_2} \int_{r_1}^{r_2} [(r^2 + H^2)^{1/2} + 25]^{-b_3\beta/b_2} \cdot r dr \quad (3.22)$$



The estimated annual probability of A exceeding a is then obtained from:

$$P[A > a] = 1 - e^{-\lambda(a)} \quad (3.23)$$

The total annual probability at a site is then obtained by summing the contributions of all sources to this probability:

$$P[A > a] = 1 - e^{-\sum_{i=1}^N \lambda_i(a)} \quad (3.24)$$

where  $\lambda_i(a)$  represents the annual mean number of events with A exceeding a occurring due to source i; and N is the total number of sources.

When the uncertainty in the attenuation law is incorporated in the analysis, the integral involved in the calculation of the annual probabilities can be calculated numerically.

The incorporation of uncertainties in the attenuation law results in more complex mathematical formulations. In Appendix A, McGuire's (1976) formulation of the mathematical expression used in such a case is briefly presented.

This type of calculation becomes problematic when in a particular study there exists a large number of sources of various shapes to be considered, and the uncertainties of the various parameters are to be incorporated in the calculation. Computer programs have been coded for the purpose of performing these calculations. The programs most widely used and which are currently available are:<sup>25</sup>

- 1) M.I.T. program by Professor C. A. Cornell, Department of Civil Engineering, Massachusetts Institute of Technology, Cambridge, MA 02139
- 2) USGS program by Dr. R. K. McGuire, Branch of Earthquake Tectonics, Denver Federal Center, Denver, Colorado 80225

#### PART 4: APPLICATIONS

This Part of the Report will discuss the various applications of seismic hazard analysis. A review of the literature has indicated that the results of seismic hazard studies have been utilized for a variety of purposes.

Cornell and Merz (1975) conducted a seismic hazard analysis in Boston, the result of which became a major contributing factor to the formulation of a new Massachusetts building code which provides for earthquake design. Seismic hazard analysis has been applied by many investigators throughout the world toward the development of hazard or zoning maps for different countries. For the United States, the most recent hazard maps (presented and discussed later) are the map of Algermissen and Perkins (1976), which provides probabilistic estimates of maximum rock acceleration, and the map developed by the Applied Technology Council (1978) providing estimates for "effective peak acceleration" and "effective peak velocity" for the contiguous 48 states.

Whitman et al. (1975) have described a seismic design decision analysis which presents a methodology for evaluating alternate structural design requirements. The procedure utilizes the results from a hazard analysis expressed in terms of Modified Mercalli Intensity.

Current earthquake mitigation efforts and earthquake insurance policy formulations consider seismic hazard results as invaluable input.

Seismic hazard analysis has been used for such purposes as the siting of nuclear power plants and in selecting the operating basis earthquake (OBE) (21, 94). Applications to other types of facilities including buildings, dams and offshore facilities are also reported in the literature (5, 6, 7, 8, 9, 17, 28, 35, 65, 85, 104).

The type of seismic hazard analysis reviewed herein has been extended to the joint probability that various levels of earthquake shaking will be experienced at a number of discrete sites (98, 100, 106). Such modifications allow for the study of seismic risk for whole communities and cities. Special attention has been focused in recent years on the seismic risk studies of lifelines (95). Seismic hazard maps are most valuable in the risk studies of networks of various lifelines extending over large seismically active regions.

In general, a seismic hazard analysis provides a probabilistic description of the seismic load on a facility which then can be used in a seismic risk analysis using a probabilistic resistance function to arrive at a probabilistic estimate of damage or consequence to that facility. The risk analysis can be described by Eq. 4.1:

$$P[F] = \int P[F|p] \cdot f_p(p)dp \quad (4.1)$$

where  $f_p(p)$  is the probability density function of the parameter  $p$ . This parameter describes the hazard at the site and constitutes the output from a seismic hazard analysis.  $P[F|p]$  is the conditional probability of failure, damage or consequence on the uncertain resistance of the facility to the hazard  $p$ . This probability is dependent on the uncertain resistance of the facility to the hazard  $p$ . The total unconditional probability of failure is then determined by the integral of the product, shown in Eq. 4.1, over all values of interest of the hazard,  $p$ .

Very often, a design level load associated with an acceptable probability of exceedence is chosen from the output of a seismic hazard analysis, and the design of a facility is carried out in a conventional, deterministic way, thus

avoiding a complete risk analysis which evaluates the contribution to this risk of a range of values of the input load. Donovan (1978) describes the common practice of selecting two levels of the design load from the hazard curves for structural design purposes. The specific seismic event for which a structure is to be designed to remain elastic should that event occur would correspond to a 50% probability of exceedence during a 50-year period. The adequacy of the design in terms of the required ductility would then be evaluated using the event with a 10% probability of being exceeded in a 50-year period. This latter level is also what the recent hazard maps have used.

The following discussions will provide descriptions of the various procedures and parameters used in describing the output of the seismic hazard analysis, which then becomes the input load in the consideration of structural and geotechnical problems. The hazard maps of Algermissen and Perkins (1976) and the Applied Technology Council (1978) appear separately at the end of this section.

#### Input to Structural Analysis

This Report has outlined and described the various parameters presently used in seismic hazard studies to describe the intensity of ground motion at a site during a seismic event, including peak ground acceleration, velocity, displacement, spectral velocity, Fourier spectrum ordinate, and duration. Design considerations for a particular structure may require input from one or more of these parameters. In most cases, peak acceleration and/or velocity is not sufficient to completely describe the ground motion characteristic (76). Frequency content and duration of motion are significant to the determination of the dynamic response of a structure. Thus, the most appropriate and desirable seismic

parameter is the spectral velocity for the structure, or preferably, the spectral velocities for the frequency range pertinent to the structure. There may be more than one approach followed in the hazard analysis in order to arrive at this design spectrum, depending on the nature of the available seismological data and the attenuation law chosen for the analysis.

The available seismological data is generally stated in terms of either Modified Mercalli Intensity or Richter Magnitude. Therefore, there will normally be two approaches to the estimation of the probability of exceedence of  $S_v$ , each of which will be discussed separately.

#### Intensity Data

Seismicity data which is stated in terms of epicentral intensities allows for two analytic options.

##### 1) $I_o \rightarrow m$

This approach necessitates the conversion of all epicentral data to earthquake magnitude figures using the relationships given in Fig. 2.4, and the analysis is then proceeded with on the basis of earthquake magnitudes. A more detailed discussion of this procedure will be presented subsequently.

##### 2) $I_o \rightarrow I_s \rightarrow P \rightarrow S_v$

This approach makes use of epicentral intensity data. The seismic hazard analysis is completed expressing the results in terms of site intensity. The site intensities are then related to peak acceleration, velocity or displacement by means of the published relationships. Krinitzsky and Chang (1977) have presented such relationships for near and far field conditions.

Alternatively, the attenuation law selected to relate epicentral intensity to site intensity can be combined with any one of the attenuation laws proposed

by McGuire (1976) (see Table 2.5) relating site intensity to acceleration. A combined relationship can then be developed which relates epicentral intensity directly to peak ground acceleration, velocity or displacement. The output from the seismic hazard analysis will directly yield the probability of exceedence of a, v or d. The question of which parameter (a, v or d) should be selected for study was discussed in Part 2 of the Report. In brief summary, peak ground acceleration may be used if the period of the structure is short, while peak ground velocity is more appropriate for intermediate period ranges (1 cps). Peak ground displacement is the recommended parameter for use in design considerations for long period structures, such as offshore towers (7, 29).

In cases where the hazard curve is expressed in terms of site intensity, duration of ground shaking can be estimated for each site intensity using the relationship given in Table 2.10. The estimation of the design response spectrum is made by scaling the standardized response spectra using the design level acceleration and velocity corresponding to an "acceptable" probability of exceedence (or non-exceedence) within a given time period. McGuire (1977b) has indicated that such spectra "are found to be inconsistent in terms of risk for building sites very close and very far from faults", and has recommended an alternate procedure which will be discussed subsequently.

#### Magnitude Data

Two alternative approaches to hazard analysis are available when the seismic data for a region is stated either in terms of earthquake magnitude or in terms of epicentral intensity, converted to magnitude for the purposes of the analysis.

$$1) \quad m, R \rightarrow p \rightarrow S_v$$

This approach utilizes a magnitude-distance attenuation law to describe the hazard at a site in terms of a parameter,  $p$ , which can be either peak ground acceleration, velocity or displacement, whichever of these parameters is thought to be most appropriate. Considerations pertinent to the selection and use of these parameters in determining a design response spectrum and in incorporating site effects were previously discussed. McGuire (1977a) has provided a function relating Fourier amplitude spectrum to earthquake magnitude, distance and soil type, presented in Part 2 in Eq. 2.24. A Fourier spectrum gives a qualitative measure of the nature of earthquake motions. The Fourier amplitude spectrum is a lower bound to the pseudo-velocity spectrum for zero damping. Employing this relationship for different frequencies, a Fourier amplitude spectrum associated with a chosen fractile can be developed.

McGuire (1977b) has also proposed a parameter,  $s$ , which is proportional to  $S_v$ , for use in scaling normalized spectra:

$$s(1 \text{ Hz, } 7\% \text{ damping}) = 0.155 \times 10^{0.382m} (R + 25)^{-0.587} (\text{in/sec}) \quad (4.2)$$

He proposes the use of  $s$  for the middle frequency range (1 Hz) and the use of acceleration,  $a$ , for the high frequency range to scale standardized Newmark-Blume-Kapur response spectra (83). Thus, the seismic hazard analysis is conducted using attenuation laws for  $s$  and  $a$ . The design values of  $s$  and  $a$ , corresponding to an "acceptable" probability level, are then selected from the hazard curve and applied as described above. In addition, design values of  $s$  and  $a$  can be used with the corresponding attenuation laws chosen for the analy-

sis to define a design earthquake of magnitude  $m_d$  and hypocentral distance  $R_d$ . The determination of a design earthquake allows for the estimation of the duration of ground shaking associated with the design criterion, using Figs. 2.21 and 2.22.

2)  $m, R \rightarrow S_v$

A seismic hazard analysis following this approach utilizes an attenuation law in order to relate earthquake magnitude and distance to  $S_v$ . Thus, a direct estimation of the probability of exceedence of  $S_v$  for a particular structure can be made using the attenuation constants for  $S_v$  corresponding to the period of the structure. If a complete response spectrum is desired, the hazard analysis may be repeated for each period, changing the attenuation constants as required.

Input to Geotechnical Analysis

While the parameter  $S_v(T)$  is most useful in structural analyses, most soil dynamics studies in earthquake engineering utilize peak ground acceleration, duration, or a time history of ground acceleration.

It is well-known that the susceptibility of soils to liquefaction is dependent not only on the peak ground acceleration (or shear stress), but also on the number of applications of the acceleration (or stress). Youd and Perkins (1978) have combined cyclic shear strength information with attenuation laws for cyclic shear stress and the number of significant cycles, expressed in terms of earthquake magnitude and distance, and have developed a criterion for liquefaction, given by Eq. 4.3:

$$m = C_1 + C_2 \log R \quad (4.3)$$

where  $C_1$  and  $C_2$  are coefficients which vary with the attenuation factors and local site conditions. Eq. 4.3 can be applied in a seismic hazard analysis for a site such that for each segment of a source zone having a distance  $R_i$ , the annual number of earthquakes with magnitudes greater than  $m_i$  is calculated. The total annual mean number of these special events causing liquefaction at the site is obtained by summing the contributions to this number of all segments from each source. The probability of  $n$  such occurrences in a period of  $t$  years can then be obtained, assuming that the events causing liquefaction follow a poisson process of arrival.

McGuire et al. (1978) have described a liquefaction risk analysis in which an attenuation law for the earthquake-induced shear stress was compared to the cyclic shear strength of the soil deposit to compute the probability of liquefaction. The constants for the shear stress attenuation law were obtained by performing a regression analysis on the results obtained from one-dimensional wave propagation studies.

Yegian and Whitman (1978) have presented a risk analysis for liquefaction which employs a parameter referred to as the liquefaction potential index, LPI, given by Eq. 4.4:

$$LPI = b_1 e^{b_2 m} (R + 25)^{-b_3} \quad (4.4)$$

The parameters  $b_1$ ,  $b_2$  and  $b_3$  are obtained based on the soil properties at the site and from interpretation of field observations of cases of liquefaction and no liquefaction, as well as on an assumed acceleration attenuation law. It is noted that the form of LPI is similar to the form of the attenuation

laws commonly used in seismic hazard analysis. Since the LPI is lognormally distributed, Eq. 4.4 can be used as an attenuation law, and the probability of liquefaction ( $LPI > 1.0$ ) can be calculated employing any of the conventional procedures of seismic hazard analysis reviewed in this Report. It is believed that the use of LPI implicitly takes into account duration of earthquake motion.

When the duration associated with a design level acceleration is desired, the seismic hazard analysis is often repeated using an attenuation law for duration. In reference to the duration considerations discussed previously, it must be brought to attention here that separate consideration of duration estimates falsely assumes that acceleration and duration are independent variables. Duration and peak ground acceleration are both related to earthquake magnitude and distance, the parameters used to describe the essential characteristic of an earthquake; and, therefore, they are not statistically independent variables. The procedure proposed by McGuire (1977b) and described earlier regarding the calculation of a design earthquake with magnitude  $m_d$  and distance  $R_d$  can be used to relate duration to design acceleration more appropriately, using the relationships presented by Chang and Krinitzsky (1977).

In general, soil dynamics problems associated with major structures, including power plants and dams, require the use of a time-history record of motion on firm ground. The proper selection of a time-history consistent with a specific design criterion is difficult. There presently exists no systematic procedure for this selection; in lieu of a tested procedure, all pertinent information, including available instrumental records of major aftershocks, should be weighed with careful professional judgment in order to select a time-history. In most cases, more than one time-history is selected and the influence of the variation in the time-history characteristics is evaluated. Among the para-

meters used in the selection process of a time-history are peak acceleration and the ratio of peak acceleration to peak velocity. McGuire (1978) has pointed out that this ratio is not a constant, but rather is dependent on the distance of the site from a potential earthquake source. Duration of ground motion and period estimates, based on design earthquake parameters  $m_d$  and  $R_d$ , provide valuable information. If a design response spectrum has been determined, an artificial time-history record can be generated using a computer program developed by Vanmarcke at M.I.T.

#### Seismic Hazard Maps

A seismic hazard map can be generated for a region by dividing the region into a grid of points and repeating the analysis treating each point as a site. Contour lines are then drawn for various levels of acceleration corresponding to a certain probability of exceedence in a given period of time. A hazard map for a region provides information regarding the expected hazard at different locations in the region as well as valuable input to the formulation of seismic provisions in building codes. In addition, hazard maps can be used in the seismic risk assessment for lifelines.

Various maps for the United States, of different forms and containing various modifications, have been published since 1947. Although certain of the early maps were labeled as risk maps, they actually provided no estimate of risk or frequency of occurrence of seismic events. This Report will concern itself with only the more recent and important of the published maps.

#### Uniform Building Code

Fig. 4.1 shows the zoning map adopted by the Uniform Building Code, in which the United States is divided into five zones identified as zones 0, 1, 2,

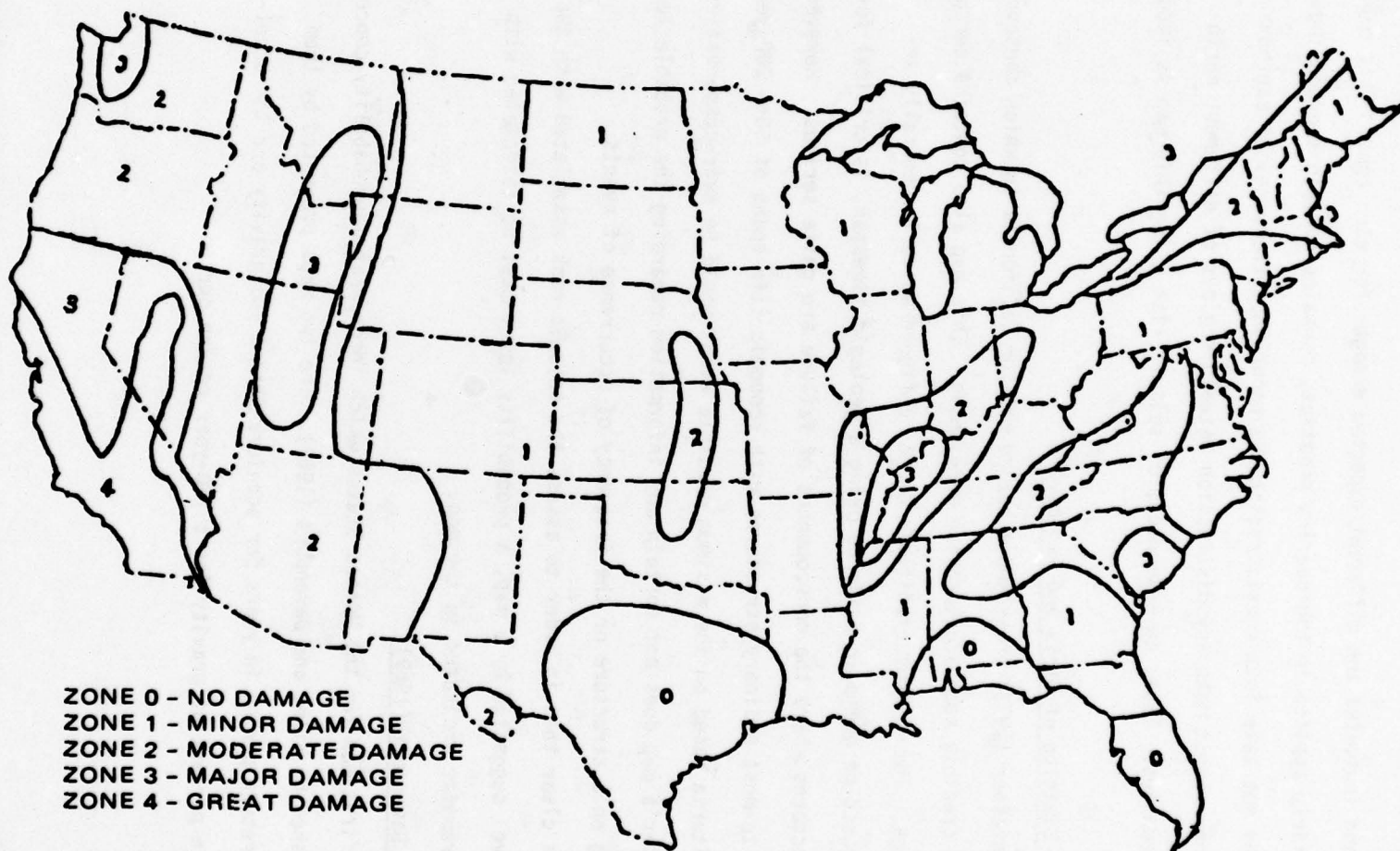


FIG. 4.1 Seismic Zone Map of the United States

3, and 4, and indicates the different expected damages for each zone. This map, although widely applied in engineering practice, contains certain shortcomings. The map does not take into consideration the occurrence frequency of earthquakes, and therefore cannot make any distinction between regions of different earthquake frequencies. Thus, an assessment of seismic risk using this map is impossible.

#### California Division of Mines and Geology

Greensfelder (1973) presented a hazard map for California in which contours of maximum credible rock acceleration were shown. This map also contains certain shortcomings. The maximum creditable event, a figure which is generally arrived at based on geologic evidence using a geologic timespan, is critical for major structures where the consequences of failure are quite serious. However, in regard to most ordinary structures with economic life-spans of 50 - 200 years, design criteria based on the maximum credible event would be over-conservative. Greensfelder's map does not contain any information regarding the probable level of loading on a structure or the frequency of occurrence of events.

It is clear that in order to assess the seismic risk associated with the hazard level suggested by a map, a probability level must be associated with the hazard parameter indicated in the map.

#### Milne and Davenport (1969)

The first map for the United States which incorporated probability concepts was published by Milne and Davenport (1969). The two maps presented by them gave the return period in years for acceleration of 10% gravity and the acceleration in percent of gravity for a 100-year return period.

Kiremidjian and Shah (1975)

More recently, a seismic hazard map for California was published by Kiremidjian and Shah (1975). This map gives peak ground acceleration values corresponding to  $P[A > a] = 0.1$ , during a period of 50 years. The return period associated with this level of probability is 475 years.

Algermissen and Perkins (1976)

Probabilistic estimates of maximum acceleration in rock in the contiguous United States were presented by Algermissen and Perkins (1976) of the U.S. Geological Survey. The map shown in Fig. 4.2 indicates the relative hazard for various parts of the United States. The contour lines for horizontal acceleration in percent gravity correspond to a 90% probability of not being exceeded in 50 years. The seismic hazard analysis conducted to arrive at these estimates was based primarily on historic data. The acceleration attenuation laws employed in the analysis for the Western and Eastern United States were shown in Fig. 2.14.

Applied Technology Council (1978)

The design earthquake ground motion and elastic spectrum provisions developed by the Applied Technology Council (ATC), associated with the Structural Engineers Association of California, were recently published (5, 105). The two parameters employed to describe the provisions are "effective peak acceleration" (EPA), and "effective peak velocity" (EPV). These parameters are used as scaling factors to develop a design response spectrum from standardized spectra. The parameters do not have physical meaning, but were chosen such that the EPA is proportional to a spectral ordinate between 0.1- to 0.5-second periods, and the EPV is proportional to a spectral ordinate of approximately 1-second period. This proportionality constant is 2.5 for a damping value of 5%. Thus, from a design spectrum, it is possible to calculate  $EPA = \frac{S_a(0.1 \text{ to } 0.5)}{2.5}$  and  $EPV = \frac{S_v(1 \text{ sec})}{2.5}$ . In general,

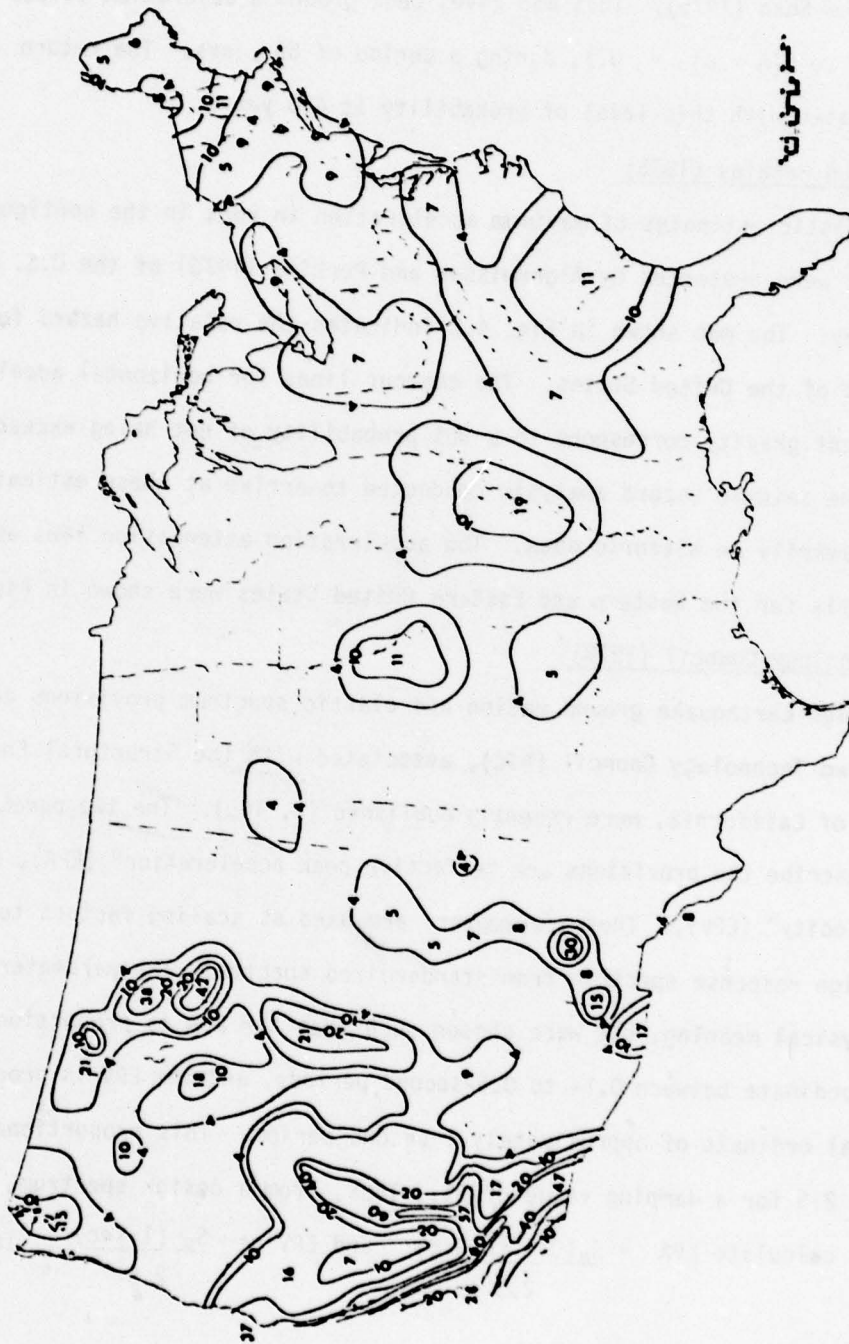


FIG. 4.2 Seismic Hazard Map Prepared by Algermissen and Perkins (1976)  
(From ATC 1978)

EPA is less than the peak ground acceleration, particularly for very high frequencies; and EPV is greater than peak ground velocity, particularly at long distances. The duration of ground motion associated with the EPA and EPV values recommended in the provision is between 20 and 32 seconds. These values should be decreased for shorter durations and increased for longer durations, as deemed appropriate.

Seismic hazard analyses were conducted using the Algermissen and Perkins (1976) map as a reference. The results were interpreted as a map for EPA, shown in Figs. 4.3 and 4.4. The map for EPV, shown in Figs. 4.5 and 4.6, was obtained by introducing modifications to the map for EPA. The numbers on the contour lines in Fig. 4.3 correspond to  $A_a$ , the value of EPA divided by gravity. The values in Fig. 4.5 correspond to  $A_v$ , which is a dimensionless parameter referred to as velocity-related acceleration, and is related to EPV as follows:

<u>EPV (sec)</u>	<u><math>A_v</math></u>
12	0.4
6	0.2
3	0.1
1.5	0.05

The contour lines correspond to a 90% probability of not exceeding, in a period of 50 years, the level of risk chosen by Algermissen and Perkins. If the EPA chosen for design differs from the value suggested by the map, the probability of not exceeding in 50 years, corresponding to the value of EPA, can be determined from Fig. 4.7.

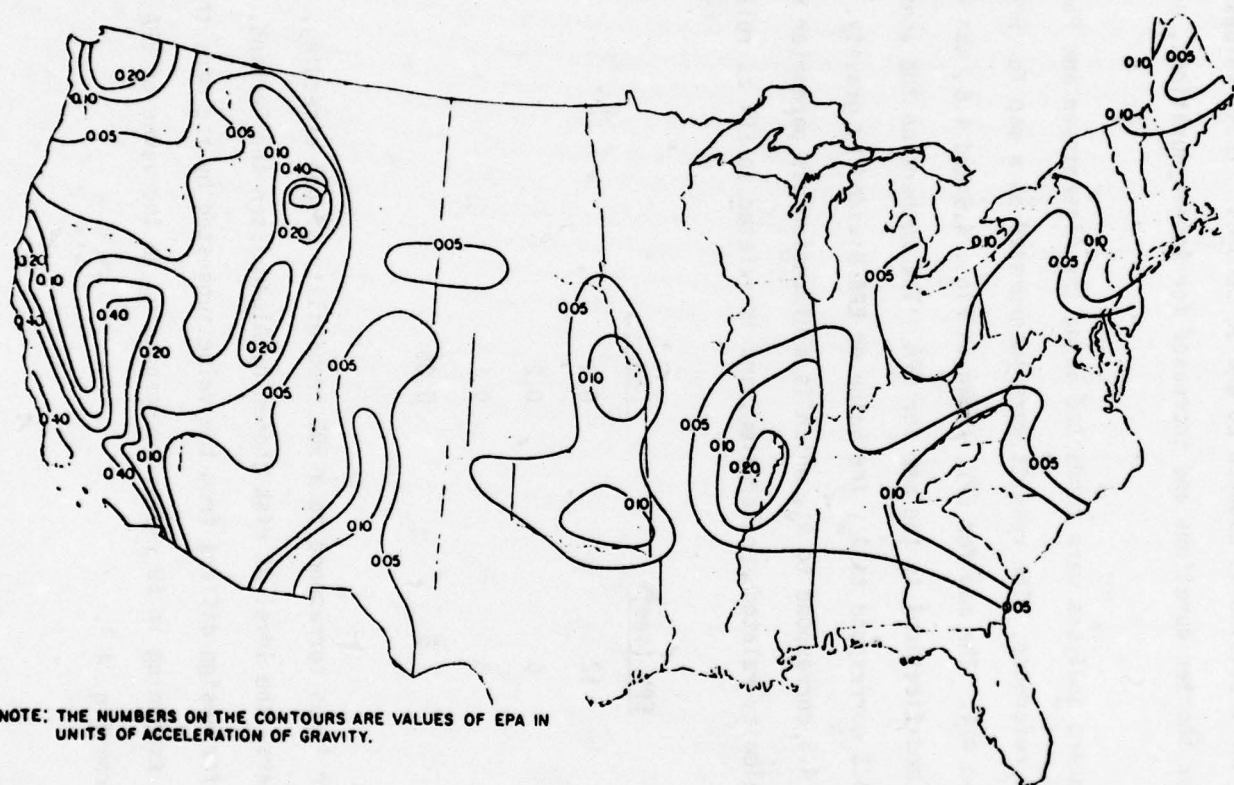
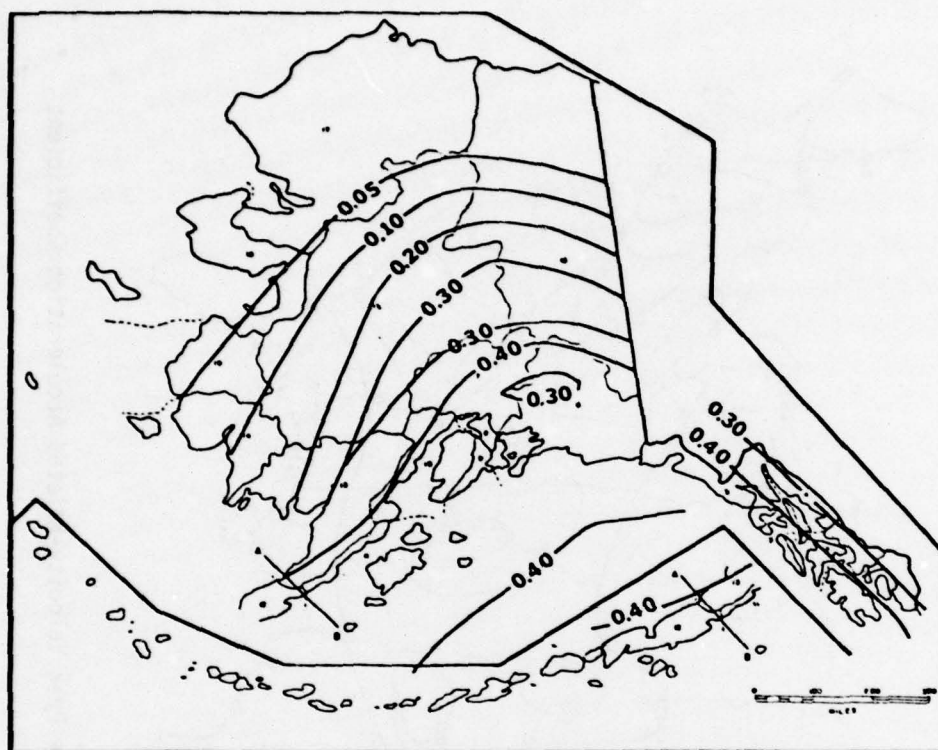
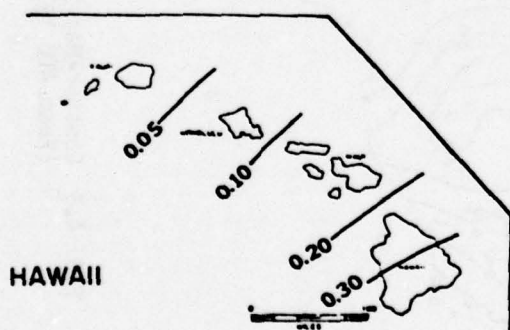


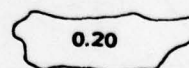
FIG. 4.3 Contour Map for Effective Peak Acceleration (From ATC 1978)



ALASKA



HAWAII



PUERTO RICO

FIG. 4.4 Contour Maps for Effective Peak Acceleration  
(From ATC 1978)

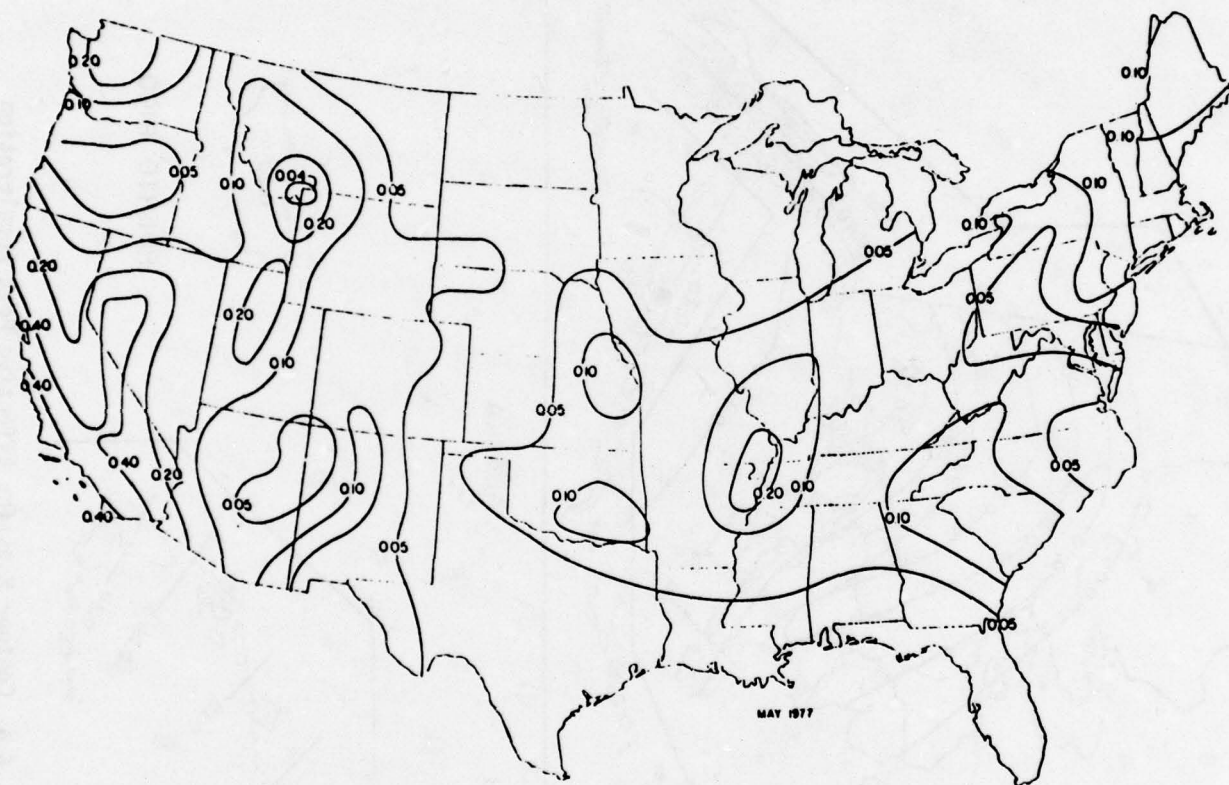


FIG. 4.5 Contour Map for Effective Peak Velocity-Related Acceleration Coefficient  
(From ATC 1978)

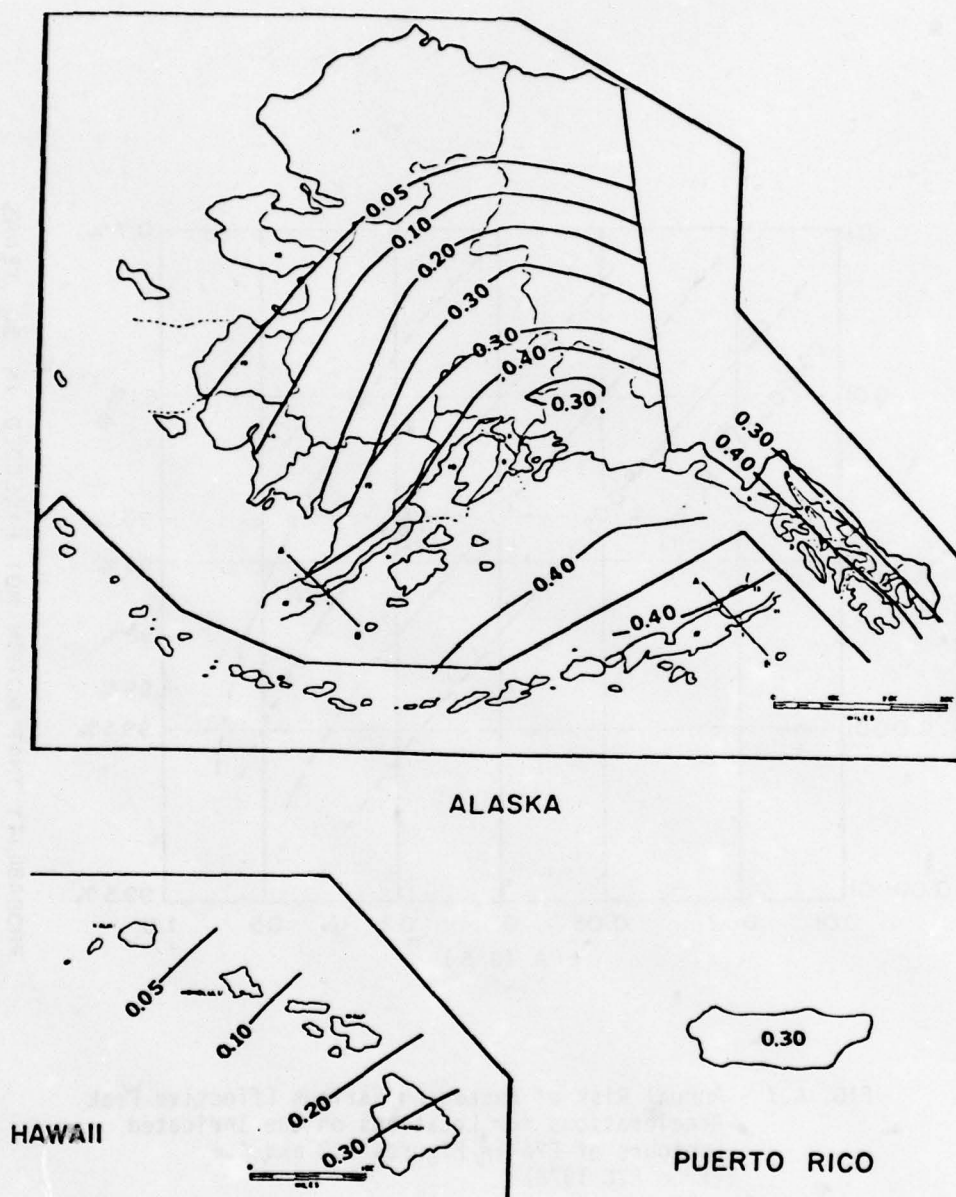


FIG. 4.6 Contour Map for Effective Peak Velocity-Related Acceleration Coefficient (From ATC 1978)

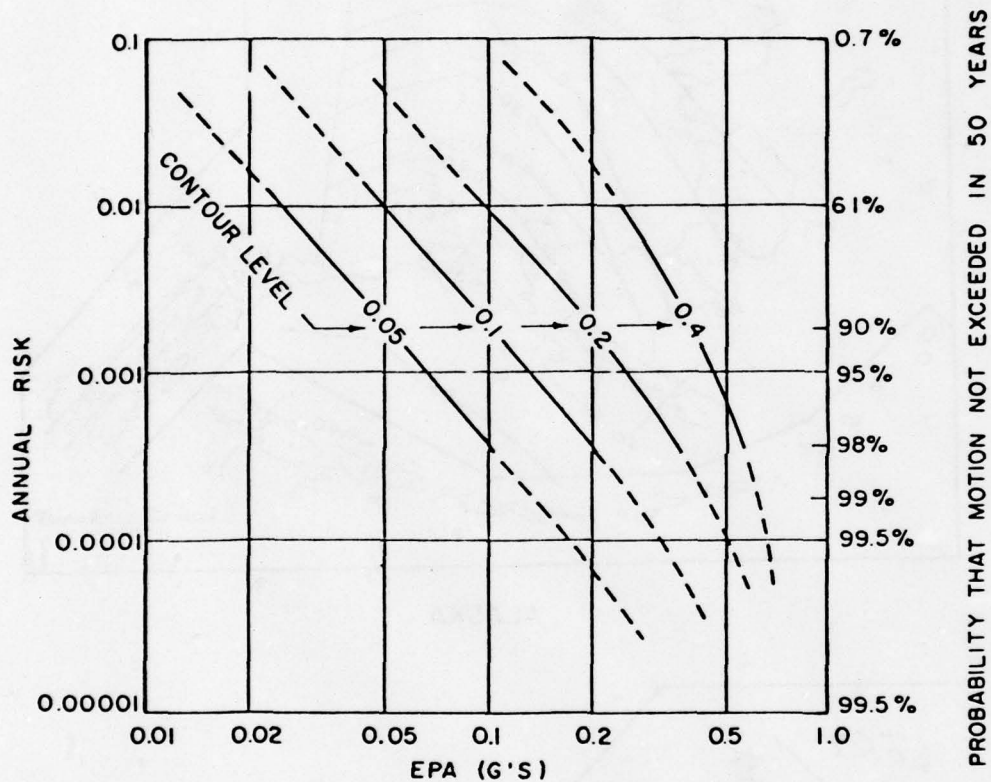


FIG. 4.7 Annual Risk of Exceeding Various Effective Peak Accelerations for Locations on the Indicated Contours of EPA in Figures 4.3 and 4.4 (From ATC 1978)

### Design Spectrum

Having estimated the EPA for a site, the design spectrum for horizontal motion can be determined by using the normalized spectra shown in Fig. 4.8 for three soil types. Briefly,  $S_1$  refers to a soil profile consisting of rock or stiff deposits (less than 200 ft\*) of sand, gravel and stiffer clays;  $S_2$  refers to deep (greater than 200-ft) cohesionless soils or stiff clay deposits; and  $S_3$  refers to deposits of 30 feet or more of clays, sands and other cohesionless materials.

In order to determine the design elastic spectrum for 5% damping, the appropriate spectrum from Fig. 4.8 is multiplied by  $EPA \times S$ , where  $S = 1.0$  for  $S_1$  and  $S_2$  profiles, and  $S = 0.8$  for  $S_3$  profiles. The design spectrum for 2% damping can be determined by multiplying the design spectrum for 5% damping by 1.25. The design elastic response spectrum for vertical motions is determined by multiplying the horizontal spectrum by 0.67.

The procedure described is applicable, provided that  $A_a$  and  $A_v$  are identical, as in the region of the innermost contours. Where  $A_a$  and  $A_v$  differ, the provision states that "the portion of the response spectrum controlled by the velocity should be increased in proportion to the EPV value and the remainder of the response spectrum extended to maintain the same overall spectral form."

---

\* A table of factors for converting U. S. customary units of measurement to metric (SI) units is presented on page 3.

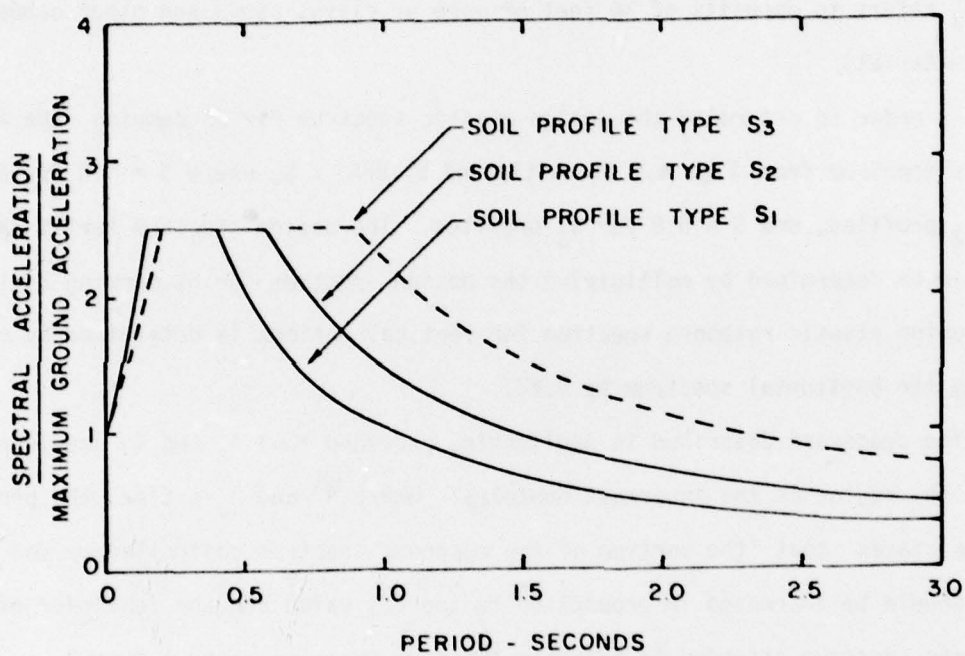


FIG. 4.8 Normalized Response Spectra Recommended for Use in Building Code (From ATC 1978)

## PART 5: CONCLUSIONS

Seismic hazard analysis provides estimates of the probability that a design parameter,  $P$ , at a given site, will exceed the value  $p$  within a certain period of time. Essentially, the procedure involves the following general steps.

- 1) A compilation of geologic, geophysical and seismological data regarding the seismicity of the region under investigation.
- 2) The establishment of potential earthquake sources within the region using all the sources of information.
- 3) For each source, the determination of the upper and lower bound magnitudes (intensities), the mean annual number of earthquake occurrences, and the relative frequency distribution for earthquake magnitude (intensity).
- 4) Selection of an appropriate attenuation law to relate the seismic design parameter at the site to earthquake magnitude (intensity), and distance to source of energy release.
- 5) Calculation of the probability of exceedence (or non-exceedence) of  $p$  for various assumed values of  $P$  using probabilistic procedures.

Calculation of the input parameters required for the analysis involves numerous uncertainties which can be accounted for and incorporated in the probability calculations. It must be noted that the reliability of the results of seismic hazard analysis depends on the accuracy of these input data. Caution is also advised regarding the calculation of small probabilities which are associated with the tails of the probability distribution for the parameter  $P$  used in the analysis (38). Proper interpretation of the results requires the application of professional judgment and experience.

The practical application of seismic hazard analysis in most cases has been limited to the definition of a design seismic parameter corresponding to an acceptable level of risk. The results of seismic hazard analysis, however, are beneficial beyond their present practical use when applied in research. Incorporating seismic hazard analysis results into an overall risk analysis can identify the major seismic parameters contributing to the risk. Furthermore, it may lead to alternate and more realistic procedures for analysis in earthquake engineering.

## REFERENCES

1. Algermissen, S.T. (1969). "Seismic Risk Studies in the United States", Proceedings, 4th World Conference on Earthquake Engineering, Vol. 1, pp. 14-27.
2. Algermissen, S.T. and Perkins, David M. (1976). "A Probabilistic Estimate of Maximum Acceleration in Rock in the Contiguous United States", U.S. Dept. of the Interior, Geological Survey, Open-file Report 76-416.
3. Allen, Clarence R. (1976). "Geological Criteria for Evaluating Seismicity", Seismic Risk and Engineering Decisions - Developments in Geotechnical Engineering, Vol. 15, C. Lomnitz and E. Rosenblueth, Editors, Chapter 3, pp. 31-40.
4. Alonso, J.L. and Larotta, J. (1977). "Seismic Risk and Seismic Zoning of the Caracas Valley", Proceedings of the 6th World Conference on Earthquake Engineering, India, January.
5. Applied Technology Council (1978). "Tentative Provisions for the Development of Seismic Regulations for Buildings", National Science Foundation, Publication 510, June.
6. Ayyaswamy, P. et al. (1974). "Estimation of the Risks Associated with Dam Failure", School of Engineering and Applied Science, UCLA - ENG - 7423, March.
7. Bea, R.G., (1978). "Earthquake Criteria for Platforms in the Gulf of Alaska", Journal of Petroleum Technology, pp. 325-340, March.
8. Bell, J.M. and Hoffman, R.A. (1978). "Design Earthquake Motions Based on Geologic Evidence", Proceedings of the ASCE Geotechnical Engineering Division Specialty Conference on Earthquake Engineering and Soil Dynamics, June 19-21, Pasadena, California.
9. Benjamin, Jack R. (1969). "A Probabilistic Model for Seismic Force Design" Proceedings of the Fourth World Conference on Earthquake Engineering, Vol. III, pp. 131-136, January.
10. Benjamin, J.R. and Cornell, C.A. (1970). Probability, Statistics and Decisions for Civil Engineers, McGraw-Hill, Inc.
11. Bernreuter, Don L. (1977). "Estimates of the Epicentral Ground Motion in the Central and Eastern United States", Sixth World Conference on Earthquake Engineering, pp. 2-09 — 2-14, January.
12. Blume, John A. (1977). "The SAM Procedure for Site-Acceleration-Magnitude Relationships", 6th World Conference on Earthquake Engineering, pp. 2-87 — 2-99, January.
13. Bollinger, G.A. (1973). "Seismicity of the Southeastern United States", Bull. Seism. Soc. Am., 63, pp. 1785-1808.
14. Bolt, B.A. (1973). "Duration of Strong Motion", Proceedings of Fifth World Conference on Earthquake Engineering, Rome.

15. Boore, D.M. (1973). "Empirical and Theoretical Study of Near-Fault Wave Propagation", Proceedings, Fifth World Conference in Earthquake Engineering, Rome.
16. Campbell, K.W. (1978). "Bayesian Estimation of Seismic Risk in a Fault with Emphasis on Lifeline Systems", Earthquake Engineering Research Institute, Course on Seismic Risk Analysis, Los Angeles, California, February 8 and 9.
17. Campbell, Kenneth W. and Duke, C. Martin (1974). "Bedrock Intensity Attenuation and Site Factors from San Fernando Earthquake Records", Bulletin of the Seismological Society of America, Vol. 64, No. 1, pp. 173-185, February.
18. Caputo, M; Keilis-Borok, V.I.; Kronrod, T.L.; Molchan, G.M.; Panza, G.F.; Pira, A.; Podgaetskaja, V.M.; and Postpischl, D. (1974) "The Estimation of Seismic Risk for Central Italy", Annali di Geofisica, Vol. XXVII-N.1-2.
19. Chang, F.K. and Krinitzsky, E.L. (1977). "Duration, Spectral Content and Predominant Period of Strong Motion Earthquake Records from Western United States", State-of-the-Art for Assessing Earthquake Hazards in the United States, Report 8, United States Army Engineer Waterways Experiment Station, Vicksburg, Miss.
20. Chinnery, Michael A. and Rogers, Donald A. (1973). "Earthquake Statistics in Southern New England", Earthquake Notes, Vol. XLIV, Nos. 3-4, July-December.
21. Christian, J.T., Borjeson, R.W. and Tringale, P.T. (1978). "Probabilistic Evaluation of OBE for Nuclear Plants", Journal of the Geotechnical Engineering Division, ASCE, Vol. 104, No. GT7, July.
22. Cluff, L.S. (1978). "Type and Significance of Geologic Input for Seismic Risk Analysis", Lecture notes for Earthquake Engineering Research Institute Course on Seismic Risk Analysis, Los Angeles, California, February 8 and 9.
23. Cornell, C.A. (1968). "Engineering Seismic Risk Analysis", Bulletin of the Seismological Society of America, Vol. 58, No. 5, pp. 1583-1606, October.
24. Cornell, C.A. (1973). "Theme Report on Topic 2: Ground Motion, Seismicity, Seismic Risk and Zoning", 5th World Conference on Earthquake Engineering, Italy.
25. Cornell, C.A. (1978). "Seismic Risk Analysis", Earthquake Engineering Research Institute, Course on Seismic Risk Analysis, Los Angeles, California, February 8 and 9.
26. Cornell, C.A. and Merz, H.A. (1975). "Seismic Risk Analysis of Boston", Journal of the Structural Division, ASCE, Vol. 101, No. ST10, Proceedings Paper 11617, pp. 2027-2043, October.
27. Cornell, C.A. and Vanmarcke, E.H. (1969). "The Major Influences on Seismic Risk", Proceedings of the 4th World Conference on Earthquake Engineering, Santiago, Chile.
28. Cornell, C.A. and Vanmarcke, E.H. (1975). "Seismic Risk Analysis for Offshore Structures", Proceedings of the Offshore Technology Conference, Houston, Texas, May 5-8.

29. DeCapua, N.J. and Liu, S.C. (1974). "Statistical Analysis of Seismic Environment in New York State", Fifth Symposium on Earthquake Engineering, Vol. 1, pp. 389-396, November.
30. DerKiureghian, A. and Ang, A. H-S. (1977). "A Fault-Rupture Model for Seismic Risk Analysis", Bulletin of the Seismological Society of America, Vol. 67, No. 4, pp. 1173-1194, August.
31. Dick, I.D. (1965). "Extreme Value Theory and Earthquakes", Proceedings of the Third World Conference on Earthquake Engineering, Vol I, pp. III-45 - III-53, January-February.
32. Dietrich, J.H. (1973). "A Deterministic Near-Fault Source Model", Proceedings of the Fifth World Conference on Earthquake Engineering, Rome.
33. Donovan, N.C. (1973). "A Statistical Evaluation of Strong Motion Data Including the February 9, 1971 San Fernando Earthquake", Proceedings of the Fifth World Conference on Earthquake Engineering, Rome.
34. Donovan, N.C. (1978). "Notes for EERI Course on Seismic Risk Analysis", Earthquake Engineering Research Institute, Los Angeles, California, February 8 and 9.
35. Donovan, N.C. and Bornstein, A.E. (1978). "Uncertainties in Seismic Risk Procedures", Journal of the Geotechnical Engineering Division, ASCE, Vol. 104, No. GT7, July.
36. Douglas, Bruce M. and Ryall, Alan (1975). "Return Periods for Rock Acceleration in Western Nevada", Bulletin of the Seismological Society of America, Vol. 65, No. 6, pp. 1599-1611, December.
37. Dowrick, D.J. (1977). Earthquake Resistant Design, John Wiley and Sons.
38. Drenich, R.F. and Yun, C.B (1977). "Prediction of Earthquake Resistance", Preprint 3039, American Society of Civil Engineers Fall Convention and Exhibit, San Francisco, October 17-21.
39. Eguchi, R.T. and Campbell, K.W. (1977). "Seismicity and Site Effects on Earthquake Risk", Proceedings 6th World Conference on Earthquake Engineering, India.
40. Espinosa, A.F. (1977). "Particle-Velocity Attenuation Relations: San Fernando Earthquake of February 9, 1971", Bulletin of the Seismological Society of America, Vol. 67, No. 4, pp. 1195-1214, August.
41. Esteva, L. (1969). "Seismicity Prediction: A Bayesian Approach", Proceedings, Fourth World Conference on Earthquake Engineering, Santiago, Chile, January.
42. Esteva, L. and Villaverde, R. (1973). "Seismic Risk, Design Spectra and Structural Reliability", Proceedings of the Fifth World Conference on Earthquake Engineering, Rome.
43. Esteva, L. (1975). "Seismicity", Seismic Risk and Engineering Decisions - Developments in Geotechnical Engineering, Vol. 15, Lomnitz and E. Rosenblueth, Editors, Chapter 6, pp. 179-224.

44. Esteva, L. (1976). "Seismic Risk and Seismic Design Decision", Seismic Design for Nuclear Power Plants, Edited by Hansen, R.J., Massachusetts Institute of Technology Press.
45. Esteva, L. and Villaverde, R. (1973). "Seismic Risk, Design Spectra and Structural Reliability", Proceedings of the Fifth World Conference on Earthquake Engineering, Rome.
46. Faccioli, Ezio (1977). "Probabilistic Assessment of Seismic Risk on Local Soil Sediments", Proceedings of the Sixth World Conference on Earthquake Engineering, pp. 2-243 to 2-248, January.
47. Ferraes, S.G. (1967a). "Statistical Relation of Magnitude to Frequency of Occurrence for Earthquakes in Mexico City", Earth Plant. Sci. Lett., 3, pp. 449-452.
48. Ferraes, S.G. (1967b). "Test of Poisson Process for Earthquakes in Mexico City", Journal of Geophysical Research, 72, pp. 3741-3742.
49. Ferraes, S.G. (1973). "Earthquake Magnitude Probabilities and Statistical Independence for Mexico City Earthquakes", Bulletin of the Seismological Society of America, Vol. 63, No. 6, pp. 1913-1919, December.
50. Grandori, G. and Benedetti, D. (1973). "On the Choice of Acceptable Seismic Risk", International Journal of Earthquake Engineering and Structural Dynamics, 2, pp. 3-9.
51. Grandori, G. and Petrini, V. (1977). "Comparative Analysis of the Seismic Risk in Sites of Different Seismicity", Earthquake Engineering and Structural Dynamics, Vol. 5, pp. 53-65.
52. Guha, S.K. et al. (1973). "Ground Motions in the Epicentral Area of Earthquakes", Proceedings of the Fifth World Conference on Earthquake Engineering, Rome.
53. Gulkan, P. and Yuceman, M.S. (1975). "A Seismic Risk Study of Izmir", Proceedings of the Fifth European Conference on Earthquake Engineering, Vol 2, Paper No. 160,11.
54. Greensfelder, A.W. (1973). "A Map of Maximum Expected Bedrock Acceleration from Earthquakes in California", California Division of Mines and Geology Publication, Sacramento, California.
55. Gumbel, E.J. (1960). Statistics of Extremes, Columbia University Press.
56. Gutenberg, B. and Richter, C.F. (1954). Seismicity of the Earth, Princeton University Press.
57. Housner, G.W. (1969). "Engineering Estimates of Ground Shaking and Maximum Earthquake Magnitude", Proceedings of the Fourth World Conference on Earthquake Engineering, Vol I, pp. 1-27, January.
58. Hsieh, T., Okrent, D., and Apostolakis, G.E. (1975). "On the Average Probability Distribution of Peak Ground Acceleration in the U.S. Continent Due to Strong Earthquakes", Prepared for National Science Foundation, Grant GI-39416, UCLA-ENG-7516, March.

59. International Atomic Energy Agency (1970). "Earthquake Guidelines for Reactor Siting", Technical Report Series No. 139, pp. 1-23, Vienna Panel, June.
60. Isacks, B. and Oliver, J. (1964). "Seismic Waves with Frequencies from 1 to 100 Cycles per Second Recorded in a Deep Mine in New Jersey", Bulletin of Seismological Society of America,
61. Isacks, B. and Page, R. (1968). Comments on paper by C. Lomnitz: "Statistical Prediction of Earthquakes", Rev. Geophys., 6, 99.
62. Kiremidjian, A.S. and Shah, H.C. (1975). "Seismic Hazard Mapping of California", The John A. Blume Earthquake Engineering Center, Technical Report No. 21, Stanford University, Stanford, California.
63. Knopoff, L. (1964). "The Statistics of Earthquakes in Southern California", Bulletin of the Seismological Society of America, 54, pp. 1871-73, December.
64. Krinitzsky, E.L. and Chang, F.K. (1977). "Specifying Peak Motions for Design Earthquakes", State-of-the-Art For Assessing Earthquake Hazards in the United States, Report 7, United States Army Engineer Waterways Experiment Station, December.
65. Liu, S.C. and Dougherty, M. (1975). "Earthquake Risk Analysis - Application to Telephone Community Dial Offices in California - Case 20133-485", Bell Laboratories, Memorandum.
66. Liu, S.C. and Fagel, L.W. (1972). "Earthquake Environment for Physical Design: A Statistical Analysis", The Bell System Technical Journal, Vol. 51, No. 9.
67. Lomnitz, C. (1964). "On Andean Structure, Part II: Earthquake Risk in Chile", Bulletin of the Seismological Society of America, Vol. 54, No. 5, Part A, pp. 1271-1281, October.
68. Lomnitz, C. (1966). "Statistical Prediction of Earthquakes", Reviews of Geophysics, Vol. 4, pp. 377-393.
69. Lomnitz, C. (1969). "An Earthquake Risk Map of Chile", Proceedings of the Fourth World Conference on Earthquake Engineering, Vol. I, pp. 161-184, January.
70. Lomnitz, C. and Singh, S.K. (1976). "Earthquake and Earthquake Prediction", Seismic Risk and Engineering Decisions - Developments in Geotechnical Engineering, Vol. 15, C. Lomnitz and E. Rosenblueth, Editors, Chapter 2, pp. 3-30.
71. Mann, O.C. and Howe, W. (1973). "Regional Earthquake Risk Study", M & H Engineering, Memphis, Tennessee.
72. McClain, W.C. and Myers, O.H. (1970). "Seismic History and Seismicity of the Southeastern Region of the United States", Report No. ORNL-4582, Oak Ridge National Laboratory, Oak Ridge, Tennessee.
73. McGuire, R.K. (1976). "FORTRAN Computer Program for Seismic Risk Analysis", United States Department of the Interior Geological Survey: Open-File Report 76-67.
74. McGuire, R.K. (1977a). "A Simple Model for Estimating Fourier Amplitude Spectra", Submitted to Seismological Society of America Bulletin.

75. McGuire, R.K. (1977b). "Seismic Design Spectra and Mapping Procedures Using Hazard Analysis Based Directly on Oscillator Response", Earthquake Engineering and Structural Dynamics, Vol. 5, pp. 211-234.
76. McGuire, R.K. (1977c). "The Use of Intensity Data in Seismic-Hazard Analysis", Proceedings of the Sixth World Conference on Earthquake Engineering, India, January.
77. McGuire, R.K. (1978). "Seismic Ground Motion Parameter Relations", Journal of the Geotechnical Engineering Division, ASCE, Vol. 104, No. GT4, April.
78. McGuire, R.K., Tatsuoka, F., Iwasaki, T. and Tokida, K. (1978). "Probabilistic Procedures for Assessing Soil Liquefaction Potential", United States Geological Survey, Denver, Colorado.
79. Merz, H.A. and Cornell, C.A. (1973). "Seismic Risk Analysis Based on Quadratic Magnitude-Frequency Law", Bulletin of the Seismological Society of America, Vol. 63, pp. 1999-2006.
80. Milne, W.G. and Davenport, A.G. (1969). "Earthquake Probability", Proceedings of the Fourth World Conference on Earthquake Engineering, Santiago de Chile, January.
81. Mortgart, C.P., Zsutty, T.C., Shah, H.C. and Lubetkin, L. (1977). "A Study of Seismic Risk For Costa Rica", Report No. 5, The John A. Blume Earthquake Engineering Center, Stanford University, April.
82. Newmark, N.M. and Rosenblueth, Emilio (1971). Fundamentals of Earthquake Engineering, Prentice-Hall, Inc., Englewood Cliffs, New Jersey.
83. Newmark, N.M., Blume, J.A. and Kapur, K.K. (1975). "Seismic Design Spectra for Nuclear Power Plants", Journal of the Power Division, ASCE, 99, pp. 287-303.
84. Nuttli, O.W. (1974). "Magnitude-Recurrence Relation for Central Mississippi Valley Earthquakes", Bulletin of the Seismological Society of America, Vol. 64, No. 4, August.
85. O'Rourke, M.J. and Solla, E. (1977). "Seismic Risk Analysis of Latham", Technical Report (SVBDUPS Project) No. 3, National Science Foundation Grant No. ENV76-14884, June.
86. Papastamatiou, D. (1977). "Near Field Stochastic Modelling", Proceedings of the Sixth World Conference on Earthquake Engineering, India, January.
87. Rosenblueth, E. (1969). "Seismicity and Earthquake Simulation - General Report", Proceedings of the Fourth World Conference on Earthquake Engineering, Vol. IV, pp. 67-76, January.
88. Rosenblueth, E. (1972). "Development of Earthquake Engineering Design Methods", Proceedings of the Fourth European Symposium on Earthquake Engineering, pp. 103-114, September.
89. Rosenblueth, E. (1973). "Analysis of Risk", Proceedings of the Fifth World Conference on Earthquake Engineering, Rome.

90. Schnabel, P.B. and Seed, B. (1973). "Accelerations in Rock for Earthquakes in the Western United States", Bulletin of the Seismological Society of America, Vol. 63, No. 2, pp. 501-516, April.
91. Seed, H.B., Murarka, R., Lysmer, J. and Idriss, I.M. (1976). "Relationships of Maximum Acceleration, Maximum Velocity, Distance from Source and Local Site Conditions", Seismological Society of America Bulletin, Vol. 66, No. 4.
92. Seed, H.B., Ugas, C. and Lysmer, J. (1974). "Site-Dependent Spectra for Earthquake-Resistant Design", Earthquake Engineering Research Center, University of California, Berkely, California, Report No. EERC 74-12.
93. Shah, H.C. (1975). "Seismic Risk Analysis: California State Water Project", Talk given to Cal. Water and Power Earthquake Engineering Forum, January.
94. Shah, H.C. (1978). "Seismic Risk Analysis", Lecture Notes, Earthquake Engineering Research Institute, Course in Seismic Risk Analysis, Los Angeles, California, February 8 and 9.
95. Shah, H.C. and Benjamin, J.R. (1977). "Lifeline Seismic Criteria and Risk, A State of the Art Report", Proceedings, Technical Council on Lifeline Earthquake Engineering, Specialty Conference, University of California, Los Angeles, California, August 30 and 31.
96. Shah, H.C., Mortgart, C.P., Kiremidjian, A. and Zsuther, T.C. (1975). "A Study of Seismic Risk for Nicaragua, Part I", The John Blume Earthquake Engineering Center, Stanford University, Report No. 11, January.
97. Slemmons, D.B. (1977). "Faults and Earthquake Magnitude", State-of-the-Art for Assessing Earthquake Hazards in the United States, Report 6, United States Army Engineer Waterways Experimental Station, May.
98. Taleb-Agha, G. and Whitman, R.V. (1975). "Seismic Risk Analysis of Discrete Systems", SDDA Report No. 23, Massachusetts Institute of Technology, Department of Civil Engineering Research Report R75-48, December.
99. Tocher, D., Patwardhau, A.S. and Cluff, L.S. (1971). "Estimation of Near Field Characteristics of Earthquake Motion", Proceedings of the Sixth World Conference on Earthquake Engineering, India, January.
100. Tong, W. (1975). "Seismic Risk Analysis for Two-Sites Case", Seismic Design Decision Analysis, Report No. 18, Department of Civil Engineering, Massachusetts Institute of Technology, June.
101. Vanmarcke, E.H. and Lai, S.P. (1977). "Strong-Motion Duration of Earthquakes", MIT, Publication No. R77-16, Order No. 569, "Evaluation of Seismic Safety of Buildings, Report No. 10", July.
102. Veneziano, D. (1975). "Probabilistic and Statistical Models for Seismic Risk Analysis", Seismic Design Decision Analysis, Report No. 21, Department of Civil Engineering, Massachusetts Institute of Technology, July.

103. Ward, P.L., Gibbs, J., Harlow, D. and Aburto, A. (1974). "Aftershocks of the Managua, Nicaragua Earthquake and the Tectonic Significance of the Tiscapa Fault", Bulletin of the Seismological Society of America, Vol. 64, No. 4, pp. 1017-1029, August.
104. Whitman, R.V. et al. (1975). "Seismic Design Decision Analysis", Journal of the Structural Division, ASCE, ST5, May.
105. Whitman, R.V., Donovan, N.C., Bolt, B., Algermissen, S.T. and Sharpe, R.L. (1977). "Seismic Design Regionalization Maps for the United States", Sixth World Conference on Earthquake Engineering, pp. 2-387 to 2-292, January.
106. Whitman, R.V. and Taleb-Agha, G. (1977). "Seismic Risk for Multiple Sites", Proceedings of the Sixth World Conference on Earthquake Engineering, pp. 2-439 to 2-448, January.
107. Yegian, M.K. and Whitman, R.V. (1978). "Risk Analysis for Ground Failure By Liquefaction", Journal of the Geotechnical Engineering Division, ASCE, Vol. 104, No. GT7, July.
108. Yegulalp, T.M. and Kuo, J.T. (1974). "Statistical Prediction of the Occurrence of Maximum Magnitude Earthquakes", Bulletin of the Seismological Society of America, Vol. 64, No. 2, April.
109. Youd, L.T. and Perkins, D.M. (1978). "Mapping Liquefaction - Induced Ground Failure Potential", Journal of the Geotechnical Engineering Division, ASCE, Vol. 104, No. GT4, April.

# APPENDIX A: SEISMIC HAZARD ANALYSIS USING PROBABILISTIC ATTENUATION LAW

McGuire (1976) presents a brief description of the theoretical formulations used in his computer program for seismic hazard analysis employing a probabilistic attenuation law. The mathematical expressions presented herein are taken from McGuire (1976).

The unconditional probability of acceleration  $A$  exceeding  $a$  is given by:

$$P[A > a] = \int_r \int_M P[A > a|m \text{ and } R] f_M(m) f_R(r) d_m d_r \quad (A.1)$$

where  $P[A > a|m \text{ and } R]$  is the complementary cumulative probability of  $a$ , given an earthquake of magnitude  $m$  and distance  $R$ ;  $f_M(m)$  and  $f_R(r)$  represent the probability density functions of  $m$  and  $R$ . The integration is carried out over the entire magnitude range of engineering interest, and over the various sources.

Assuming an attenuation law of the form

$$\bar{a} = c_1 e^{c_2 m} (r + r_0)^{c_3} \quad (A.2)$$

where  $\bar{a}$  represents the mean value of the acceleration, which is lognormally distributed with a standard deviation  $\sigma_{\ln a}$ , and using the truncated magnitude recurrence relationship given in Eq. 2.10, the density function on magnitude is given by:

$$f_M(m) = \beta K m_1 \exp(-\beta(m - m_0)) \quad m_0 < m < m_1 \quad (A.3)$$

Using Eqs. A.2 and A.3, Eq. A.1 can be written as:

$$P[A > a] = \int_r \int_{m_0}^{m_1} \phi^* \left( \frac{\ln \bar{a} - C_1 - C_2 m - C_3 \ln(r + r_0)}{\sigma_{\ln a}} \right) \quad (A.4)$$

$$\beta K_{m_1} \exp(-\beta(m - m_0)) f_R(r) d_m dr$$

where  $\phi^*$  is the complementary cumulative of the standardized normal distribution. Performing the integration on magnitude analytically, Eq. A.4 can be written as:

$$P[A > a] = \int_r \left\{ (1 - K_{m_1}) \phi^* \left( \frac{Z}{\sigma_{\ln a}} \right) + K_{m_1} \phi^* \left( \frac{Z'}{\sigma_{\ln a}} \right) + K_{m_1} (r + r_0)^{\beta C_3 / C_2} \right. \\ \left. \exp \left( -\frac{\ln a \beta}{C_2} + \frac{\beta C_1}{C_2} + \beta m_0 + \frac{\beta^2 \sigma^2 \ln a}{2 C_2^2} \right) \right\} f_R(r) dr \quad (A.5)$$

$$\left[ \phi^* \left( \frac{Z - \beta \sigma_{\ln a}^2 / C_2}{\sigma_{\ln a}} \right) - \phi^* \left( \frac{Z' - \beta \sigma_{\ln a}^2 / C_2}{\sigma_{\ln a}} \right) \right] \left\{ f_R(r) dr \right.$$

in which

$$Z = \ln a - C_1 - C_2 m_1 - C_3 \ln(r + r_0)$$

$$Z' = \ln a - C_1 - C_2 m_0 - C_3 \ln(r + r_0)$$

The density function on distance,  $f_R(r)$ , is dependent on the locations of the sources and subsources relative to the site. The integral shown in Eq. A.5

is evaluated numerically for each value of acceleration  $a$ . The output from McGuire's program includes values for the total expected number of events causing intensities or accelerations exceeding some specified values, as well as the annual probabilities of exceedence associated with each specified event. The probability of exceedence during a time interval  $t$  can be calculated from the computed expected number of occurrences of an event using Eq. 3.5.

In accordance with letter from DAEN-RDC, DAEN-ASI dated 22 July 1977, Subject: Facsimile Catalog Cards for Laboratory Technical Publications, a facsimile catalog card in Library of Congress MARC format is reproduced below.

Yegian, Mishac K

State-of-the-art for assessing earthquake hazards in the United States; Report 13: Probabilistic seismic hazard analysis / by M. K. Yegian, Department of Civil Engineering, Northeastern University, Boston, Mass. Vicksburg, Miss. : U. S. Waterways Experiment Station ; Springfield, Va. : available from National Technical Information Service, 1979. 130, 3 p. : ill. ; 27 cm. (Miscellaneous paper - U. S. Army Engineer Waterways Experiment Station ; S-73-1, Report 13) Prepared for Office, Chief of Engineers, U. S. Army, Washington, D. C., under Contract No. DACW39-78-M-2652. References: p. 123-130.

1. Earthquake engineering. 2. Earthquake hazards. 3. Earthquakes. 4. Ground motion. 5. Probability theory. 6. Seismic investigations. 7. Seismic risks. 8. State-of-the-art studies. I. Northeastern University, Boston. Dept. of Civil Engineering. II. United States. Army. Corps of Engineers. III. Series: United States. Waterways Experiment Station, Vicksburg, Miss. Miscellaneous paper ; S-73-1, Report 13. TA7.W34m no.S-73-1 Report 13